Title
Distributed Sliding Mode Control for Nonlinear Consensus

Author
Wu, Yujia

Publication Date
2019

Peer reviewed|Thesis/dissertation

Distributed Sliding Mode Control for Nonlinear Consensus

by

Yujia Wu

A dissertation submitted in partial satisfaction of the

requirements for the degree of

Doctor of Philosophy

in

Mechanical Engineering

in the

Graduate Division

of the

University of California, Berkeley

Committee in charge:

Professor Kameshwar Poolla, Chair
Professor Francesco Borrelli
Professor Claire Tomlin

Spring 2019

Distributed Sliding Mode Control for Nonlinear Consensus

Abstract

Distributed Sliding Mode Control for Nonlinear Consensus

by

Yujia Wu

Doctor of Philosophy in Mechanical Engineering

University of California, Berkeley

Professor Kameshwar Poolla, Chair

This dissertation is concerned with the distributed control of nonlinear multi-agent consensus problems. The main objective of the consensus study is to design distributed algorithms that rely on only local interaction to achieve global group behavior. We propose a distributed sliding mode control (DSMC) framework for nonlinear heterogeneous multi-agent systems under different information exchange topologies. The DSMC constructs the topological sliding surface and reaching law via a so-called "topological structured function". The control law obtained by matching the topological sliding surface and topological reaching law is naturally distributed. Under this framework, topological diversity is explicitly incorporated. Also, the consensus problem is significantly simplified by mapping N interconnected higher-order dynamics into an N-th order sliding variable. The DSMC framework supports both leaderless consensus and consensus with a leader. For both cases, we show asymptotic stability when the topology contains a spanning tree, and further prove finite-time convergence under the undirected topologies. We also extend the DSMC framework to MIMO systems.

To demonstrate the usage and show the effectiveness of DSMC, we discuss two major applications with simulation results. The first application is for heterogeneous platoon systems. The control objective is to regulate vehicles to travel at a common speed while maintaining desired inter-vehicle gaps. The information flow topology dictates the pattern of communication between vehicles in the platoon. The second application is for flocking of nonholonomic unicycle agents.

to family and friends.

Contents

List of Figures

List of Tables

Acknowledgments

First, I would like to thank my advisor Kameshwar Poolla. Professor Poolla took me under his wing at my most difficult time. He inspires and enlightens me with his genius. He shows me how to be a warm, accessible, and caring person by being a role-model. My best time at Berkeley is when I wrote papers with him in his small messy office.

I also wish to thank my advisor Karl Hedrick, he introduced me to nonlinear control theory. His advice and words of wisdom always came at the right time. His encouragement and support towards my work have been invaluable.

During my years at Berkeley, I worked with many amazing professors. I would like to express gratitude to Francesco Borrelli, he has been supporting the whole VDL since Prof. Hedrick passed away. I thank Andy Packard, not only because he helped me during his generous office hours, also because he treats all students as family. His work ethics is contagious. I thank Masayoshi Tomizuka for giving me the opportunity to come to Berkeley, this opportunity has changed my life. I would like to thank Murat Arcak and Claire Tomlin for their stimulating and throught-provocking discussions on nonlinear control theory.

I would like to express my gratitude to my co-authors. Particular thanks go to Shengbo Li for devoting countless hours in our collaboration. I thank Jorge Cortes for helpful discussions and insights on discontinuous dynamical systems and consensus thory.

I would like to mention my Berkeley colleagues. Special thanks goes to Minghui Zheng, Andy Hasen, Donghan Lee, Chang Liu, Grace Liao, Eric Choi, Selina Pan, Chan-Kyu Lee, and Shih-Yuan Liu. I would like to thank my friends, there are numerous enlightening moments and good memories during our working lunches, coffee breaks, Saturday dinners and badminton games. Special thanks go to Sheng Liu, Wei Qi, Arun Hedge, Ke Te, He Long, Tao Hong, and Shuxin Xu.

Finally, I would like to thank my family back in Yichun. To my parents Hanzhen and Yongping for their loving care and unconditional support. They are always my safety net.

My last thought goes to my wife Vivian. I could not accomplish this without your support.

Chapter 1

Introduction

The coordination problem of multi-agent systems has received tremendous attention from the automation community in the past decade due to the broad applications in many areas including control of vehicular platoons [77, 84], coordination of unmanned air vehicles [16], flocking [57], distributed sensor networks [11], and congestion control in communication networks [49]. One critical issue arising from multi-agent systems is to develop the distributed control law based on local information that enables all agents to reach an agreement on certain quantities of interest, which is known as the consensus problem [40].

1.1 Consensus Problem

Consensus problems have a long history in computer science as the foundation of distributed computing [46]. The consensus problem was later applied to statistics [12] in 1960s. The ideas of statistical consensus theory reappeared two decades later in aggregation of information with uncertainty obtained from multiple sensors and medical experts [73].

Distributed computation and consensus over a network has a tradition in systems and control theory starting with the pioneering work in distributed estimation [6], decentralized decision making [69], rendezvous problems [43], asynchronous asymptotic agreement problems [70].

Since [48] introduced the distributed coordination of networked dynamical systems, we witnessed dramatic advances of various distributed algorithms that achieve agreements. In [48], a general framework for consensus for networked single-integrators with balanced graph topologies is established. The authors addressed the *leaderless consensus* (cooperative regulation) problem with a linear consensus protocol

based on disagreement functions, and discovered the connection between the algebraic connectivity and performance. Later, [54] extended this result to consensus with second-order agents under directed topologies. This work showed that containing a spanning tree is a necessary condition with the proposed protocol. [28, 27] introduced the *leader-following consensus* (cooperative tracking) protocol with a distributed observer under bidirectional topologies. The state of the leader keeps changing and is partially measured. It was proved that the agents can follow the leader if the input of the leader is known. Leader-following consensus is also studied under directed topologies, proving asymptotic tracking is guaranteed with the condition of a static leader and the existence of a spanning tree [55]. All the aforementioned works limited the agent model to first or second order integrators. [40] address the consensus problem with general linear node dynamics by introducing a distributed observer-type consensus protocol (with an essence from the complex networks synchronization problem). This method converts the consensus problem of multi-agent system into a stability analysis of a set of matrices with the same low dimension (as a single agent).

Following this, consensus problem has been studied from different angles. [2] showed that for multi-agent systems with bidirectional topologies, the closed-loop system exhibits a special interconnection structure inherited from the passivity properties of its components. A passivity-based design framework was proposed for additional design flexibility. For multi-agent systems with external disturbances and model uncertainties, [44] developed $\mathcal{H}_\infty$ consensus control based on a reduced-order system. For finite-time convergence, [10] considers a discontinuous control law for bidirectional topologies. A distributed observer is brought up [65] for consensus problems with general linear dynamics and an active leader. Consensus of general linear agents with intermittent interactions is studied in [56, 74]. Distributed model predictive control is introduced in [83] for consensus problems under bidirectional topologies. There are other advances in topics such as nonholonomic agents, formation transition and scaling, actuator saturation, and event-based consensus, etc. There is no way to cover the literature exhaustively in this dissertation, interested readers can consult recent surveys [52, 47].

Sliding mode control, with its robustness and easy-to-design nature, is widely applied in platoon systems, which is often viewed as a subcategory of multi-agent systems. The main shortcoming of existing research on SMC for multi-agent consensus is that it is dedicated to specific fixed topologies. [66, 67] conducted the research under a fixed leader-predecessor following topology. Here, each following agent has access to the state information to its predecessor as well as the leader. Based on this framework, [45] explored the effects of network communication delays on the stability, and [36] applied the fuzzy-sliding mode control to address nonlinear

paper	type	agent	topology	controller
[48]	leaderless	single-integrator	balanced graph	linear
[54]	leaderless	double-integrator	spanning tree	linear
[28]	active-leader	double-integrator	bidirectional	linear
[55]	static-leader	single-integrator	spanning tree	linear
[41]	active-leader	LTI	spanning tree	linear
[10]	leaderless	single-integrator	bidirectional	discontinuous
[2]	leaderless	single-integrator	bidirectional	passive
[44]	leaderless	single-integrator	spanning tree	$\mathcal{H}_\infty$
[65]	active-leader	LTI	bidirectional	output-feedback
[74]	leaderless	LTI	spanning tree	intermittent
[83]	leaderless	LTI	bidirectional	MPC
	all	*nonlinear*	*all*	*sliding mode*

Table 1.1: Listing of some literature

node dynamics. [35] extended coupled sliding mode control to a specific bidirectional topology. Similar structures were used in [23] to integrate tracking errors into the sliding surface design to overcome bounded disturbances.

In this dissertation, we present a distributed sliding mode control (DSMC) framework for nonlinear heterogeneous node dynamics, and all types of leaders and communication topologies mentioned above.

1.2 Application of Consensus: Platoon Systems

The platooning of connected and automated vehicles is attracting increasing attention due to its potential in increasing traffic throughput and infrastructure utilization, enhancing driving safety, and reducing fuel consumption. The objective of the platoon control system is to regulate vehicles to travel at a common speed while maintaining desired inter-vehicle gaps [29, 84].

Platooning was first proposed in the well-known PATH project [61], where linear control strategies were designed and implemented based on linearized vehicle models. Importantly, this work focused on a fixed communication topology of information exchange between vehicles. Following this, diverse aspects of platoon control have been explored, including control architecture, platoon modeling, spacing policy, controller synthesis, and performance requirements. Some representative examples of research include selection of spacing policies [68], string stability [66], scalability [85], direct

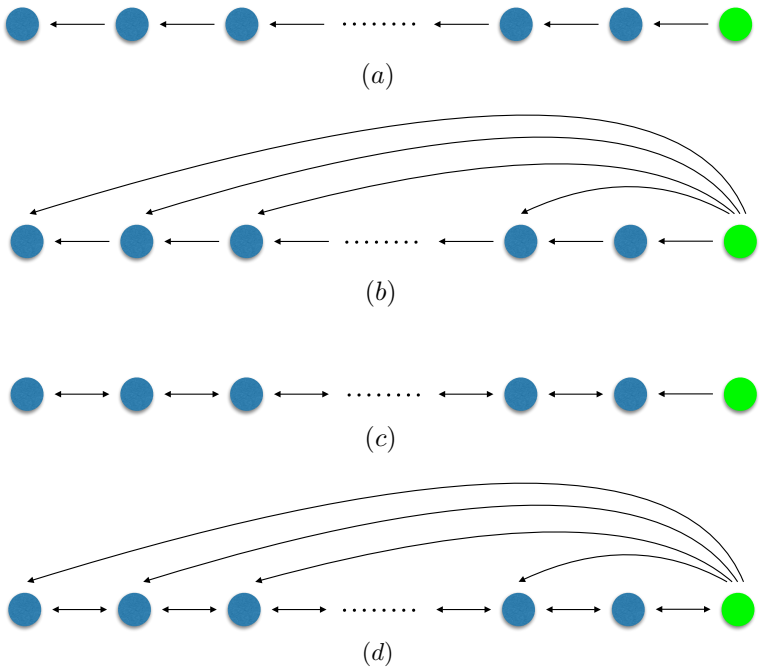

Figure 1.1: Common topologies: (a) predecessor following topology, (b) leader-predecessor following topology, (c) bidirectional topology, (d) leader-bidirectional topology.

consideration of powertrain dynamics [79], dynamic homogeneity and heterogeneity [60]. A recent review on platoon control can be found in [37].

The information exchange topology plays a key role in the design of platoon control systems [37]. Much of the early research on platoon control focused on radar-based sensing systems, where information topologies were limited to predecessor following topology [25], [17]. The topology is shown in Figure 1.1 (a), where directed links denote information exchange. With the rapid adoption of vehicle-to-vehicle (V2V) communications [75], a variety of new information topologies can be supported, which offer the promise of high performance and robust platoon control. These include leader-predecessor following topology [66], bidirectional topology [35] and leader-bidirectional topologies (see Figure 1.1).

Under this diversity of possible information topologies, new control challenges emerge, in particular when systematically considering nonlinear vehicle dynamics, communication delay and topology switching. As a result, *it is advantageous to view the vehicle platoon as a multi-agent system, and to employ a networked control perspective to design distributed controllers* [85]. This has led to new advanced control

methods for platoon control.

Here we survey several distributed design methods specifically for platooning systems.

- Linear consensus control.

  Linear control is one of the most commonly used methods for platoon control [68, 60], since it can not only facilitate theoretical analysis but is also suitable for hardware implementations. Many existing results on stability region, stability margin, and string stability requirements are based on linear controllers [60, 22, 63].

- Distributed robust control.

  The robustness of platoon control systems is an important topic. One practical way to handle model mismatches in vehicle dynamics is to use the consistent and accurate input-out behavior of node dynamics [39]. But it is not easy to accommodate the heterogeneity in node dynamics.

  Considering the requirements of string stability, robustness, and tracking performance [19] proposed an $\mathcal{H}_\infty$ control method for a heterogeneous platoon with uncertain dynamics and uniform time delays. In this study, all nodes were combined as a big system. One disadvantage is that the designed controller only works for a specific platoon and it needs to be redesigned when the scale or interaction topology changes. Similar to the case of linear control, the decoupling strategy of robust control is also an effective way to overcome this problem.

- Distributed MPC.

  MPC is an optimization-based control technique to anticipate future behavior of plants and take control actions accordingly. Using MPC techniques, the control input is obtained by numerically optimizing a finite horizon optimal control problem where both nonlinearity and constraints can be explicitly handled. This technique has been embraced by many industrial applications, for instance, collision avoidance and vehicle stability [72, 13].

  Currently, most MPCs are implemented in a centralized way. The distributed MPC is proposed by [83], where each vehicle is assigned a local optimal control problem only relying on its neighboring vehicles information. This method is suitable for an unidirectional topologies.

Sliding mode control (SMC) is a promising method to handle nonlinear dynamics, actuator constraints, and information topology diversity. The pioneering work of

SMC research on platoon control was conducted by Swaroop and Hedrick (1996) under a fixed leader-predecessor following topology. Here, each following vehicle can access the position, velocity and acceleration information of both the lead vehicle and the preceding vehicle [66]. This work was the first to introduce and analyze the key notion of string stability of interconnected nonlinear systems. Under this information topology, Liu *et al.* (2001) explore the effects of network communication delays on the stability of the sliding-mode-controlled platoon system [45]. This research studies the effects of preceding-vehicle information delay and lead-vehicle information delay on string stability. Lee and Kim (2002) used fuzzy-sliding mode control for platoons with leader-predecessor following topology to address nonlinear vehicle dynamics and time-varying parametric uncertainty [36]. The fuzzy SMC controller generate throttle and brake commands without requiring high-fidelity vehicle models. For the predecessor-following topology, Ferrara (2009) designed a sliding mode controller for each vehicle in a platoon to track its preceding vehicle under a constant time-headway spacing policy [17]. Kwon and Chwa (2014) extended coupled sliding mode control to bidirectional topology where the preceding vehicle information is used in the sliding surface design [35]. Similar controller structures were used in [23] to integrate tracking errors into the sliding surface design, and to overcome bounded disturbances under different kinds of spacing policies.

The main shortcoming of existing research on SMC for vehicle platoons is that they are dedicated to *fixed* information topologies: leader-predecessor following topology in [66], [67], [45], and [36]; predecessor following topology in [25] and [17]; bidirectional topology in [35] and [23]. However, in a practical context, information topologies can vary as platoons are formed, or can change as topologies switch. Chapter 7 focuses on sliding mode control design for vehicle platoons that is agnostic to the dynamic nature of the information topology.

1.3 Statement of Contributions

We present a distributed sliding mode control (DSMC) design framework for nonlinear heterogeneous multi-agent systems. We propose a new "topologically structured function" that is used to construct the topological sliding surface and reaching law. This design results naturally in a distributed control architecture. The distributed control law is obtained by properly matching the topological sliding surface and topological reaching law. The consensus problem is significantly simplified by casting N interconnected higher-order dynamics into N-th order sliding variable. The stability and convergence property are proved in the sense of Filippov to cope with the discontinuity originated from switching terms.

The advantage of our method is it explicitly supports both consensus problems with/without leader. It also incorporates all possible information topologies ranging from undirected topology to directed topologies with spanning tree, and gives stability justifications for each one of them. Also, it fits all nonlinear feedback-linearizable systems.

1.4 Outline of Dissertation

A brief outline of content of the various chapters is as follows:

Chapter 2: Here we review the necessary mathematical tools. The discontinuous dynamical systems and the Filippov method are introduced.

Chapter 3: In this chapter, we present graph theory, the modeling of information topologies, and some algebraic results for graphs.

Chapter 4: This chapter presents the problem formulation, definition of the topological structured function, and DSMC design for consensus 1. without a leader, 2. with a static leader, 3. with an active leader. The design process includes the introduction of topological structured sliding surface and reaching law. We will show how to match the sliding surface and reaching law to arrive at a distributed control formula.

Chapter 5: Here we presents the stability analysis results. This chapter includes the discussions on Lyapunov stability, finite-convergence, input-to-state stability, robustness, and the relation between graph and performance.

Chapter 6: This chapter contains the application of DSMC to a platooning system. In addition, we have a discussion on propogation of disturbance and topology.

Chapter 7: In this chapter, we present the MIMO DSMC design. We also show an application of using DSMC to study the sparsity-promoting optimal control framework.

Chapter 8: This chapter presents some conclusions, a summary and some directions for future research.

Chapter 2

Discontinuous Dynamical Systems

Discontinuous dynamical systems appear in many real-world applications. There are applications in minimum-time trajectory generation, thermostats on-off controllers, robot manipulation, etc. In sliding mode control, discontinuities are also intentionally designed to achieve regulation and stabilization.

Usually, we describe nonlinear time-invariant systems as:

$$\dot{x}(t) = f(x(t)), \quad x(t_0) = x_0, \tag{2.1}$$

where $x \in \mathbb{R}^n$, n is a positive integer, $f : \mathbb{R}^n \to \mathbb{R}^n$. If $x(t)$ is a solution for (2.1), $x(t)$ has to be continuously differentiable (due to the right-hand side). If $x(t)$ satisfies $\dot{x}(t) = f(x(t))$ and $x(t_0) = x_0$, and $x(t)$ is continuously differentiable, then it is called a classical solution. Usual Lyapunov analysis relies on the existence and uniqueness of the classical solution [32]. One common sufficient condition for the classical condition to exist and being unique is f being Lipschitz continuous [32].

If f is not continuous, then the classical solution $x(t)$ might not exist. Consider the example [9]:

$$f(x) = \begin{cases} -1 & x > 0 \\ 1 & x \leq 0 \end{cases}$$

does not have a classical solution from zero. Suppose that there exists a continuously differentiable function $x : [0, T] \to \mathbb{R}$ such that $\dot{x}(t) = f(x(t))$ and $x(0) = 0$. Then $\dot{x}(0) = 1$, and $\dot{x}(t) = -1$ for any $t > 0$, which shows $x(t)$ is not continuous at $t = 0$.

One sufficient condition on the existence of the classical solution is $x \mapsto f(x)$ being continuous. One common sufficient condition on the uniqueness of the classical solution is $x \mapsto f(x)$ being locally Lipschitz, which can be relaxed to one-sided Lipschitz.

However, for sliding mode control, f is not continuous, under this case, classical solution-based Lyapunov analysis could not be applied. Fortunately, for discontin-

uous dynamical systems, there are several other solutions, such as Caratheodory, Filippov, Krasovskii, Sample-and-Hold, etc.

A Caratheodory solution for (2.1) is a absolutely continuous function $x : [0, T] \to \mathbb{R}^n$ that satisfies (2.1) except for a μ-null set. A Filippov solution for (2.1) is a absolutely continuous function satisfies the differential inclusion

$$\dot{x}(t) \in \mathcal{F}(x(t)),$$

where $\mathcal{F} : \mathbb{R}^n \to \mathfrak{B}(\mathbb{R}^n)$ is the Filippov set-valued map generated from f, which will be introduced in the next subsection.

Based on the properties of different systems, we should employ different solutions. Caratheodory solutions are employed for time-depend vector fields that depend discontinuously on time, such as dynamical systems involving impulses and discontinuous inputs. Filippov solutions are for systems with switches and sliding. Krasovskii solution is similar to Filippov solution, and it applies to discontinuous systems with delay.

It is hard for us to survey many of solutions in this dissertation due to the space limit, readers could consult: Caratheodory and Filippov [9], [18], Krasovskii [34], Sample-and-Hold [33], Hermes [26], [3], Ambrosio [1], and Yahubovich-Leonov-Gelig [31].

By the nature of our system, we choose the Filippov solution, and carry out our Lyapunov analysis under this framework. In the following part of this section, we introduce mathematical preliminaries and Filippov solution. This framework extends Lyapunov theorems to dynamical systems (2.1) with measurable and locally essential bounded f.

2.1 Preliminaries

Notation

For a set M, its closure is written $\overline{M}$. The smallest convex set containing M (i.e., its convex hull) is denoted by co$M$. Equivalently, co$M$ is the set of all convex combination of points drawn from M. The set of positive real numbers is denoted as $\mathbb{R}^+$. For a function f, define $f(M)$ to be the image of M under f. For the affine function $f(x) = Ax + b$, where $A \in \mathbb{R}^{m\times n}$, we write $f(M) = AM + b$. If M is closed and bounded (i.e., compact), co$(AM + b) = A$co$M + b$.

For a symmetric matrix A, the maximum and minimum eigenvalues are denoted by $\lambda_{\max}(A)$ and $\lambda_{\min}(A)$, respectively. If A is positive definite, the square root of the

matrix is denoted by $A^{\frac{1}{2}}$, which is also symmetric and positive definite. For a vector $x = [x_1, x_2, \cdots, x_n]^\top \in \mathbb{R}^n$, define $\text{sgn}(x)$ as

$$\text{sgn}(x) = [\text{sgn}(x_1), \text{sgn}(x_2), \cdots, \text{sgn}(x_n)]^\top,$$

where

$$\text{sgn}(x_i) = \begin{cases} -1, & x_i < 0, \\ 0, & x_i = 0, \\ 1, & x_i > 0. \end{cases} \quad \text{for } i \in \{1, \cdots, n\}.$$

Measure theory

Our later analysis relies on the measure theory and the Lebesgue measure. In this section, we will give a quick review on measure theory to help us understand basic concepts.

Definition 1. *Let X be a non-empty set, $\mathcal{M}$ is said to be an algebra on X if it satisfies*

1. *contains empty set and X: $\emptyset \in \mathcal{M}$ and $X \in \mathcal{M}$.*
2. *closed under complement: if $E \in \mathcal{M}$ then $X \setminus E \in \mathcal{M}$.*
3. *closed under finite intersection and union: if $E_1, \cdots, E_n \in \mathcal{M}$, then $\bigcup_i^n E_i \in \mathcal{M}$ and $\bigcap_i^n E_i \in \mathcal{M}$.*

The algebra is a σ-algebra if the intersection and union can be countable infinite many.

Let $\mathcal{A}$ denotes σ-algebra, $(X, \mathcal{A})$ is called a measurable space. The sets in $\mathcal{A}$ are called measurable sets.

Definition 2. *For topological space X, let $\mathcal{G}$ be the collection of open sets. $\sigma(\mathcal{G})$ is the smallest σ-algebra containing open sets. $\mathcal{B} := \sigma(\mathcal{G})$ is called Borel σ-algebra. The elements of $\mathcal{B}$ are called Borel sets.*

Denote the Borel σ-algebra in $\mathbb{R}$ as $\mathcal{B}_\mathbb{R}$, it will play an important role in the construction of set-valued map. $\mathcal{B}_\mathbb{R}$ can be generated by each of the following

1. the open intervals,
2. the closed intervals,
3. half open intervals: $E = \{(a, b] : a < b\}$ or $E = \{[a, b) : a < b\}$,

4. the open rays: $E = \{(a, \infty) : a \in \mathbb{R}\}$ or $E = \{(-\infty, a) : a \in \mathbb{R}\}$,
5. the closed rays: $E = \{[a, \infty) : a \in \mathbb{R}\}$ or $E = \{(-\infty, a] : a \in \mathbb{R}\}$.

The Borel σ-algebra in $\mathbb{R}^n$ is the product Borel σ-algebra generated by sets:

$$\{\pi_i^{-1}(E_i) : E_i \in \mathcal{M}_i, i \in \{1, \cdots, n\}\},$$

where $\pi_i : \mathbb{R}^n \to \mathbb{R}$ are the coordinate maps, $\mathcal{M}_i$ is the Borel σ-algebra on the i-th coordinate.

Definition 3. *A measure $\mu : \mathcal{A} \to [0, \infty]$ is defined on measurable space $(X, \mathcal{A})$, satisfying:*

1. *$\mu(\emptyset) = 0$,*
2. *countable additive: if $\{E_i\}$ is a collection of disjoint sets in $\mathcal{M}$, then $\mu(\bigcup_{i=1}^{\infty} E_i) = \sum_{i=1}^{\infty} E_i$*

By μ-null set, we mean a measurable set with zero measure.
By the definition of measure, some properties follow:

1. $A \subseteq B \in \mathcal{A} \Rightarrow \mu(A) \leq \mu(B)$,
2. countable sub-additivity for $A = \bigcup_i^{\infty} A_i$, $\mu(A) \leq \sum_{i=1}^{\infty} \mu(A_i)$
3. continuity from above, $A_i \uparrow A$, then $\mu(A) = \lim_{n\to\infty} \mu(A_n)$
4. continuity from below, $A_i \downarrow A$ with $\mu(A_1) < \infty$, $\mu(A) = \lim_{n\to\infty} \mu(A_n)$.

Definition 4. *Outer measure μ^* is defined on all subsets of X.*

1. *$\mu^*(\emptyset) = 0$*
2. *$\mu^*(A) \leq \mu^*(B)$ if $A \subset B$.*
3. *$\mu^*(\bigcup_i^{\infty} A_i) \leq \sum_i^{\infty} \mu^*(A_i)$ countable sub-additivity.*

Definition 5. *μ^*-measurable of a set A is $\mu^*(E) = \mu^*(E \cap A) + \mu^*(E \cap A^c)$.*

This guarantees the inner measure is equal to the outer measure.

Theorem 1. *Caratheodory's theorem: If μ^* is an outer measure on X, the collection $\mathcal{M}$ of μ^*-measureable sets is an σ-algebra, and the restriction of μ^* to $\mathcal{M}$ is a complete measure.*

Definition 6. *A mapping $f : (X, \mathcal{A}_X) \to (Y, \mathcal{A}_Y)$ is said to be measurable iff $f^{-1}(E) \in \mathcal{A}_X$ for all $E \in \mathcal{A}_Y$.*

Remark 1. *The functions we discuss in this dissertation are all measurable. Almost all functions we see on mechanical systems are measurable. To my knowledge, the constructions of a non-measurable set and non-measurable require the invocation of the axiom of choice or Zorn's lemma. One famous example of non-measurable set is called the Vitali set.*

To construct Lebesgue measure on the real line, we also need the concept, called premeasure. Compared to the outer measure, which is defined on all subsets on X, the premeasure is defined on an algebra on X.

Definition 7. *Let $\mathcal{A} \in \mathfrak{B}(X)$ be an algebra, a function $\mu_0 : \mathcal{A} \to [0, \infty]$ is a premeasure if it satisfies:*

1. $\mu(\emptyset) = 0$,
2. *countablely additive: let $\{A_j\}_1^\infty$ be a collection of disjoint sets in the algebra $\mathcal{A}$, then $\mu_0(\bigcup_{i=1}^\infty A_j) = \sum_{i=1}^\infty \mu_0(A_j)$.*

One way to construct outer measure from premeasure is:

$$\mu^*(E) = \inf\{\sum_1^\infty \mu_0(A_j) : A_j \in \mathcal{A}, E \in \bigcup_{i=1}^\infty A_j\} \tag{2.2}$$

Theorem 2. *Let $\mathcal{A} \subseteq \mathfrak{B}(X)$ be an algebra, μ_0 be a premeasure on $\mathcal{A}$, and $\mathcal{M}$ is the σ-algbra generated by $\mathcal{A}$. Then the outer measure generated by (2.2) restricted on $\mathcal{M}$ is a complete measure.*

On the real line, the Borel algebra can be generated with half-open intervals. We construct the premeasure, if $(a_j, b_j]$ are disjoint half-open intervals, let

$$\mu_0(\bigcup_1^n (a_j, b_j]) = \sum_1^n (b_j - a_j), \tag{2.3}$$

and let $\mu(\emptyset) = 0$. The measure induced by the premeausre (2.3) is called Lebesgue measure.

2.2 Discontinuous systems

Sliding mode control is used to stabilize a platoon by intentionally introducing discontinuities in the feedback loop [71]. The closed-loop dynamics with discontinuity do not satisfy the traditional Lipschitz conditions that assure the existence and the uniqueness of continuous differentiable solutions. Solutions of discontinuous ordinary differential equations can be analyzed using Filippov methods [18]. Our exposition here follows [9].

Consider the vector-valued ordinary differential equation

$$\dot{x}(t) = f(x(t)). \tag{2.4}$$

Here, $x(t) \in \mathbb{R}^n$, $f : \mathbb{R}^n \to \mathbb{R}^n$, and f is discontinuous.

The framework of Filippov solution for discontinuous f is formulated around the concept of set-valued maps $\mathcal{F} : \mathbb{R}^n \to \mathfrak{B}(\mathbb{R}^n)$, where $\mathfrak{B}(\mathbb{R}^n)$ is the power set of $\mathbb{R}^n$. The idea is to associate a set-valued map to f by looking at the neighboring values of f at each point. Specifically, for $x \in \mathbb{R}^n$, the vector field of f is evaluated at the points belonging to $B(x, \delta)$ (open ball). We examine the effect of $\delta > 0$ approaching 0. For additional flexibility, we can exclude a μ-null set when doing this evaluation.

The Filippov set-valued map $\mathcal{F}[f] : \mathbb{R}^n \to \mathfrak{B}(\mathbb{R}^n)$ associated with f is defined as

$$\mathcal{F}[f](x) \triangleq \bigcap_{\delta>0} \bigcap_{\mu(H)=0} \overline{\text{co}}\{f(B(x,\, \delta) \setminus H)\},\ x \in \mathbb{R}^n, \tag{2.5}$$

where $B(x,\, \delta)$ is a open ball of radius $\delta > 0$ centered at x, and the intersection is taken over all sets H with zero Lebesgue measure.

Example 1. *Computation of of Filippov set-valued map when f is piecewise continuous. Let $f : \mathbb{R}^n \to \mathbb{R}^n$ be a piecewise continuous mapping. Let there exist finite of disjoint open sets $\{D_i\}_1^m$, where $D_i \subseteq \mathbb{R}^n$ and $\mathbb{R}^n = \bigcup_1^n \bar{D}_i$, and f is continuous on each D_i. Denote S as the set of unions of all boundaries of D_i, note that S is the set where f is discontinuous, and $\mu(S) = 0$.*

- *For $x \in D_i$,*
$$\mathcal{F}[f](x) = \{f(x)\}$$
- *For $x \in S$,*
$$\mathcal{F}[f](x) = \overline{\text{co}}\{\lim_{i\to\infty} f(x_i) : x_i \to x, x_i \notin S\}$$

Definition 8. *An absolutely continuous function $x(t) : [0, T] \to \mathbb{R}^n$ is said to be a solution of (2.4) in the sense of Filippov if for almost all $t \in [0, T]$,*

$$\dot{x}(t) \in \mathcal{F}[f](x(t)). \tag{2.6}$$

The point x_e is an equilibrium of the differential inclusion (2.6) if $0 \in \mathcal{F}[f](x_e)$.

Lemma 1. *[9] (*Existence of Filippov solution*) Let $f : \mathbb{R}^n \to \mathbb{R}^n$ be measurable and locally essentially bounded, i.e., bounded on a bounded neighborhood of every point, excluding sets of measure zero. Then for all $x_0 \in \mathbb{R}^n$, there exists a Filippov solution of (2.4) with initial condition $x(0) = x_0$.*

The existence of solution is implicitly required for stability in the sense of Lyapunov and asymptotic stability [32], while the solutions for a discontinuous system are not necessarily unique.

Example 2. *Consider the system $\dot{x}(t) = \operatorname{sgn}(x(t))$, for initial condition $x(0) = 0$, there are three solutions $x_1(t) = -t$, $x_2 = t$, $x_3 = 0$.*

Remark 2. *The traditional sliding mode control does not need the Filippov solution treatment [32], [62]. The reason for this is that under usual sliding mode control, with the 1 dimensional sliding variable, and specific set-up of the reaching law, the solution exists and is unique. This does not holds in our case, in the distributed sliding mode control, the reaching law is multi-dimensional. We will introduce this in the subsequent sections.*

Filippov solutions for discontinuous system are not necessarily unique for each initial condition. Therefore, when considering properties such as stability in the sense of Lyapunov, asymptotic stability and invariance, we must specify whether attention is being paid to a particular solution starting from an initial condition ("weak") or to all the solutions starting from an initial condition ("strong"). For example, "weakly stable equilibrium point" means that at least one solution starting close to the equilibrium point remains close to it, whereas "strongly stable equilibrium point" means that all solutions starting close to the equilibrium point remain close to it. Detailed definitions can be found in [18, 9].

To compute the Lie derivative of a set-valued map, we need to introduce the generalized gradient [8]. Let $V : \mathbb{R}^n \to \mathbb{R}$ be a locally Lipschitz function, and let $S_V \subseteq \mathbb{R}^n$ denote the set of points where f fails to be differentiable.

Definition 9. *The generalized gradient $\partial V : \mathbb{R}^n \to \mathfrak{B}(\mathbb{R}^n)$ is defined by*

$$\partial V \triangleq \operatorname{co}\{\lim_{i \to \infty} \nabla V(x_i) : x_i \to x, x_i \notin K \cup S_V\}, \tag{2.7}$$

where K is a μ-null set arbitrarily chosen to simplify the computation.

The Lie derivative of a set-valued map is defined as follows. Given a locally Lipschitz function $V : \mathbb{R}^n \to \mathbb{R}$ and a set-valued map $\mathcal{F} : \mathbb{R}^n \to \mathfrak{B}(\mathbb{R}^n)$, the set-valued Lie derivative $\mathscr{L}_{\mathcal{F}} V : \mathbb{R}^n \to \mathfrak{B}(\mathbb{R}^n)$ of V with respect to $\mathcal{F}$ at x is defined as

$$\begin{aligned}\mathscr{L}_{\mathcal{F}} V(x) \triangleq \{a \in \mathbb{R} :\ &\text{there exists } v \in \mathcal{F}(x), \text{ such that} \\ &\xi^\top v = a \text{ for all } \xi \in \partial V(x)\},\end{aligned}$$

where $\partial V(x)$ denotes the generalized gradient [8]. If the function $V(x)$ is continuously differentiable, the generalized Lie derivative takes the following form:

$$\mathscr{L}_{\mathcal{F}} V(x) \triangleq \left\{\nabla V(x)^\top v : v \in \mathcal{F}(x)\right\}.$$

Lemma 2. *Let $x : [0, t_1] \to \mathbb{R}^n$ be a solution of the differentiable inclusion (2.6), and let $V : \mathbb{R}^n \to \mathbb{R}$ be locally Lipschitz and regular. Then,*

i. The composition $t \mapsto V(x(t))$ is differentiable at almost all $t \in [0, t_1]$.

ii. The derivative of $t \mapsto V(x(t))$ satisfies

$$\frac{d}{dt}(V(x(t))) \in \mathscr{L}_{\mathcal{F}} V(x(t)) \quad \text{for a.e. } t \in [0,\, t_1].$$

Lemma 3. *[9] (*Discontinuous Lyapunov theorem*) Let $f : \mathbb{R}^n \to \mathbb{R}^n$ satisfy the hypotheses of Lemma 1, and $\mathcal{F}[f] : \mathbb{R}^n \to \mathfrak{B}(\mathbb{R}^n)$ be the set-valued map corresponding to f. Let x_e be an equilibrium of the differential inclusion (2.6), and let $\mathcal{D} \subset \mathbb{R}^n$ be an open and connected set with $x_e \in \mathcal{D}$. Furthermore, let $V : \mathbb{R}^n \to \mathbb{R}$ be such that the following holds:*

i. V is locally Lipschitz and regular on $\mathcal{D}$.

ii. $V(x_e) = 0$, and $V(x) > 0$ for $x \in \mathcal{D} \setminus \{x_e\}$.

iii. $\max \mathscr{L}_{\mathcal{F}} V(x) \leq 0$ for each $x \in \mathcal{D}$. Then, x_e is a strongly stable equilibrium of (2.6). In addition, if (iii) above is replaced by

iv. $\max \mathscr{L}_{\mathcal{F}} V(x) < 0$ for each $x \in \mathcal{D} \setminus \{x_e\}$.
Then, x_e is a strongly asymptotic stable equilibrium of (2.6).

Note that a continuously differentiable function is automatically locally Lipschitz and regular, and hence one can invoke Lemma 3 for such functions.

Lemma 4. *[9] (*Discontinuous version of Lasalle's invariance principle*) Let* $f : \mathbb{R}^n \to \mathbb{R}^n$ *satisfy the hypotheses of Lemma 1, and let* $\mathcal{F}[f] : \mathbb{R}^n \to \mathfrak{B}(\mathbb{R}^n)$ *be the set-valued map corresponding to* f*. Let* $\Omega \subset \mathbb{R}^n$ *be compact and strongly invariant for (2.6), and assume* $\max \mathscr{L}_{\mathcal{F}} V(x) \leq 0$ *for each* $x \in \Omega$*. Then, all solutions* $x : [0, \infty) \to \mathbb{R}^n$ *of (2.6) starting at* Ω *converge to the largest weakly invariant set* M *contained in*

$$\Omega \cap \mathcal{Z}_{\mathcal{F},V},$$

where $\mathcal{Z}_{\mathcal{F},V} = \overline{\{x \in \mathbb{R}^n : 0 \in \mathscr{L}_{\mathcal{F}} V(x)\}}$.

Chapter 3

Graph Theory

In the multi-agent consensus problem, one of the most important properties is the information topology. The information flow topology dictates the pattern of communication between agents in the system. This information is essential to effective control, and therefore plays a central role in affecting the design and performance of control strategies.

The information topology is described by graph. We will introduce graph theory in this section.

3.1 Introduction to Graph

A *graph* $\mathcal{G} = (\mathcal{V}, \mathcal{E})$ is a tuple consisting of a finite set $\mathcal{V}$ of vertices and a finite set $\mathcal{E}$ of edges where each edge is an unordered pair of vertices. The two vertices associated with an edge e are called the *end-vertices* of e. The *edge* between two vertices v_1 and v_2 is denoted by $e = (v_1, v_2)$. We also denote the set of vertices of a graph by $\mathcal{V}(\mathcal{G})$ and the set of edges of $\mathcal{G}$ by $\mathcal{E}(\mathcal{G})$. A vertex of a graph is also called a node. The number of vertices is denoted with $|\mathcal{V}|$, and number of edges is denoted with $|\mathcal{E}|$.

We call a graph a *directed graph* or *digraph* if each edge is associated with a direction. The elements of $\mathcal{E}$ are called *directed edge* or *arc*. For a directed graph $\mathcal{G} = (\mathcal{V}, \mathcal{E})$, $e = (u, v) \in \mathcal{E}$, this means there is a directed edge from u to v. u is the *tail* of e, and v is the *head* of v. We say the edge e is leaving u and terminating at v. A node is a *source (sink)* if there is no edge terminating at (leaving) the node.

The *degree* of a vertex v in a graph $\mathcal{G}$ is denoted by $\deg(v)$, is defined as the number of edges incident to v.

Lemma 5. *Let $\mathcal{G} = (\mathcal{V}, \mathcal{E})$ be a graph, $\sum_{v \in \mathcal{V}} deg(v) = 2|\mathcal{E}|$.*

The concept of the degree of vertex of graphs also extends to digraphs. The *indgree* of a vertex v of a digraph is the number of directed edges terminating at v, and the *outdegree* of v is the number of directed edges leaving v.

Lemma 6. *Let $\mathcal{G} = (\mathcal{V}, \mathcal{E})$ be a directed graph, then $\sum_{v\in\mathcal{V}} indeg = \sum_{v\in\mathcal{V}} outdeg = |\mathcal{E}|$.*

let $\mathcal{G} = (\mathcal{V}, \mathcal{E})$ be a directed graph, the undirected graph $\mathcal{G}' = (\mathcal{V}, \mathcal{E}')$ is called the *underlying graph* of $\mathcal{G}$ if $\mathcal{G}'$ is constructed from $\mathcal{G}$ such that $(u, v) \in \mathcal{E}'$ if and only if $(u, v) \in \mathcal{E}$. A sequence of successive edges $\{(i, k), (k, l), \cdots, (m, j)\}$ is a *directed path* from node i to node j. A directed graph $\mathcal{G}$ is *weakly connected* if its underlying graph is connected. A vertex u is said to be reachable from a vertex v, if there is a directed path from v to u. A digraph is *strongly connected* if every pair of vertices is reachable from each other.

A *tree* is an undirected graph in which any two vertices are connected by exactly one path. An example is shown in fig. 3.1. Photo credit: `https://en.wikipedia.org/wiki/Tree_(graph_theory)`

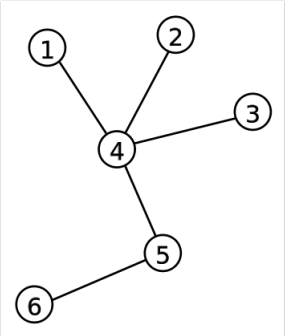

Figure 3.1: Example: tree

A directed graph $\mathcal{G}$ contains a spanning tree if there exists a node v, such that all other nodes can be reached via a directed path. v is also called the root of the spanning tree.

A subgraph of a graph $\mathcal{G}$ is a graph $\mathcal{G}' = (\mathcal{V}', \mathcal{E}')$ such that $\mathcal{V}' \subseteq \mathcal{V}$ and $\mathcal{E}' \subset \mathcal{E}$. A graph with an empty edge set is called a null graph. A graph in which each pair of distinct vertices are adjacent is called complete graph.

Let $\mathcal{G}_1 = (\mathcal{V}_1, \mathcal{E}_1)$ and $\mathcal{G}_2 = (\mathcal{V}_2, \mathcal{E}_2)$ be two graphs. The union of $\mathcal{G}_1$ and $\mathcal{G}_2$ denoted by $\mathcal{G}_1 \cup \mathcal{G}_2$ is defined as $\mathcal{G}_3 = (\mathcal{V}_1 \cup \mathcal{V}_2, \mathcal{V}_1 \cup \mathcal{E}_2)$. Similarly, the intersection of $\mathcal{G}_1$ and $\mathcal{G}_2$ denoted by $\mathcal{G}_1 \cap \mathcal{G}_2$ is defined as $\mathcal{G}_4 = (\mathcal{V}_1 \cap \mathcal{V}_2, \mathcal{V}_1 \cap \mathcal{E}_2)$.

Let $\mathcal{G}$ be a graph with the vertex set $\mathcal{V} = \{v_1, v_2, \cdots, v_n\}$, and the edge set $\mathcal{E} = \{e_1, e_2, \cdots, e_m\}$. The adjacency matrix of $\mathcal{G}$ is an $n \times n$ matrix $\mathcal{A} = [a_{ij}]$ defined as

$$\begin{cases} a_{ij} = 1, & \text{If } (j,\, i) \in \mathcal{E}, \\ a_{ij} = 0, & \text{Otherwise.} \end{cases}$$

A directed graph $\mathcal{G}$ is called balanced if $\sum_{i \neq j} a_{ij} = \sum_{j \neq i} a_{ji}$ for all $i \in \mathcal{V}$. An example from [48] of balanced graphs is shown in 3.2.

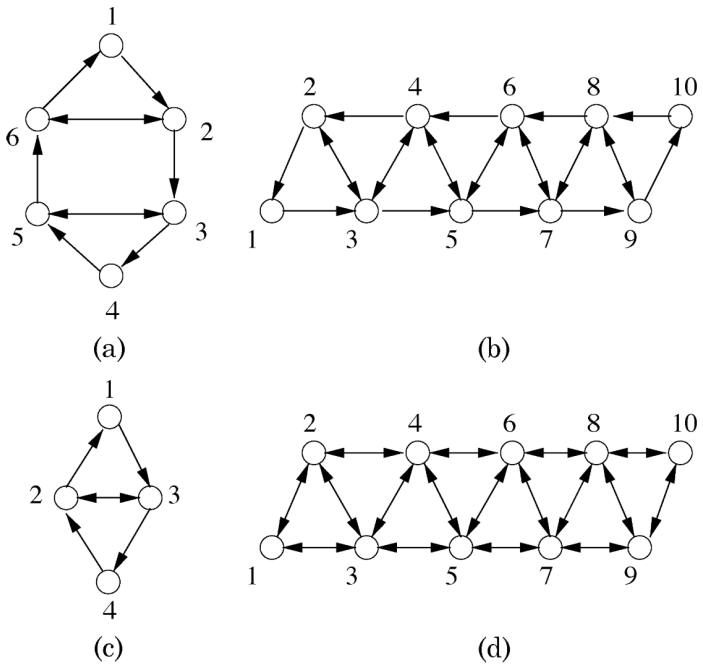

Figure 3.2: Example: balanced graphs [48]

The Laplacian matrix $\mathcal{L} = [l_{ij}] \in \mathbb{R}^{N \times N}$ is defined as:

$$l_{ij} = \begin{cases} -a_{ij}, & \text{if } i \neq j, \\ \sum\limits_{k=1,\, k \neq i}^{N} a_{ik}, & \text{if } i = j, \end{cases} \qquad \forall i,\, j \in \mathcal{V}.$$

For an undirect graph, the adjacency matrix and the Laplacian matrix are symmetric. This does not hold for the direct graph.

We also define incidence matrix $\mathbf{E} = [e_{ij}] \in \mathbb{R}^{|\mathcal{E}| \times |\mathcal{V}|}$ as:

$$e_{ij} = \begin{cases} \sqrt{a_{ij}}, & (i,j) \in \mathcal{E} \text{ and } i < j, \\ -\sqrt{a_{ij}}, & (i,j) \in \mathcal{E} \text{ and } i > j, \\ 0, & \text{otherwise.} \end{cases} \tag{3.1}$$

We can easily check that $\mathbf{E}^\intercal\mathbf{E} = \mathcal{L}$.

3.2 Graph for Consensus Problem

The communication topology of the networked system is described by a directed graph (digraph) $\mathcal{G}$ with two subgraphs $\mathcal{G}_{\text{agent}}$ and $\mathcal{G}_{\text{leader}}$.

The subgraph $\mathcal{G}_{\text{agent}} = (\mathcal{V}, \mathcal{E})$ describes the communication topology among the agents with the node set $\mathcal{V} = \{1, \ldots, N\}$ and the edge set $\mathcal{E} \subseteq \mathcal{V} \times \mathcal{V}$. An edge of $\mathcal{G}_{\text{agent}}$ leaving node i and terminating at node j is denoted by $e_{ij} = (i, j)$. We say node i is the *tail* and node j is the *head* of e_{ij}. The connectivity of $\mathcal{G}_{\text{agent}}$ is represented by adjacency matrix $\mathcal{A}$ and Laplacian matrix $\mathcal{L}$.

The subgraph $\mathcal{G}_{\text{leader}}$ describes the communication topology between the virtual leader and the agents. Assume the virtual leader is a source, we use the pinning matrix $\mathcal{P}$ to denote the edges leaving the leader and terminating at nodes in $\mathcal{V}$:

$$\mathcal{P} = \text{diag}(p_1, p_2, \ldots, p_N),$$

where $p_i \in \{0, 1\}$. If there is an edge from leader to node i, $p_i = 1$; otherwise, $p_i = 0$.

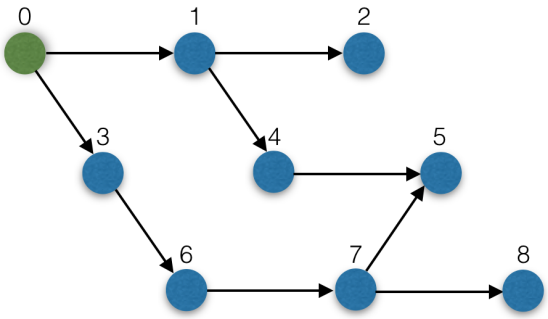

Figure 3.3: Example: directed topology

Example 3. *Pinning matrix and Laplacian matrix of Figure. 3.3*

$$\mathcal{P} = \text{diag}([1, 0, 1, 0, 0, 0, 0, 0])$$

$$\mathcal{L} = \begin{bmatrix} 0 & 0 & 0 & 0 & 0 & 0 & 0 & 0 \\ -1 & 1 & 0 & 0 & 0 & 0 & 0 & 0 \\ 0 & 0 & 0 & 0 & 0 & 0 & 0 & 0 \\ -1 & 0 & 0 & 1 & 0 & 0 & 0 & 0 \\ 0 & 0 & 0 & -1 & 1 & 0 & -1 & 0 \\ 0 & 0 & -1 & 0 & 0 & 1 & 0 & 0 \\ 0 & 0 & 0 & 0 & 0 & -1 & 1 & 0 \\ 0 & 0 & 0 & 0 & 0 & 0 & -1 & 1 \end{bmatrix}$$

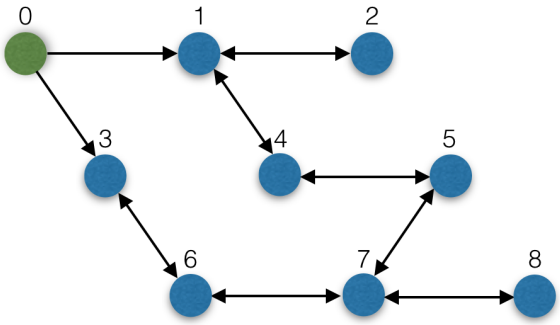

Figure 3.4: Example: undirected topology

Example 4. *Pinning matrix and Laplacian matrix of Figure. 3.4*

$$\mathcal{P} = \text{diag}([1, 0, 1, 0, 0, 0, 0, 0])$$

$$\mathcal{L} = \begin{bmatrix} 2 & -1 & 0 & -1 & 0 & 0 & 0 & 0 \\ -1 & 1 & 0 & 0 & 0 & 0 & 0 & 0 \\ 0 & 0 & 1 & 0 & 0 & -1 & 0 & 0 \\ -1 & 0 & 0 & 2 & -1 & 0 & 0 & 0 \\ 0 & 0 & 0 & -1 & 2 & 0 & -1 & 0 \\ 0 & 0 & -1 & 0 & 0 & 2 & -1 & 0 \\ 0 & 0 & 0 & 0 & -1 & -1 & 3 & -1 \\ 0 & 0 & 0 & 0 & 0 & 0 & -1 & 1 \end{bmatrix}$$

3.3 Algebraic Results

In this section, we present some of the algebraic results related to graph theory. The exposition and results follow [82, 48, 77, 38, 78] with minor modifications.

Theorem 3. *[48] Let $\mathcal{G} = (\mathcal{V}, \mathcal{E})$ be a weighted directed graph with Laplacian $\mathcal{L}$. If $\mathcal{G}$ is strongly connected, then rank$(\mathcal{L}) = |\mathcal{V}| - 1$.*

Corollary 1. *Let $\mathcal{G} = (\mathcal{V}, \mathcal{E})$ be undirected graph with Laplacian $\mathcal{L}$. If $\mathcal{G}$ is connected, then rank$(\mathcal{L}) = |\mathcal{V}| - 1$.*

Theorem 4. *[48] (Balanced graph) Let $\mathcal{G} = (\mathcal{V}, \mathcal{E})$ be a directed graph with adjacency matrix $\mathcal{A}$. Then, all the following statements are equivalent.*

- *$\mathcal{G}$ is balanced.*
- *$\eta = \mathbf{1}$ is the left eigenvector of the Laplacian $\mathcal{L}$ of $\mathcal{G}$ associated with the zero eigenvalue. i.e. $\mathbf{1}^\top \mathcal{L} = \mathbf{0}$.*
- *$\sum_{i=1}^{n} u_i = 0$, $\forall x \in \mathbb{R}^{|\mathcal{V}|}$ with $u_i = \sum_{j \neq i} a_{ij}(x_j - x_i)$.*

Theorem 5. *[53] Suppose that directed graph $\mathcal{G} = (\mathcal{V}, \mathcal{E})$ is strongly connected. Let $\mathbf{x} = [x_1, x_2, \cdots, x_N]^\top$ be a left eigenvector for the Laplacian associated with the eigenvalue 0. Define*

$$\begin{aligned} \Lambda =& \operatorname{diag}\{x_1, x_2, \cdots, x_{|\mathcal{V}|}\}, \\ Q =& \Lambda\mathcal{L} + \mathcal{L}^\top \Lambda. \end{aligned}$$

Then $P \succ 0$ and $Q \succeq 0$.

More specifically, let's apply the upper theorems to real topologies.

Theorem 6. *[78] Consider a network of agents with topology $\mathcal{G} = \mathcal{G}_{leader} \cup \mathcal{G}_{agent}$. Assume $\mathcal{G}_{agent}$ is undirected and connected, and there exists at least one edge from the leader to one of the followers. Then $\mathcal{L} + \mathcal{P} \succ 0$.*

Proof. When $\mathcal{G}_{\text{agent}}$ is undirected and connected, $\mathcal{L}$ is positive semi-definite, and the algebraic multiplicity of the zero eigenvalue is one. The eigenvector corresponding to zero eigenvalue is $\mathbf{1} \triangleq [1, 1, \ldots, 1]^\top \in \mathbb{R}^N$ [21]. Define eigenvalues of $\mathcal{L}$ to be $\lambda_1 = 0 < \lambda_2 \leq \ldots \leq \lambda_N$, and the corresponding eigenvectors are $\eta_1, \eta_2, \ldots, \eta_N$, where $\eta_1 = \mathbf{1}$. Since $\mathcal{L}$ is symmetric, it can be diagonalized by a orthogonal matrix composed of N linearly independent eigenvectors, so any vector $x \in \mathbb{R}^N$ can be written as a linear combination of the eigenvectors, $x = \sum_{i=1}^{N} c_i \eta_i$, where c_i, $i \in \mathcal{N}$ are constants. Since G contains a spanning tree, $\mathcal{P} \neq 0$, and $\eta_1^\top \mathcal{P} \eta_1 > 0$. For any $x \neq 0$, there is

$$x^\top (\mathcal{L} + \mathcal{P}) x = \sum_{i=2}^{N} \lambda_i c_i^2 \eta_i^\top \eta_i + x^\top \mathcal{P} x > 0.$$

□

The following theorems are about spanning trees.

Theorem 7. *[82] Consider a network of agents with topology $\mathcal{G} = \mathcal{G}_{leader} \cup \mathcal{G}_{agents}$. Assume there is a spanning tree rooted from the leader. Then, $\mathcal{L} + \mathcal{P}$ is nonsingular and eigenvalues have positive real part, i.e., $Re[\lambda(\mathcal{L} + \mathcal{P})] > 0$.*

Theorem 8. *[82] Consider a network of agents with topology $\mathcal{G} = \mathcal{G}_{leader} \cup \mathcal{G}_{agents}$. Assume there is a spanning tree rooted from the leader. Define*

$$\begin{aligned}
\mathbf{a} =& [a_1, \cdots, a_N]^\top = (\mathcal{L} + \mathcal{P})^{-1}\mathbf{1}, \\
\mathbf{b} =& [b_1, \cdots, b_N]^\top = (\mathcal{L} + \mathcal{P})^{-\top}\mathbf{1}, \\
\mathcal{D} =& \operatorname{diag}\left(\frac{b_1}{a_1}, \frac{b_2}{a_2}, \cdots, \frac{b_N}{a_N}\right), \qquad (3.2) \\
\mathcal{Q} =& \mathcal{D}(\mathcal{L} + \mathcal{P}) + (\mathcal{L} + \mathcal{P})^\top \mathcal{D}. \qquad (3.3)
\end{aligned}$$

Then, $\mathcal{D} \succ 0$ and $\mathcal{Q} \succ 0$.

Corollary 2. *[41] Consider a network of agents with topology $\mathcal{G} = \mathcal{G}_{leader} \cup \mathcal{G}_{agents}$. Assume there is a spanning tree rooted from the leader. Let*

$$\begin{aligned}
[\lambda_1, \lambda_2, \cdots, \lambda_N] &= (\mathcal{L} + \mathcal{P})^{-\top}\mathbf{1}, \\
\Lambda &= \operatorname{diag}\{\lambda_1, \lambda_2, \cdots, \lambda_N\}, \\
\mathcal{Q} &= \Lambda(\mathcal{L} + \mathcal{P}) + (\mathcal{L} + \mathcal{P})^\top \lambda.
\end{aligned}$$

Then $\Lambda \succ 0$ and $\mathcal{Q} \succ 0$.

The following theorems are about strongly connected graphs.

Theorem 9. *[82] Consider a network of agents with topology $\mathcal{G} = \mathcal{G}_{leader} \cup \mathcal{G}_{agents}$. Assume there is a spanning tree rooted from the leader, and $\mathcal{G}$ is strongly connected. Denote $\lambda = \max_{i \le N}(l_{ii} + p_i)$ and $\mathcal{B} = \lambda I_N - (\mathcal{L} + \mathcal{P})$. Let $x > 0$ and $y > 0$ be the first right and left eigenvectors of $\mathcal{L} + \mathcal{P}$ with respect to the eigenvalue $\lambda - \rho(\mathcal{B})$, where $\rho(\mathcal{B})$ denotes the largest absolute value of its eigenvalues.*

Define

$$\begin{aligned}
\mathcal{D} =& \operatorname{diag}\left\{\frac{y_1}{x_1}, \cdots, \frac{y_N}{x_N}\right\}, \\
\mathcal{Q} =& \mathcal{D}(\mathcal{L} + \mathcal{P}) + (\mathcal{L} + \mathcal{P})^\top \mathcal{D}.
\end{aligned}$$

Then $\mathcal{D} \succ 0$ and $\mathcal{Q} \succ 0$.

Corollary 3. *[82] Consider a network of agents with topology $\mathcal{G} = \mathcal{G}_{leader} \cup \mathcal{G}_{agents}$. Assume there is a spanning tree rooted from the leader, and $\mathcal{G}$ is strongly connected. Denote $\lambda = \max_{i\leq N}(l_{ii}+p_i)$ and $\mathcal{B} = \lambda I_N - (\mathcal{L}+\mathcal{P})$. Let $x > 0$ and $y > 0$ be the first right and left eigenvectors of $\mathcal{L}+\mathcal{P}$ with respect to the eigenvalue $\lambda - \rho(\mathcal{B})$, where $\rho(\mathcal{B})$ denotes the largest absolute value of its eigenvalues.*

Define

$$\begin{aligned}\mathcal{D} =& \operatorname{diag}\left\{\frac{y_1}{x_1}, \cdots, \frac{y_N}{x_N}\right\},\\ \mathcal{Q} =& \mathcal{D}(\mathcal{L}+\mathcal{P})^\top + (\mathcal{L}+\mathcal{P})\mathcal{D}.\end{aligned}$$

Then $\mathcal{D} \succ 0$ and $\mathcal{Q} \succ 0$.

The following theorem is the discontinuous version of the former theorems, we will use this in the discontinuous analysis.

Theorem 10. *Consider a network of agents with topology $\mathcal{G} = \mathcal{G}_{leader} \cup \mathcal{G}_{agents}$. Assume there is a spanning tree rooted from the leader. Let $\mathcal{D}$ be as defined in* (3.2)*. For $x \in \mathbb{R}^N$, define set $\mathcal{W}$ as*

$$\begin{aligned}\mathcal{W} = co\{\bar{x} = [\bar{x}_1, \cdots, \bar{x}_N]^\top : \bar{x}_i = \operatorname{sgn}(x_i),\ if x_i \neq 0;\\ \bar{x}_i = \{-1,\ 1\},\ if x_i = 0\}.\end{aligned} \tag{3.4}$$

Then $x^\top \mathcal{D}(\mathcal{L}+\mathcal{P})w \geq 0$ for all $x \in \mathbb{R}^N$ and $w \in \mathcal{W}$.

Proof. From (3.4), we have

$$x_i w_i = \begin{cases} 0, & \text{if } x_i = 0,\\ x_i \operatorname{sgn}(x_i), & \text{if } x_i \neq 0,\end{cases}$$

where w_i is the i-th element of w. Hence, we have

$$x^\top \mathcal{D}(\mathcal{L}+\mathcal{P})w = \sum_{i=1}^{N} d_i p_i |x_i| + x^\top \mathcal{D}\mathcal{L}w, \tag{3.5}$$

where d_i and p_i is the i-th diagonal term of $\mathcal{D}$ and $\mathcal{P}$. With Lemma 8, there is $\mathcal{D} \succ 0$, we have $d_i p_i |x_i| \geq 0$.

Define $\mathcal{H} = [h_{ij}] \in \mathbb{R}^{N\times N}$ as

$$h_{ij} = \begin{cases} l_{ii}, & \text{if } i = i,\\ w_i l_{ij} w_j, & \text{if } i \neq j\end{cases}$$

where l_{ij} is the $(i,j)^{\text{th}}$ term of $\mathcal{L}$. One can easily check

$$x^\top \mathcal{D}\mathcal{L}w = |x|^\top \mathcal{D}\mathcal{H}\mathbf{1}. \tag{3.6}$$

Also, we have $h_{ii} = l_{ii}$ for all $i \in \mathcal{V}$, and $h_{ij} \geq l_{ij}$ for $i, j \in \mathcal{V}$ and $i \neq j$ ($l_{ij} \in \{0, 1\}$ and w_i, $w_j \in [0, 1]$). We can conclude $\mathcal{H} \geq \mathcal{L}$.

Since $\mathcal{L}\mathbf{1} = \mathbf{0}$ and $\mathcal{H} - \mathcal{L} \geq 0$, we have

$$\begin{aligned} x^\top \mathcal{D}\mathcal{L}w =& |x|^\top \mathcal{D}\mathcal{H}\mathbf{1} - |x|^\top \mathcal{D}\mathcal{L}\mathbf{1} \\ =& |x|^\top \mathcal{D}(\mathcal{H} - \mathcal{L})\mathbf{1} \geq 0. \end{aligned} \tag{3.7}$$

Thus, we have $x^\top \mathcal{D}(\mathcal{L} + \mathcal{P})w = \sum_{i=1}^{N} d_i p_i |x_i| + x^\top \mathcal{D}\mathcal{L}w \geq 0$ for all $w \in \mathcal{W}$.

□

3.4 Graph and Stability

From the results Theorem 5 to Corollary 3, we see the equation

$$\mathcal{Q} = \mathcal{D}(\mathcal{L} + \mathcal{P})^\top + (\mathcal{L} + \mathcal{P})\mathcal{D}, \tag{3.8}$$

several times.

Recall the Lyapunov equation of linear systems. Consider a continuous-time linear-invariant system:

$$\dot{x}(t) = Ax(t),$$

where $x \in \mathbb{R}^n$, $A \in \mathbb{R}^{n \times n}$.

Select the specific positive definite equation $V(x) = x^\top Px$ with $P \succ 0$, $P \in \mathbb{R}^{n \times n}$, if we have

$$\frac{\mathrm{d}}{\mathrm{d}t} V(x) = x^\top A^\top Px + x^\top PAx = x^\top (A^\top P + PA)x,$$

with

$$Q := A^\top P + PA. \tag{3.9}$$

Stability conditions are:

- If $Q \succeq 0$, then the system is stable in the sense of Lyapunov.
- If $Q \succ 0$, the system is asymptotically stable.
- If $Q \succeq 0$, and $(A, Q^{\frac{1}{2}})$ is observable, then the system is asymptotically stable.
- if $Q \succeq 0$, then all trajectories of $x(t)$ from all initial conditions are bounded.

Chapter 4

Design of Distributed Sliding Mode Control

In this section, we will formulate the consensus problem and then design the distributed sliding mode control.

4.1 Problem Formulation

Nonlinear node dynamics

Consider a network of single-input-single-output nonlinear heterogeneous agents with n-th order dynamics,

$$\begin{aligned} \dot{x}_{i,1} =& x_{i,2}, \\ \dot{x}_{i,2} =& x_{i,3}, \\ & \vdots \\ \dot{x}_{i,n} =& f_i(\mathbf{x}_i) + g_i(\mathbf{x}_i)u_i, \\ y_i =& x_{i,1} \end{aligned} \tag{4.1}$$

where $\mathbf{x}_i = [x_{i,1}, x_{i,2}, \cdots, x_{i,n}]^\top \in \mathbb{R}^n$ is the state vector, $u_i \in \mathbb{R}$ and $y_i \in \mathbb{R}$ are the input and output of i-th node, respectively. The smooth functionals $f_i : D \to \mathbb{R}$ and $g_i : D \to \mathbb{R}$ are defined on domain of interest $D \subset \mathbb{R}^n$, and $g_i(\mathbf{x}_i) \neq 0$ for all $\mathbf{x}_i \in D$.

Remark 3. *For any nonlinear feedback (input-output) linearizable system, there exists a diffeomorphism which transforms the system to* (4.1).

Leader and leaderless

Based on the existence of a leader, the consensus problems can be categorized into *consensus with a leader* and *leaderless consensus*.

For the consensus with a leader, we assume there is a leader with output y_0. The information of the leader is only available to the subset of the agents which are linked to the leader. For those agents, the corresponding elements of the pinning matrix $p_i = 1$. The objective of the control design is to achieve:

$$y_i(t) \to y_0, \text{ as } t \to +\infty, \ \forall\, i \in \mathcal{V}.$$

For the leaderless consensus, we assume there is no leader. In this case, we treat the graph $\mathcal{G}_{\text{leader}}$ as a null-graph, and the corrosponding pinning matrix $\mathcal{P}$ to be a zero matrix. The objective of the control design is to achieve:

$$\|y_i(t) - y_j(t)\| \to 0, \text{ as } t \to +\infty, \ \forall\, i, j \in \mathcal{V}.$$

Assumptions on information exchange topology

From Chapter 3, we know that different assumptions lead to various stability results. Here for consensus with a leader and leaderless consensus, we list 4 different Assumptions.

- Consensus with a leader

  Assumption 1. *Consider a network of agents with topology $\mathcal{G} = \mathcal{G}_{leader} \cup \mathcal{G}_{agents}$. Assume the graph $\mathcal{G}$ contains a spanning tree rooted from the leader.*

  Assumption 2. *Consider a network of agents with topology $\mathcal{G} = \mathcal{G}_{leader} \cup \mathcal{G}_{agents}$. Assume the graph $\mathcal{G}$ contains a spanning tree rooted from the leader. Also $\mathcal{G}_{agents}$ is bidirectional (undirected).*

- Leaderless consensus

  Assumption 3. *Consider a network of agents with topology $\mathcal{G} = \mathcal{G}_{agents}$. Assume the graph $\mathcal{G}$ contains a spanning tree.*

  Assumption 4. *Consider a network of agents with topology $\mathcal{G} = \mathcal{G}_{agents}$. Assume the graph $\mathcal{G}$ is bidirectional (undirected) and connected.*

4.2 Consensus with a Static Leader

In this section, we mainly consider a consensus problem with a static virtual reference $y_0 \in \mathbb{R}$. Note that y_0 is only available to a subset of the agents. The objective of control design is to achieve:

$$y_i(t) \to y_0, \text{ as } t \to +\infty, \ \forall\, i \in \mathcal{V}.$$

The Distributed SMC is composed of two parts: (a) topological sliding surface, and (b) topological reaching law. The two parts share a common designing structure defined by a newly-proposed topologically structured function.

Topologically structured function

Definition 10. *(Topologically structured function) For a set of vectors $\{\mathbf{z}_i\}_1^N$, $\mathbf{z}_i \in \mathbb{R}^n$, the topologically structured function for the i-th node is defined as*

$$t_i^{TS}(Z) = \sum_{j=1, j\neq i}^{N} a_{ij}(\mathbf{z}_i - \mathbf{z}_j) + p_i \mathbf{z}_i, \tag{4.2}$$

where $Z = [\mathbf{z}_1^\top, \mathbf{z}_2^\top, \ldots, \mathbf{z}_N^\top]^\top \in \mathbb{R}^{nN}$, a_{ij} is the $(i, j)^{th}$ entry of $\mathcal{A}$, and p_i is the i-th diagonal entry of $\mathcal{P}$.

We define the topologically structured function for the entire multi-agent system as

$$T^{TS}(Z) = \begin{bmatrix} t_1^{TS}(Z) \\ t_2^{TS}(Z) \\ \vdots \\ t_N^{TS}(Z) \end{bmatrix} = ((\mathcal{L} + \mathcal{P}) \otimes I_n)\, Z, \tag{4.3}$$

where $\otimes$ denotes Kronecker product, and I_n is the n-th order identity matrix.

Remark 4. *Under Assumption 1 and Assumption 2, the topologically structured function for the entire multi-agent system* (4.3) *is an isomorphism.*

Design of topological sliding surface

The tracking error of node i is

$$e_i = y_i - y_0.$$

We define an intermediate error δ_i,

$$\delta_i \triangleq (\frac{\mathrm{d}}{\mathrm{d}t} + \rho)^{n-1} e_i, \tag{4.4}$$

where $\rho \in \mathbb{R}_+$ is a positive real tuning parameter. This parameter determines the converging rate of tracking error.

The intermediate error vector is

$$\Delta \triangleq [\delta_1, \delta_2, \ldots, \delta_N]^\top.$$

We define the individual sliding variable for the i-th node as

$$s_i \triangleq t_i^{TS}(\Delta).$$

The sliding variable array is

$$S \triangleq \begin{bmatrix} s_1 \\ s_2 \\ \vdots \\ s_N \end{bmatrix} = T^{TS}(\Delta) = (\mathcal{L} + \mathcal{P})\Delta. \tag{4.5}$$

The topological sliding surface for the entire multi-agent system is the manifold defined by $S = \mathbf{0}$.

Remark 5. *Under Assumption 1 and Assumption 2, T^{TS} is an isomorphism, $S = T^{TS}(\Delta) = \mathbf{0}$ if and only if $\Delta = \mathbf{0}$.*

Remark 6. *It is easily observed that each s_i only depends on local states as well as the states of neighboring agents constrained by $\mathcal{G}$, which means s_i is a distributed sliding variable. Note that $\delta_i - \delta_j$ does not depend on the virtual leader information, since*

$$\delta_i - \delta_j = \sum_{k=0}^{n-1} \binom{n-1}{k} \rho^k (x_{i,n-k} - x_{j,n-k}),$$

where $\binom{n-1}{i}$ denotes the binomial coefficient.

Design of topological reaching law

To design the DSMC, the reaching law has to conform with the associated sliding surface. The topological reaching law for node i is

$$\dot{s}_i \triangleq -\psi t_i^{ST}(S) - \phi t_i^{ST}(\mathrm{sgn}(S))$$

where ψ, $\phi \in \mathbb{R}_+$ are tuning parameters. We define $\mathrm{sgn}(S) \triangleq [\mathrm{sgn}(s_1), \cdots, \mathrm{sgn}(s_N)]^\top$, where

$$\mathrm{sgn}(s_i) = \begin{cases} -1, & s_i < 0, \\ 0, & s_i = 0, \\ 1, & s_i > 0. \end{cases}$$

Combining all nodes, we arrive at the compact form array

$$\dot{S} = -(\mathcal{L} + \mathcal{P})(\psi S + \phi\,\mathrm{sgn}(S)). \tag{4.6}$$

With (4.5) and (4.6), we observe that

$$(\mathcal{L} + \mathcal{P})\dot{\Delta} = -(\mathcal{L} + \mathcal{P})(\psi S + \phi\,\mathrm{sgn}(S)).$$

Since $\mathcal{L} + \mathcal{P}$ is nonsingular, we obtain

$$\dot{\Delta} = -(\psi S + \phi\,\mathrm{sgn}(S)). \tag{4.7}$$

Note that the invertibility of $\mathcal{L} + \mathcal{P}$ is critical in designing a distributed SMC suitable for a broad range of communication topologies. The i-th row of (4.7) is

$$\dot{\delta}_i = -\psi s_i - \phi\,\mathrm{sgn}(s_i). \tag{4.8}$$

Substituting (4.1) and (4.4) to (4.8), the distributed SMC control law is

$$u_i = -\frac{1}{g_i(\mathbf{x}_i)}(\psi s_i + \phi\,\mathrm{sgn}(s_i) + f_i(\mathbf{x}_i) + \gamma(\mathbf{x}_i)), \tag{4.9}$$

where

$$\gamma(\mathbf{x}_i) = \sum_{k=1}^{n-1} \binom{n-1}{k} \rho^k x_{i,n-k+1}. \tag{4.10}$$

Remark 7. *The control law* (4.9) *is distributed since* s_i *is distributed and* $f_i(\mathbf{x}_i)$, $g_i(\mathbf{x}_i)$, $\gamma(\mathbf{x}_i)$ *only depends on local states.*

4.3 Consensus with an Active Leader

Consider an active leader with dynamics as follows:

$$\begin{aligned} \dot{\mathbf{x}}_0 =& A_0\mathbf{x}_0, \\ y_0 =& C_0\mathbf{x}_0, \end{aligned} \tag{4.11}$$

where $\mathbf{x}_0 \in \mathbb{R}^q$, $y_0 \in \mathbb{R}$, $A_0 \in \mathbb{R}^{q\times q}$, and $C_0 \in \mathbb{R}^{1\times q}$. The objective of control design is to achieve:

$$y_i(t) \to y_0(t), \text{ as } t \to +\infty, \ \forall\, i \in \mathcal{V}.$$

The reference state $\mathbf{x}_0$ is available to node i if and only if $p_i = 1$.

We apply the same design principle (4.5) and (4.6). For theoretical simplicity, we eliminate the switching term by setting $\phi = 0$. The following control law is obtained:

$$u_i = -\frac{1}{g_i(\mathbf{x}_i)}(\psi s_i + f_i(\mathbf{x}_i) + \gamma(\mathbf{x}_i) - \zeta(\mathbf{x}_0)), \tag{4.12}$$

where $\zeta : \mathbb{R}^n \to \mathbb{R}$ is a linear functional defined as:

$$\zeta(\mathbf{x}_0) = \sum_{k=0}^{n-1} \binom{n-1}{k} \rho^k C_0 A_0^{n-k} \mathbf{x}_0. \tag{4.13}$$

Controller (4.12) is not distributed since $\mathbf{x}_0$ is not available to all agents in the network. To address this issue we follow [65] to construct a distributed observer to estimate $\mathbf{x}_0$,

$$\dot{\hat{\mathbf{x}}}_{0,i} = A_0\hat{\mathbf{x}}_{0,i} - k(\sum_{i=1}^{N} a_{ij}(\hat{\mathbf{x}}_{0,i} - \hat{\mathbf{x}}_{0,j}) + p_i(\hat{\mathbf{x}}_{0,i} - \mathbf{x}_0)), \tag{4.14}$$

where $\hat{\mathbf{x}}_{0,i}$ is the estimated $\mathbf{x}_0$ for the i-th agent, and $k \in \mathbb{R}_+$ is tuning parameter. We define the observing error as $\epsilon_i \triangleq \hat{\mathbf{x}}_{0,i} - \mathbf{x}_0$, and $E \triangleq [\epsilon_1^\top, \epsilon_2^\top, \cdots, \epsilon_N^\top]^\top$, (4.14) is reformed as:

$$\dot{\hat{\mathbf{x}}}_{0,i} = A_0\hat{\mathbf{x}}_{0,i} - kt_i^{TS}(E).$$

Replacing $\mathbf{x}_0$ in (4.12) with $\hat{\mathbf{x}}_{0,i}$, the control law becomes fully distributed:

$$u_i = -\frac{1}{g_i(\mathbf{x}_i)}(\psi s_i + f_i(\mathbf{x}_i) + \gamma(\mathbf{x}_i) - \zeta(\hat{\mathbf{x}}_{0,i})). \tag{4.15}$$

4.4 Leaderless Consensus

We mainly consider a consensus problem without a leader, which means $\mathcal{P} = 0$.

The objective of a leaderless consensus is to satisfy

$$\lim_{t\to\infty} \|y_i(t) - y_j(t)\| = 0,$$

for all $i, j \in \mathcal{N}$, then we say the consensus is achieved. Furthermore, if there exists $y^* \in \mathbb{R}$ such that

$$\lim_{t\to\infty} \|y_i(t) - y^*\| = 0,$$

for all $i \in \mathcal{N}$ then we call y^* is the consensus state of the multi-agent system.

For a leaderless consensus, the control law is simply to apply $\mathcal{P} = 0$ in the topologically structured function (4.3), then apply control law (4.9) and (4.10).

In this case, the topologically structured function becomes:

$$\begin{aligned} t_i^{TS}(Z) &= \sum_{j=1, j\neq i}^{N} a_{ij}(\mathbf{z}_i - \mathbf{z}_j) + 0\mathbf{z}_i, \\ &= \sum_{j=1, j\neq i}^{N} a_{ij}(\mathbf{z}_i - \mathbf{z}_j). \end{aligned} \tag{4.16}$$

The topologically structured function for the entire multi-agent system becomes

$$T^{TS}(Z) = \begin{bmatrix} t_1^{TS}(Z) \\ t_2^{TS}(Z) \\ \vdots \\ t_N^{TS}(Z) \end{bmatrix} = (\mathcal{L} \otimes I_n)\, Z. \tag{4.17}$$

Design of topological sliding surface

Directly define e_i as

$$e_i = y_i.$$

We define an intermediate error δ_i,

$$\delta_i \triangleq (\frac{\mathrm{d}}{\mathrm{d}t} + \rho)^{n-1} e_i, \tag{4.18}$$

where $\rho \in \mathbb{R}_+$ is a positive real tuning parameter. This parameter determines the converging rate of tracking error once the intermediate error equals zero.

The intermediate error vector is

$$\Delta \triangleq [\delta_1,\, \delta_2, \ldots, \delta_N]^\top.$$

We define the individual sliding variable for the i-th node as

$$s_i \triangleq t_i^{TS}(\Delta).$$

The sliding variable array is

$$S \triangleq \begin{bmatrix} s_1 \\ s_2 \\ \vdots \\ s_N \end{bmatrix} = T^{TS}(\Delta) = \mathcal{L}\Delta. \tag{4.19}$$

The topological sliding surface for the entire multi-agent system is the manifold defined by $S = \mathbf{0}$.

DSMC control law for leaderless consensus

For leaderless consensus, since $\mathcal{L} + \mathcal{P}$ is not invertible, we give the control law directly, we will deliver the stability analysis in a different fashion.

The DSMC control law:

$$u_i = -\frac{1}{g_i(\mathbf{x}_i)}(\psi s_i + \phi\,\mathrm{sgn}(s_i) + f_i(\mathbf{x}_i) + \gamma(\mathbf{x}_i)), \tag{4.20}$$

where

$$\gamma(\mathbf{x}_i) = \sum_{k=1}^{n-1} \binom{n-1}{k} \rho^k x_{i,n-k+1}. \tag{4.21}$$

ψ, $\phi \in \mathbb{R}_+$ are tuning parameters.

Remark 8. *The control law* (4.20) *is distributed since* s_i *is distributed and* $f_i(\mathbf{x}_i)$, $g_i(\mathbf{x}_i)$, $\gamma(\mathbf{x}_i)$ *only depends on local states.*

Chapter 5

Stability and Performance Analysis

5.1 Consensus with a Static Leader

The stability proof of DSMC is divided into two phases, i.e., reaching phase and sliding phase. The stability of reaching phase is analyzed by Lyapunov method in the sense of Filippov, while that of sliding phase follows the traditional SMC analysis.

Reaching Phase

Theorem 11. *Consider a network of agents with nonlinear heterogeneous node dynamics* (4.1) *and communication topology* $\mathcal{G}$ *under Assumption 3. With the distributed control law* (4.9)*, and tuning parameters* ψ, ϕ, $\rho \in \mathbb{R}_+$*, the sliding variable* S*, defined by* (4.5)*, converges to* $\mathbf{0}$ *asymptotically.*

Proof. With the control law (4.9), the dynamics of sliding variable is

$$\dot{S} = (\mathcal{L} + \mathcal{P})(-\psi S - \phi \operatorname{sgn}(S)). \tag{5.1}$$

Define $f_{sld} : \mathbb{R}^N \to \mathbb{R}^N$ as

$$f_{sld}(S) = (\mathcal{L} + \mathcal{P})(-\psi S - \phi \operatorname{sgn}(S)). \tag{5.2}$$

Although f_{sld} is not Lipschitz continuous, it is measurable and essentially locally bounded. Therefore, Lemma 1 is satisfied, the Filippov solution of (5.1) exists.

From (2.5), the Filippov set-valued map associated with (5.2) is

$$\mathcal{F}[f_{sld}](S) = -(\mathcal{L} + \mathcal{P})(\psi S + \phi \mathcal{W}),$$

where $\mathcal{W}$ is the set defined by

$$\begin{aligned}\mathcal{W} \triangleq \mathrm{co}\{\bar{S} = [\bar{s}_1, \cdots, \bar{s}_N]^\top : &\bar{s}_i = \mathrm{sgn}(s_i), \text{ if } s_i \neq 0; \\ &\bar{s}_i = \{-1, 1\}, \text{ if } s_i = 0\}.\end{aligned} \tag{5.3}$$

We choose a Lyapunov candidate for the networked system,

$$V_1(S) = S^\top \mathcal{D} S, \tag{5.4}$$

where $\mathcal{D} \succ 0$ is defined as in (3.2).

The set-valued Lie derivative of (5.4) is

$$\begin{aligned}\mathscr{L}_{\mathcal{F}[f_{sld}]} V_1(S) =& \{\nabla V_1(S)^\top v : v \in \mathcal{F}[f_{sld}](S)\} \\ =& -\psi S^\top \mathcal{Q} S - 2\phi S^\top \mathcal{D}(\mathcal{L} + \mathcal{P})\mathcal{W},\end{aligned} \tag{5.5}$$

where $\mathcal{Q} = \mathcal{D}(\mathcal{L} + \mathcal{P}) + (\mathcal{L} + \mathcal{P})^\top \mathcal{D}$. By Theorem 8, we have $\mathcal{Q} \succ 0$, thus the first term of (5.5) is negative for all $S \in \mathbb{R}^N \setminus \{\mathbf{0}\}$. By Theorem 10, all elements in the second term of (5.5) are non-positive.

Then, for all $S \in \mathbb{R}^N \setminus \{\mathbf{0}\}$, we have

$$\max \mathscr{L}_{\mathcal{F}[f_{sld}]} V_1(S) < 0. \tag{5.6}$$

By Lemma 3, we establish asymptotic stability of system (5.1). □

Next, we give a sufficient condition for finite-time convergence.

Corollary 4. *Consider a network of agents satisfying the hypotheses of Theorem 11. Let $\mathcal{G}_{agent}$ be undirected. Then, the sliding variable S converges to $\mathbf{0}$ in finite time.*

Proof. With Theorem 6, we have $\mathcal{L} + \mathcal{P} \succ 0$. Choose the Lyapunov candidate,

$$V_2(S) = \frac{1}{2} S^\top (\mathcal{L} + \mathcal{P})^{-1} S.$$

Taking the set-valued Lie derivative, we have

$$\begin{aligned}\mathscr{L}_{\mathcal{F}[f_{sld}]} V_2(S) =& \{-\psi \|S\|_2^2 - \phi S^\top \mathrm{sgn}(S)\} \\ =& \{-\psi \|S\|_2^2 - \phi \|S\|_1\}\end{aligned}$$

Since $\|S\|_1 \geq \|S\|_2$, we have

$$\max \mathscr{L}_{\mathcal{F}[f_{sld}]} V_2(S) \leq -\psi \|S\|_2^2 - \phi \|S\|_2 \tag{5.7}$$

Instead of proving the finite-time convergence of S directly, we prove that $\sqrt{2V_2} = \|(\mathcal{L}+\mathcal{P})^{-\frac{1}{2}}S\|_2$ converges to 0 in finite time. For $S \in \mathbb{R}^N \setminus \{\mathbf{0}\}$, the set-valued Lie derivative of $\sqrt{2V_2}$ is

$$\mathscr{L}_{\mathcal{F}[f_{sld}]}\sqrt{2V_2} = \frac{1}{\|(\mathcal{L}+\mathcal{P})^{-\frac{1}{2}}S\|_2}\mathscr{L}_{\mathcal{F}[f_{sld}]}V_2. \tag{5.8}$$

By Rayleigh's quotient, we have

$$\|(\mathcal{L}+\mathcal{P})^{-\frac{1}{2}}S\|_2 \leq \frac{1}{\sqrt{\lambda_{\min}(\mathcal{L}+\mathcal{P})}}\|S\|_2. \tag{5.9}$$

From (5.7), (5.8), and (5.9), one can establish

$$\max \mathscr{L}_{\mathcal{F}[f_{sld}]}\sqrt{2V_2} \leq -\sqrt{\lambda_{\min}(\mathcal{L}+\mathcal{P})}\phi.$$

From Lemma 2, we have

$$\frac{\mathrm{d}}{\mathrm{d}t}\|(\mathcal{L}+\mathcal{P})^{-\frac{1}{2}}S(t)\|_2 \in \mathscr{L}_{\mathcal{F}[f_{sld}]}\sqrt{2V_2} \tag{5.10}$$

for almost every $t \in [0, +\infty)$. We have

$$\begin{aligned}\|(\mathcal{L}+\mathcal{P})^{-\frac{1}{2}}S(t_f)\|_2 =& \|(\mathcal{L}+\mathcal{P})^{-\frac{1}{2}}S(0)\|_2 \\ &+ \int_0^{t_f}\frac{\mathrm{d}}{\mathrm{d}\tau}\|(\mathcal{L}+\mathcal{P})^{-\frac{1}{2}}S(\tau)\|_2\mathrm{d}\tau.\end{aligned} \tag{5.11}$$

With (5.10) and (5.11), in the region $\mathbb{R}^N \setminus \{\mathbf{0}\}$, we have

$$\begin{aligned}\|(\mathcal{L}+\mathcal{P})^{-\frac{1}{2}}S(t_f)\|_2 \leq& \|(\mathcal{L}+\mathcal{P})^{-\frac{1}{2}}S(0)\|_2 \\ &-t_f\phi\sqrt{\lambda_{\min}(\mathcal{L}+\mathcal{P})}.\end{aligned}$$

We argue that there must exist t_f such that $S(t_f) = \mathbf{0}$. Otherwise, $\|(\mathcal{L}+\mathcal{P})^{-\frac{1}{2}}S(t_f)\|_2 \to -\infty$ as $t_f \to +\infty$. □

Sliding Phase

Lemma 7. *Consider a linear time-invariant system $\dot{x} = Ax + Bu$, if A is Hurwitz, then $u(t) \to 0$ as $t \to +\infty$ implies $x(t) \to \mathbf{0}$ as $t \to +\infty$.*

Proof. Since A is Hurwitz, the system is input-to-state stable (ISS). Then, there exists class-$\mathcal{KL}$ function $\beta : [0, +\infty) \times [0, +\infty) \to [0, +\infty)$, and class-$\mathcal{K}$ function $\kappa : [0, +\infty) \to [0, +\infty)$, such that

$$\|x(t)\|_2 \leq \beta(\|x(0)\|_2, t) + \kappa(\sup_{\tau \in [0,t]} |u(\tau)|). \tag{5.12}$$

To prove $\|x(t)\|_2 \to 0$ as $t \to +\infty$, it is equivalent to show for any $\varepsilon \in \mathbb{R}_+$, there exist a $T \in \mathbb{R}_+$, s.t. $\|x(t)\|_2 \to \varepsilon$ for all $t \geq T$.

Since $u(t) \to 0$, there exists T_1, s.t. $\kappa(\sup_{\tau \geq T_1} |u(\tau)|) \leq \varepsilon/2$. Then, because β is class-$\mathcal{KL}$, there exist an T_2, s.t. $\beta(x(T_1), t - T_1) \leq \varepsilon/2$ for all $t \geq T_2$.

From (5.12), we have $\|x(t)\|_2 \leq \varepsilon$ for all $t \geq T_1 + T_2$. □

Theorem 12. *Consider a network of agents satisfying the hypotheses of Theorem 11. The tracking error $e_i(t)$ for each agent converges to 0 asymptotically.*

Proof. From Theorem 11, we know $S(t) \to \mathbf{0}$ as $t \to +\infty$. With (4.5), we have $\Delta(t) = (\mathcal{L} + \mathcal{P})^{-1} S(t) \to \mathbf{0}$ as $t \to +\infty$. System (4.4) is asymptotic stable, since $\rho > 0$. From Lemma 7, we have $e_i(t) \to 0$ as $t \to +\infty$. □

5.2 Consensus with an Active Leader

The stability result is presented as follows.

Theorem 13. *Consider a network of agents with nonlinear heterogeneous node dynamics* (4.1) *and communication topology $\mathcal{G}$ under Assumption 1. With the distributed control law* (4.15)*, and the distributed observer* (4.14) *with a sufficiently large positive k, both the sliding variable S in* (4.5) *and the observing error E converge to $\mathbf{0}$ asymptotically.*

Proof. First, we prove observing error E converges to $\mathbf{0}$ asymptotically. The observing error dynamics is

$$\dot{E} = (I_N \otimes A_0 - k(\mathcal{L} + \mathcal{P}) \otimes I_q)E. \tag{5.13}$$

From [65], the eigenvalues of $I_N \otimes A_0 - k(\mathcal{L} + \mathcal{P}) \otimes I_q$ are:

$$\{\lambda_i(A_0) - k\lambda_j(\mathcal{L} + \mathcal{P}) : i \in \{1, \cdots, q\};\ j \in \{1, \cdots, N\}\}$$

where $\lambda_i(A_0)$ and $\lambda_j(\mathcal{L} + \mathcal{P})$ are the eigenvalues of A_0 and $\mathcal{L} + \mathcal{P}$, respectively. With a sufficiently large k, we can ensure all the eigenvalues of $I_N \otimes A_0 - k(\mathcal{L} + \mathcal{P}) \otimes I_q$ in the left-half complex plane. Then, we conclude asymptotic stability of system (5.13).

Secondly, we prove the asymptotic convergence of the sliding variable. The dynamics of sliding variable is

$$\dot{S} = -\psi(\mathcal{L} + \mathcal{P})S + \overline{\zeta}(E),$$

where $\overline{\zeta} : \mathbb{R}^{qN} \to \mathbb{R}^N$ defined as

$$\overline{\zeta}(E) = T^{TS}(\begin{bmatrix} \zeta(\epsilon_1) \\ \vdots \\ \zeta(\epsilon_N) \end{bmatrix}) = (\mathcal{L} + \mathcal{P}) \begin{bmatrix} \zeta(\epsilon_1) \\ \vdots \\ \zeta(\epsilon_N) \end{bmatrix}. \tag{5.14}$$

From (4.13) and (5.14), we see $\overline{\zeta}$ is linear. Since $\overline{\zeta}(E) \to \mathbf{0}$ and $-\psi(\mathcal{L} + \mathcal{P})$ is Hurwitz, we conclude $S \to \mathbf{0}$ as $t \to +\infty$ by Lemma 7.

□

Theorem 14. *Consider a network of agents satisfies the hypotheses of Theorem 13. The tracking error $e_i(t)$ for each agent converges to 0 asymptotically.*

Proof. The proof is the same as in Theorem 12. □

5.3 Leaderless Consensus

Also, the stability proof of leaderless consensus is divided into two phases, i.e. reaching phase and sliding phase.

Theorem 15. *Consider a network of agents with nonlinear heterogeneous node dynamics* (4.1) *and communication topology $\mathcal{G}$ under Assumption 3. With the distributed control law* (4.20)*, and tuning parameters ψ, ϕ, $\rho \in \mathbb{R}_+$, the sliding variable S, defined by* (4.19)*, converges to a consensus equilibrium $S^* = c\mathbf{1}$ asymptotically, where $c \in \mathbb{R}$. This means $\lim_{t\to\infty} \|s_i(t) - s_j(t)\| = 0$.*

Proof. By (4.19), the sliding mode variable is

$$s_i = \sum_{i=1, i\neq j}^{N} a_{ij}(\delta_i - \delta_j). \tag{5.15}$$

Taking derivative of (5.15) we get

$$\dot{s}_i = \sum_{i=1, i\neq j}^{N} a_{ij}(\dot{\delta}_i - \dot{\delta}_j) \tag{5.16}$$

With equation (4.18), there is

$$\begin{aligned}\dot{\delta}_i =&\frac{\mathrm{d}}{\mathrm{d}t}((\frac{\mathrm{d}}{\mathrm{d}t}+\rho)^{n-1}y_i)\\ =&\frac{\mathrm{d}}{\mathrm{d}t}((\frac{\mathrm{d}}{\mathrm{d}t}+\rho)^{n-1}x_{i,1})\\ =&f_i(\mathbf{x}_i)+\gamma(\mathbf{x}_i)+g_i(\mathbf{x}_i)u_i\\ =&f_i(\mathbf{x}_i)+\gamma(\mathbf{x}_i)+g_i(\mathbf{x}_i)(-\frac{1}{g_i(\mathbf{x}_i)}(\psi s_i+\phi\,\mathrm{sgn}(s_i)+f_i(\mathbf{x}_i)+\gamma(\mathbf{x}_i)))\\ =&-\psi s_i-\phi\,\mathrm{sgn}(s_i)\end{aligned} \tag{5.17}$$

Substituting (5.16) to (5.17), we get

$$\dot{s}_i=\sum_{i=1,i\neq j}^{N}a_{ij}(-\psi s_i-\phi\,\mathrm{sgn}(s_i)+\psi s_j+\phi\,\mathrm{sgn}(s_j)). \tag{5.18}$$

The dynamics of the sliding surface is

$$\dot{S}=-\mathcal{L}(\psi S+\phi\,\mathrm{sgn}(S)), \tag{5.19}$$

Define the right-hand-side of (5.19) as $f_{sld}:\mathbb{R}^n\to\mathbb{R}^n$,

$$f_{sld}(S)=-\mathcal{L}(\psi S+\phi\,\mathrm{sgn}(S)). \tag{5.20}$$

Although f_{sld} is not Lipschitz continuous, it is measurable and essentially locally bounded. Therefore, Lemma 1 is satisfied, the Filippov solution of (5.19) exists.

From (2.5), the Filippov set-valued map associated with (5.20) is

$$\mathcal{F}[f_{sld}](S)=-\mathcal{L}(\psi S+\phi\mathcal{W}),$$

where $\mathcal{W}$ is the set defined by

$$\begin{aligned}\mathcal{W}\triangleq\mathrm{co}\{\bar{S}=[\bar{s}_1,\cdots,\bar{s}_N]^\top:&\bar{s}_i=\mathrm{sgn}(s_i),\ \text{if}\ s_i\neq 0;\\ &\bar{s}_i=\{-1,\,1\},\ \text{if}\ s_i=0\}.\end{aligned}$$

Choose Lyapunov candidate:

$$V_3(S)=\max_i\{s_i\}-\min_i\{s_i\},$$

where V_3 is continuous but not differentiable with respect to S. From [8], Proposition 2.3.1, one deduces that V_3 is locally Lipschitz, with generalized gradient

$$\begin{aligned}\partial V_3(S)=&\,\mathrm{co}\{e_j\in\mathbb{R}^n|j\ \text{such that}\ s_j=\max_i\{s_i\}\}\\ &-\mathrm{co}\{e_k\in\mathbb{R}^n|j\ \text{such that}\ s_k=\min_i\{s_i\}\},\end{aligned} \tag{5.21}$$

where e_i is the i-th vector of orthonormal basis of Euclidean space.

According to [10],

$$\begin{aligned} V_3(S) =& \max_i\{s_i\} - \min_i\{s_i\} \\ =& \|2S - 2(\max_i\{s_i\} + \min_i\{s_i\})\mathbf{1}\|_\infty. \end{aligned}$$

The set-valued Lie derivative is:

$$\begin{aligned} \mathscr{L}_{\mathcal{F}[f_{sld}]}V_3(S) =& \{a \in \mathbb{R} : \text{ there exists } v \in \mathcal{F}[f_{sld}], \text{ such that} \\ & \xi^\top v = a \text{ for all } \xi \in \partial V_3(x)\}, \end{aligned}$$

which is hard to compute directly. We take S with $v_3(S) \neq 0$. Let $j, k \in \{1, \cdots, N\}$ such that $s_j = \min_i\{s_i\}$ and $s_k = \max_i\{s_i\}$. Then $e_k - e_i \in \partial V_3$.

Then we have

$$a := (e_k - e_j)^\top(-\mathcal{L}(\psi S + \phi W)) \in \mathscr{L}_{\mathcal{F}[f_{sld}]}V_3(S),$$

where $W \in \mathcal{W}$.

We can easily check

$$\begin{aligned} a =& \psi \sum_{i=1, i\neq k}^{N} a_{ik}(s_i - s_k) - \psi \sum_{i=1, i\neq j}^{N} a_{ij}(s_i - s_k) \\ & + \phi \sum_{i=1, i\neq k}^{N} a_{ik}(w_i - w_k) - \psi \sum_{i=1, i\neq j}^{N} a_{ij}(w_i - w_k). \end{aligned} \tag{5.22}$$

Since s_k is the maximum of $\{s_i\}$, and s_i is the minimum of $\{s_i\}$. We can conclude $a < 0$ for $s_k \neq s_j$. With lemma 3 we conclude the system converges asymptotically to the equilibrium. □

The final consensus value of the multi-agent system over control law (4.20) is unknown and can be determined by many factors, such as the initial value of all agents, the sliding surface and the communication typologies.

We can argue that since we set the sliding variable of all agents with the same manner, the transfer functions from s_i to y_i are the same, then they will have the same steady state gain. So all the system will converge to the same y^*.

Chapter 6

Application of DSMC

In this section we show the application of distributed sliding mode control. The first application will be on platoon systems.

6.1 Platoon Systems

A vehicle platoon is a multi-agent system as shown in Fig. 6.1. We refer to the vehicles that comprise the platoon as nodes. From a network control perspective, a platoon has four main components: node dynamics, distributed controllers, information flow topology, and formation geometry [37]. The node dynamics describes the behavior of each vehicle; the information flow topology defines how nodes exchange information with each other; the distributed controller implements feedback control algorithms for each vehicle; and the formation geometry defines the desired distance between any two successive vehicles.

The platoon contains a virtual leader, denoted by 0, and N following vehicles, denoted by $i \in \mathcal{N} \triangleq \{1, \ldots, N\}$. The displacement and velocity of the virtual leader are denoted by x_0 and v_0, respectively. We assume the information topology satisfies Assumption 2. The stability analyses are carried out under two cases: (a) $\dot{v}_0$ is zero (Lyapunov stability analysis), and (b) $\dot{v}_0 = \delta_0(t)$ is nonzero, unknown and bounded (robust analysis). The convergence to the equilibrium is analyzed in case (a) in the sense of Lyapunov stability, and the Input-to-State stability (ISS) is used in case (b) to demonstrate the disturbance attenuation performance of the platoon system.

The desired distance between two neighboring vehicles is assumed to be a constant $d \in \mathbb{R}^+$. The desired position for vehicle i is then

$$x_{i,des}(t) = x_0(t) - i \cdot d.$$

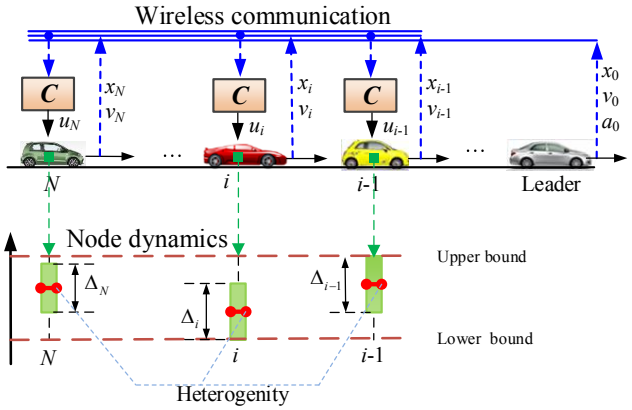

Figure 6.1: Platoon : (a) vehicle dynamics, (b) information flow topology, (c) distributed controller, (d) geometry formation [85]

The purpose of platoon control is to ensure all the vehicles run at a harmonized speed while maintaining the desired inter-vehicle spaces.

6.2 Dynamics

The vehicle longitudinal dynamics are nonlinear, which are composed of engine, drive line, brake systems, aerodynamics drag, tire friction, rolling resistance, gravitational forces, *etc.* To strike a balance between accuracy and conciseness, we assume that: (1) the vehicle body is rigid and left-right symmetric, the vehicle length is assumed to be zero; (2) the platoon is on a flat and dry-asphalt road, and the tire slip in the longitudinal direction is neglected; (3) the driving and braking torques are integrated into one control input [15]. For a heterogeneous vehicle platoon, the i-th node dynamics are described by a nonlinear model:

$$\dot{x}_i(t) = v_i(t), \tag{6.1}$$

$$\dot{v}_i(t) = \frac{1}{m_i}\left(\eta_i \frac{T_i(t)}{R_i} - C_{A,i} v_i^2(t)\right) - gf, \tag{6.2}$$

where $x_i(t)$ and $v_i(t)$ are position and velocity, respectively; $T_i(t)$ is the control input, representing the driving/braking torque; m_i is the mass of vehicle; η_i is the mechanical efficiency of the driveline; R_i is the radius of wheel; $C_{A,i}$ is the coefficient of aerodynamic drag; g is the acceleration due to gravity; and f is the coefficient of rolling resistance.

6.3 DSMC for Platoon

Design of topological sliding surface

The tracking error of the i-th vehicle is defined as

$$e_i \triangleq x_i - x_{i,des}.$$

Define an intermediate error Δ_i,

$$\Delta_i \triangleq \dot{e}_i + \rho e_i, \tag{6.3}$$

where $\rho \in \mathbb{R}^+$ is a tuning parameter. This parameter determines the converging rate of tracking error once the intermediate error equals zero. The intermediate error vector is defined as

$$\overline{\Delta} \triangleq [\Delta_1, \Delta_2, \ldots, \Delta_N]^\top.$$

We define the individual sliding variable for node i as

$$s_i \triangleq f_i^{TS}(\overline{\Delta}).$$

The sliding variable array of the platoon is then

$$S = \begin{bmatrix} s_1 \\ s_2 \\ \vdots \\ s_N \end{bmatrix} = (\mathcal{L} + \mathcal{P})\overline{\Delta}. \tag{6.4}$$

The topological sliding surface for the platoon is defined by $S(t) = \mathbf{0}$.

Remark 9. *Each sliding variable s_i depends on local node states, i.e., states of vehicle i as well as states of neighboring vehicles as constrained by the information topology. Note that $\Delta_i - \Delta_j$ does not depend on leader states since*

$$\Delta_i - \Delta_j = v_i - v_j + \rho(x_i - x_j + d(i-j)).$$

Remark 10. *The sliding variable S is a bijective linear function of $\bar{\Delta}$ defined in (6.4) because $\mathcal{L} + \mathcal{P}$ is invertible. (see Theorem 6).*

Design of topological reaching law

To design the DSMC controller, the reaching law has to conform with the associated sliding surface. The topological reaching law for node i is

$$\dot{s}_i = -\psi f_i^{ST}(S) - \phi f_i^{ST}(\mathrm{sgn}(S))$$

where ψ, $\phi \in \mathbb{R}^+$ are tuning parameters. Combining these for all nodes, we arrive at the compact form array

$$\dot{S} = -(\mathcal{L}+\mathcal{P})(\psi S + \phi\,\mathrm{sgn}(S)). \tag{6.5}$$

We observe that

$$(\mathcal{L}+\mathcal{P})\dot{\overline{\Delta}} = -(\mathcal{L}+\mathcal{P})(\psi S + \phi\,\mathrm{sgn}(S)).$$

Since $\mathcal{L}+\mathcal{P}$ is invertible, we obtain

$$\dot{\overline{\Delta}} = -(\psi S + \phi\,\mathrm{sgn}(S)). \tag{6.6}$$

Invertibility of $\mathcal{L}+\mathcal{P}$ is critical in designing a distributed SMC suitable for a broad range of topologies. Component i of the vector-valued equation (6.6) is then

$$\dot{\Delta}_i = -\psi s_i - \phi\,\mathrm{sgn}(s_i). \tag{6.7}$$

Differentiating (6.3) and equating the result to (6.7) provides an expression for $\dot{v}_i$. Substituting this in (6.2) yields the control law for node i:

$$\begin{aligned} T_i =& \frac{R_i}{\eta_i}(m_i f g + C_{A,i} v_i^2) - \frac{m_i R_i \rho}{\eta_i}(v_i - v_0) \\ & - \frac{m_i R_i}{\eta_i}(\psi s_i + \phi\,\mathrm{sgn}(s_i)). \end{aligned} \tag{6.8}$$

Remark 11. *The control law (6.8) is not quite distributed because of its possible dependence on the leader velocity v_0. We therefore need to design a distributed observer for v_0 to derive a truly distributed control law. This is done in the next subsection.*

Design of topologically structured velocity observer

Let $\hat{v}_{0,i}$ denote the estimation of v_0 produced by the i-th vehicle. The observer of i-th vehicle for the virtual leader's velocity is

$$\dot{\hat{v}}_{0,i} = -k s_i. \tag{6.9}$$

Since s_i is computed in a distributed fashion with (6.4), the observer is distributed (i.e., compatible with the underlying information topology). Using the estimated leader velocity $\hat{v}_{0,i}$ from the observer, the control law (6.8) becomes:

$$\begin{aligned} T_i =& \frac{R_i}{\eta_i}(m_i f g + C_{A,i} v_i^2) - \frac{m_i R_i \rho}{\eta_i}(v_i - \hat{v}_{0,i}) \\ & - \frac{m_i R_i}{\eta_i}(\psi s_i + \phi \operatorname{sgn}(s_i)). \end{aligned} \tag{6.10}$$

Remark 12. *For simplicity, we have used second-order nonlinear node dynamics. Our approach easily generalizes to higher-order nonlinear dynamics. A regulation example with more complex vehicle dynamics is offered in our previous work [77].*

6.4 Stability analysis

The stability analysis of DSMC is divided into two phases, i.e., the reaching phase and the sliding phase. The stability of the reaching phase is analyzed by Lyapunov method, while that of the sliding phase follows traditional SMC analysis.

Reaching Phase

We state our first main result:

Theorem 16. *Consider a platoon with nonlinear node dynamics (6.1) and (6.2) with information topology under Assumption 1. Under the distributed control law (6.10) and tuning parameters ψ, ϕ, ρ, $k \in \mathbb{R}^+$, the sliding variable S in (6.4) and the observer error $\epsilon \triangleq [\hat{v}_{0,1} - v_0, \ldots, \hat{v}_{0,N} - v_0]^\top$ converge to $\mathbf{0}$ asymptotically.*

Proof. With the sliding variable (6.4), velocity observer (6.9) and control law (6.10), the dynamics of (S, ϵ) becomes

$$\begin{aligned} \dot{S} =& (\mathcal{L} + \mathcal{P})(-\psi S - \phi \operatorname{sgn}(S) + \rho \epsilon), \\ \dot{\epsilon} =& -kS. \end{aligned} \tag{6.11}$$

The first equation of (6.11) is obtained by differentiating both sides of (6.4), and substituting (6.3), agent dynamics (6.1), (6.2), and control law (6.10) to the right-hand side of the equation.

For simpler presentation, define

$$\begin{aligned} \mathbf{x} &\triangleq \begin{bmatrix} S \\ \epsilon \end{bmatrix}, \\ f(\mathbf{x}) &\triangleq \begin{bmatrix} (\mathcal{L}+\mathcal{P})(-\psi S - \phi\,\mathrm{sgn}(S) + \rho\epsilon) \\ -kS \end{bmatrix}. \end{aligned} \tag{6.12}$$

To discuss the existence and stability of solution of a discontinuous system (6.11), we take the concepts of differential inclusion and Filippov set-valued map from [9]. Since f is measurable and essentially locally bounded, then the associated Filippov set-valued map satisfies all the conditions of Lemma 1, this guarantees the existence of Filippov solution.

The Filippov set-valued map associated with (6.12) is

$$\mathcal{F}[f](\mathbf{x}) = \begin{bmatrix} (\mathcal{L}+\mathcal{P})(\rho\epsilon - \psi S) \\ -kS \end{bmatrix} - \begin{bmatrix} (\mathcal{L}+\mathcal{P})\phi\mathcal{W} \\ 0 \end{bmatrix},$$

where $\mathcal{W}$ is the set defined by

$$\begin{aligned} \mathcal{W} = \mathrm{co}\{\bar{S} = [\bar{s}_1, \cdots, \bar{s}_N]^\top \,|\, \bar{s}_i = \mathrm{sgn}(s_i), \text{ if } s_i \neq 0; \\ \bar{s}_i = \{-1,\, 1\}, \text{ if } s_i = 0\}. \end{aligned} \tag{6.13}$$

We choose a Lyapunov candidate for the networked system,

$$V_1(\mathbf{x}) = \frac{1}{2}\mathbf{x}^\top \begin{bmatrix} (\mathcal{L}+\mathcal{P})^{-1} & 0 \\ 0 & \frac{\rho}{k} I_N \end{bmatrix} \mathbf{x}, \tag{6.14}$$

where I_N is the N dimensional identity matrix. The gradient of (6.14) is

$$\nabla V_1(\mathbf{x}) = \begin{bmatrix} (\mathcal{L}+\mathcal{P})^{-1} S \\ \frac{\rho}{k}\epsilon \end{bmatrix}.$$

Taking the Lie derivative of the Lyapunov candidate,

$$\begin{aligned} \tilde{\mathcal{L}}_{\mathcal{F}[f]} V_1(\mathbf{x}) =& \{\nabla V_1(\mathbf{x})^\top v \,|\, v \in \mathcal{F}[f](\mathbf{x})\} \\ =& \nabla V_1(\mathbf{x})^\top \mathcal{F}[f](\mathbf{x}) \\ =& -\psi S^\top S - \phi S^\top \mathcal{W}. \end{aligned} \tag{6.15}$$

The second term of (6.15) is

$$\begin{aligned} -\phi S^\top \mathcal{W} =& \{-\phi S^\top w \,|\, w \in \mathcal{W}\} \\ =& \{-\phi \sum_{i=1}^{N} s_i w_i \,|\, w \in \mathcal{W}\}, \end{aligned}$$

where w_i is the i-th element of w. Using the definition of $\mathcal{W}$ in (6.13), each $s_i w_i$ is

$$s_i w_i = \begin{cases} 0, & \text{if } s_i = 0, \\ s_i \operatorname{sgn}(s_i), & \text{if } s_i \neq 0. \end{cases}$$

Hence,

$$-S^\top \phi \mathcal{W} = \{-\phi \sum_{i=1}^{N} s_i \operatorname{sgn}(s_i)\} = \{-\phi \|S\|_1\}.$$

The Lie derivative $\tilde{\mathcal{L}}_{\mathcal{F}[f]} V_1(\mathbf{x})$ is therefore a singleton,

$$\tilde{\mathcal{L}}_{\mathcal{F}[f]} V_1(\mathbf{x}) = \{-\psi \|S\|_2^2 - \phi \|S\|_1\}. \tag{6.16}$$

We check the three conditions of Lemma 3: i. $V_1(\mathbf{x})$ is continuously differentiable; ii. $V_1(\mathbf{x}) > 0$ for $\mathbf{x} \in \mathbb{R}^{2N} \setminus \{\mathbf{0}\}$; iii. By (6.16), $\max \tilde{\mathcal{L}}_{\mathcal{F}[f]} V_1(\mathbf{x}) \leq 0$. We conclude closed-loop system is stable in the sense of Lyapunov.

The next step is to prove asymptotic stability. For any initial condition $\mathbf{x}(0)$, choose a constant $c \geq V_1(\mathbf{x}(0))$, define Ω_c to be the level set of $V_1(\mathbf{x})$,

$$\Omega_c = \{\mathbf{x} = \begin{bmatrix} S \\ \epsilon \end{bmatrix} \mid V_1(\mathbf{x}) \leq c\}. \tag{6.17}$$

From (6.16), Ω_c is positively invariant for all $c > 0$. Define

$$\begin{aligned} \mathcal{Z}_{F,V_1} \triangleq & \overline{\{\mathbf{x} \in \mathbb{R}^{2N} \mid 0 \in \tilde{\mathcal{L}}_{\mathcal{F}[f]} V_1(\mathbf{x})\}} \\ = & \{\mathbf{x} \mid S = \mathbf{0}\}. \end{aligned} \tag{6.18}$$

Then we have

$$\Omega_c \cap \mathcal{Z}_{F,V_1} = \{\mathbf{x} \mid S = \mathbf{0},\ \frac{\rho}{k} \|\epsilon\|_2^2 \leq 2c\}.$$

From (6.15), the largest weakly invariant set M in $\Omega_c \cap \mathcal{Z}_{F,V_1}$ is $M = \{\mathbf{x} \mid \mathbf{x} = \mathbf{0}\}$. Since the Lyapunov function $V_1(\mathbf{x})$ is radially unbounded, we can use Lemma 4 to conclude global asymptotic stability. □

Next, we offer a sufficient condition for finite-time convergence to the topological sliding surface $S = \mathbf{0}$.

Theorem 17. *Consider again the assumptions and parameter settings of Theorem 16, with the set Ω_c and $\mathcal{Z}_{F,V_1}$ defined in (6.17) and (6.18). For all $c \in \{c_f | 0 < c_f < \frac{\phi^2}{2k\rho}\}$, the set $\mathcal{Z}_{F,V_1} \cap \Omega_c = \{(S, \epsilon) | S = \mathbf{0},\ \|\epsilon\|_2 \leq \sqrt{2ck/\rho}\}$ is positively invariant; and any solution $\mathbf{x}(t) = [S(t), \epsilon(t)]^\top$ of system (6.11) with initial condition $\mathbf{x}(0) \in \Omega_c$ reaches $\mathcal{Z}_{F,V_1} \cap \Omega_c$ in finite time.*

Proof. To discuss the topological sliding surface dynamics, let us choose the Lyapunov candidate

$$V_2(S) = \frac{1}{2} S^\top (\mathcal{L} + \mathcal{P})^{-1} S. \tag{6.19}$$

The Lie derivative of (6.19) is

$$\begin{aligned} \tilde{\mathcal{L}}_{\mathcal{F}[f]} V_2(S) =& -\psi S^\top S - \phi S^\top \mathcal{W} + \rho \epsilon^\top S \\ =& \{-\psi \|S\|_2^2 - \phi \|S\|_1 + \rho \epsilon^\top S\}. \end{aligned} \tag{6.20}$$

Since we have already proved that the set Ω_c from (6.17) is positively invariant for any $c > 0$, if $\mathbf{x}(0) \in \Omega_c$, then

$$\|\epsilon(t)\|_2 \leq \sqrt{\frac{2ck}{\rho}}, \quad \forall t \in [0, +\infty).$$

With the condition $c < \frac{\phi^2}{2k\rho}$, we derive the upper bound of (6.20),

$$\begin{aligned} \max \tilde{\mathcal{L}}_{\mathcal{F}[f]} V_2(S) \leq& -\psi \|S\|_2^2 - (\phi - \sqrt{2ck\rho}) \|S\|_1 \\ <& 0. \end{aligned} \tag{6.21}$$

We can conclude that $\{\mathbf{x} \,|\, S = \mathbf{0}\} \cap \Omega_c$ is a positive-invariant set.

Next, we show finite-time convergence to S. Instead of proving the finite-time convergence of S directly, we prove that $\sqrt{2V_2} = \|(\mathcal{L} + \mathcal{P})^{-\frac{1}{2}} S\|_2$ converges to 0 in finite time.

In the region $\{\mathbf{x} | \mathbf{x} \in \Omega_c,\, s \neq \mathbf{0}\}$, the set-valued Lie derivative of $\sqrt{2V_2}$ is

$$\tilde{\mathcal{L}}_{\mathcal{F}[f]} \sqrt{2V_2} = \frac{1}{\|(\mathcal{L} + \mathcal{P})^{-\frac{1}{2}} S\|_2} \tilde{\mathcal{L}}_{\mathcal{F}[f]} V_2. \tag{6.22}$$

From (6.21), we have

$$\begin{aligned} &\max \tilde{\mathcal{L}}_{\mathcal{F}[f]} V_2(S) \\ &\quad \leq -\psi \|S\|_2^2 - (\phi - \sqrt{2ck\rho}) \|S\|_1 \\ &\quad \leq -\psi \|S\|_2^2 - \frac{1}{\sqrt{N}} (\phi - \sqrt{2ck\rho}) \|S\|_2. \end{aligned} \tag{6.23}$$

By Rayleigh's quotient, we have

$$\|(\mathcal{L} + \mathcal{P})^{-\frac{1}{2}} S\|_2 \leq \frac{1}{\sqrt{\lambda_{\min}(\mathcal{L} + \mathcal{P})}} \|S\|_2. \tag{6.24}$$

From (6.22), (6.23) and (6.24), one can establish

$$\max \tilde{\mathcal{L}}_{\mathcal{F}[f]} \sqrt{2V_2} \leq -\sqrt{\frac{\lambda_{\min}(\mathcal{L}+\mathcal{P})}{N}}(\phi - \sqrt{2ck\rho}),$$

for all $\{\mathbf{x} \,|\, \mathbf{x} \in \Omega_c,\, S \neq \mathbf{0}\}$.

From Lemma 2, we have

$$\frac{\mathrm{d}}{\mathrm{d}t}\|(\mathcal{L}+\mathcal{P})^{-\frac{1}{2}} S(t)\|_2 \in \tilde{\mathcal{L}}_{\mathcal{F}[f]} \sqrt{2V_2} \tag{6.25}$$

for almost every $t \in [0, +\infty)$. We have

$$\begin{aligned} \|(\mathcal{L}+\mathcal{P})^{-\frac{1}{2}} S(t_f)\|_2 =& \|(\mathcal{L}+\mathcal{P})^{-\frac{1}{2}} S(0)\|_2 \\ &+ \int_0^{t_f} \frac{\mathrm{d}}{\mathrm{d}\tau}\|(\mathcal{L}+\mathcal{P})^{-\frac{1}{2}} S(\tau)\|_2 \mathrm{d}\tau. \end{aligned} \tag{6.26}$$

With (6.25) and (6.26), in the region $\{\mathbf{x}|\mathbf{x} \in \Omega_c,\, S \neq \mathbf{0}\}$ we have

$$\begin{aligned} \|(\mathcal{L}+\mathcal{P})^{-\frac{1}{2}} S(t_f)\|_2 \leq& \|(\mathcal{L}+\mathcal{P})^{-\frac{1}{2}} S(0)\|_2 \\ &-t_f(\phi - \sqrt{2ck\rho})\sqrt{\frac{\lambda_{\min}(\mathcal{L}+\mathcal{P})}{N}}. \end{aligned} \tag{6.27}$$

We argue that there must exist t_f such that $S(t_f) = \mathbf{0}$. Otherwise, $\|(\mathcal{L}+\mathcal{P})^{-\frac{1}{2}} S(t_f)\|_2 \to -\infty$ as $t_f \to +\infty$. □

Remark 13. *The above result establishes that every trajectory starting in Ω_c approaches $\{(S,\epsilon)|S = \mathbf{0},\, \|\epsilon\|_2 \leq \sqrt{2ck/\rho}\}$ in finite time. By choosing c sufficiently large, any compact set in $\mathbb{R}^{2N}$ will fall inside Ω_c. As a result, $\frac{\phi^2}{2k\rho}$ can be made arbitrarily large, and Theorem 17 offers a sufficient semi-global condition for finite-time convergence to the sliding surface.*

Sliding Phase

Theorem 18. *Consider a vehicle platoon with nonlinear dynamics described by (6.1) and (6.2) and information topology under Assumption 1. During the sliding phase where $S = \mathbf{0}$, the tracking error for each vehicle $e_i \to 0$ as $t \to \infty$.*

Proof. In the sliding surface $S = \mathbf{0}$, with the definition of sliding error, we have

$$S = (\mathcal{L}+\mathcal{P})\overline{\Delta} = \mathbf{0}.$$

With $\mathcal{L}+\mathcal{P}$ being positive definite, we have

$$\overline{\Delta} = [\Delta_1,\, \Delta_2, \ldots, \Delta_N]^\top = \mathbf{0}.$$

For each Δ_i,

$$\Delta_i = \dot{e}_i + \rho e_i = 0, \tag{6.28}$$

where $\rho > 0$. Hence (6.28) is a stable differential equation, $e_i \to 0$ as $t \to \infty$. □

Due to practical realities of switching devices, the control law (6.10) can cause chattering. The following result assures that asymptotic stability of (6.11) is preserved with a smooth control law by setting $\phi = 0$.

Corollary 5. *Consider again the set-up and assumptions of Theorem 16 with tuning parameter $\psi, k \in \mathbb{R}^+$ and $\phi = 0$. Then, the closed-loop system (6.11) is asymptotic stable.*

Proof. By setting $\phi = 0$, the closed-loop system (6.11) becomes linear

$$\dot{\mathbf{x}}(t) = A\mathbf{x}(t), \tag{6.29}$$

where A is defined as

$$A \triangleq \begin{bmatrix} -\psi(\mathcal{L}+\mathcal{P}) & \rho(\mathcal{L}+\mathcal{P}) \\ -kI_N & 0 \end{bmatrix}. \tag{6.30}$$

Let

$$P \triangleq \begin{bmatrix} \frac{k}{\psi}(\mathcal{L}+\mathcal{P})^{-1} + \frac{\rho}{\psi}I_N & -I_N \\ -I_N & \frac{\rho}{\psi}I_N + (\frac{\rho^2}{\psi k} + \frac{\psi}{k})(\mathcal{L}+\mathcal{P}) \end{bmatrix}.$$

Using the characterization of positive definite matrices with Schur complements [81] to prove matrix P is positive definite, two conditions have to be satisfied:

1. The first diagonal block is positive definite

$$\frac{k}{\psi}(\mathcal{L}+\mathcal{P})^{-1} + \frac{\rho}{\psi}I_N \succ 0.$$

2. The Schur complement is positive definite

$$\frac{\rho}{\psi}I_N + (\frac{\rho^2}{\psi k} + \frac{\psi}{k})(\mathcal{L}+\mathcal{P}) - (\frac{k}{\psi}(\mathcal{L}+\mathcal{P})^{-1} + \frac{\rho}{\psi}I_N)^{-1} \succ 0.$$

One can check easily that the first condition holds since $\mathcal{L}+\mathcal{P}$ is positive definite. The second part is proved by using the matrix inversion lemma (Woodbury matrix identity). Since the algebraic process is simple, we omit this part for brevity.

Next, choose a Lyapunov candidate $V_3(\mathbf{x}) = \frac{1}{2}\mathbf{x}^\top P\mathbf{x}$. The derivative of $V_3(\mathbf{x})$ with respect to system (6.29) is

$$\begin{aligned}\dot{V}_3(\mathbf{x}) =& \frac{1}{2}\mathbf{x}^\top(A^\top P + PA)\mathbf{x} \\ =& -\mathbf{x}^\top Q\mathbf{x} < 0,\end{aligned} \tag{6.31}$$

where matrix Q is defined as the positive definite matrix

$$Q \triangleq \rho \begin{bmatrix} (\mathcal{L}+\mathcal{P}) & 0 \\ 0 & (\mathcal{L}+\mathcal{P}) \end{bmatrix} \succ 0.$$

We conclude matrix A is Hurwitz. □

Remark 14. *By eliminating the switching term, the asymptotic stability result of Theorem 16 is preserved, however, the finite-time convergence property from Theorem 17 is compromised. As is done with traditional SMC, a suitable trade-off between tracking precision and finite-time convergence can be arranged by introducing a thin boundary layer neighboring the topological sliding surface, $\{S \mid \|S\|_2 \leq \varepsilon\}$. Using the negative definiteness condition (6.31), one can prove that the boundary layer is invariant and can be reached in finite time. Within the boundary layer, the tracking error for each vehicle remains bounded.*

6.5 Discussion on String Stability and Robustness

String stability

String stability in a broad sense implies that the disturbances in the system will be attenuated when propagating through the platoon system. One of the common string stability definitions in the time-domain is given by [66]:

Definition 11. *[66]. Consider a interconnected system*

$$\dot{x}_i = f(x_i, x_{i-1}, \cdots, x_{i-r+1}) \tag{6.32}$$

The origin $x_i = 0$, $i \in \mathbb{R}$ of (6.32) is string stable, if for any $\epsilon > 0$, there exists a $\delta > 0$, such that $\|x_i(0)\|_\infty < \delta \Rightarrow \sup_i \|x_i(t)\|_\infty < \epsilon$.

This definition strongly relies on a specific information flow topology. The structure of the system (6.32) implies that the error propagates from the front cars to the rear cars. Without (6.32), the definition reduces to normal Lyapunov stability of the whole platoon.

String stability definition also relies on specific information flow topology in frequency-domain.

Definition 12. *[51] The system is string stable if the transfer function of outputs between the vehicle i and the predecessor vehicle $i-1$, denoted as $G_{i-1,i}$, is such that $\|G_{i-1,i}(j\omega)\|_{\mathcal{H}_\infty} \leq 1$.*

The definition is based on the predecessor following topology, and does not apply to other other information flow topology, since the existence of $G_{i-1,i}$ is not guaranteed.

There are other definitions of string stability based on specific information flow topologies: [50][51] used a predecessor following topology, [66] used a leader-predecessor following topology, [58] used a unidirectional ring topology, and [4] used nearest-neighbor bidirectional topology.

For a general class of topologies, it is very difficult to define the concept of "disturbance attenuation through the system", since the direction of disturbance propagation is not specified. To our knowledge, there are loose versions of string stability for general topologies [51] [5] [64]. These definitions emphasize Bounded-Input-Bounded-Output (BIBO) or Input-to-State stability (ISS) of the platoon under external disturbances. However, we refrain ourselves using the notion of string stability on these definitions, since we think it deviates from the original string stability idea, which focuses on disturbance attenuation. The BIBO and Input-to-State stability is immediate attainable with the proposed DSMC design.

In the dissertation, we added a section below discussing Input-to-State stability of the system. We include the unknown leader acceleration and physical disturbances as input disturbance. We proved Input-to-State (BIBO) stability of the closed-loop system, this implies with a bounded disturbance input, the error is also bounded. Furthermore, we relate the amplification effect with the eigenvalue of $\mathcal{L}+\mathcal{P}$ matrix and tuning parameter of the controller.

Robust analysis

In this section, we analyze the performance of DSMC under external disturbance. For theoretical simplicity, we assume tuning parameter $\phi = 0$.

Assume all vehicles are subject to persistent external disturbances δ_i:

$$\begin{aligned}\dot{x}_i(t) =& v_i(t),\\ \dot{v}_i(t) =& \frac{1}{m_i}\left(\eta_i \frac{T_i(t)}{R_i} - C_{A,i} v_i^2(t)\right) - gf + \delta_i(t),\end{aligned}$$

and the acceleration of the leader is non-zero $\dot{v}_0 = \delta_0(t)$, where δ_0 is unknown.

The closed-loop dynamics (6.11) with external disturbances becomes

$$\dot{\mathbf{x}}(t) = A\mathbf{x}(t) + Bd(t), \tag{6.33}$$

where $\mathbf{x} = [S, \epsilon]^\top$, A is defined in (6.30), B and $d(t)$ is defined as

$$B \triangleq \begin{bmatrix} \mathcal{L} + \mathcal{P} \\ 0 \end{bmatrix} \text{ and } d \triangleq \begin{bmatrix} \delta_1 - \delta_0 \\ \vdots \\ \delta_N - \delta_0 \end{bmatrix}.$$

The Hurwitz A matrix implies the Input-to-State Stability (ISS) of system (6.33):

$$\begin{aligned}\mathbf{x}(t) =& e^{At}\mathbf{x}(0) + \int_0^t e^{A(t-\tau)} B d(\tau) \mathrm{d}\tau,\\ |\mathbf{x}(t)| \leq& \|e^{At}\||\mathbf{x}(0)| + \int_0^t \|e^{A(t-\tau)}\|\|B\||d(\tau)|\mathrm{d}\tau\\ \leq& \kappa e^{-\alpha t}|\mathbf{x}(0)| + \|B\| \sup_{\tau\in[0,t]} |d(\tau)| \int_0^t \kappa e^{-\alpha t}\mathrm{d}\tau\\ \leq& \kappa e^{-\alpha t}|\mathbf{x}(0)| + \frac{\kappa}{\alpha}\|B\| \sup_{\tau\in[0,t]} |d(\tau)|,\end{aligned} \tag{6.34}$$

where $|\cdot|$ denotes vector norm (e.g 1, 2, ∞ norm) in Euclidean space, $\|\cdot\|$ denotes the corresponding matrix norm, $\kappa, \alpha \in \mathbb{R}_+$ and $\max \mathrm{Re}\{\lambda(A)\} < -\alpha$. We further define:

$$\begin{aligned}\beta(|\mathbf{x}(0)|, t) \triangleq& \kappa e^{-\alpha t}|\mathbf{x}(0)|,\\ \gamma(\sup_{\tau\in[0,t]} |d(\tau)|) \triangleq& \frac{\kappa}{\alpha}\|B\| \sup_{\tau\in[0,t]} |d(\tau)|.\end{aligned}$$

We can easily check function β is class-$\mathcal{KL}$ and γ is class-$\mathcal{K}$, then conclude ISS.

Remark 15. *The disturbance attenuation effect is closely related to* $\max Re\{\lambda(A)\}$. *For a smaller* $\max Re\{\lambda(A)\}$, *the error bound of* $\mathbf{x}(t)$ *will be smaller. From (6.30), we observe that the eigenvalues of* A *are affected by the information flow topology* $\mathcal{L} + \mathcal{P}$ *and the tuning parameters* ψ, ρ.

Remark 16. *The inequality (6.34) is related to* collision avoidance. *The sliding variable S is bounded due to the boundness of $\mathbf{x}(t)$. Sliding variable S and $\overline{\Delta}$ are isomorphic (6.4). Each Δ_i and tracking error e_i are related through a stable linear system (6.3):*

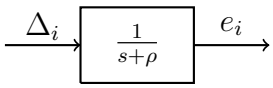

We can conclude that the tracking error e_i is bounded. Then we can guarantee collision avoidance for a finite length platoon if properly selecting spacing policy, tuning parameter and information flow topology [80].

Remark 17. *Since system (6.33) is ISS, if $\delta_i(t) = 0$ for all $i \in \mathcal{N}$, and δ_0 eventually converges to 0, then the tracking error $e_i \to 0$ as $t \to 0$.*

Parameter	Value	Uncertainty
m_i	$(1445 + i \times 50)$ kg	0%
η_i	0.85	$\pm$10%
$C_{A,i}$	0.43 kg/ m	$\pm$10%
R_i	$(0.28 + i \times 0.005)$m	0%
f	0.02	$\pm$10%

Table 6.1: Simulation parameters

6.6 Simulation Results

We now illustrate the effectiveness of proposed DSMC through numerical simulations. A heterogeneous platoon with 1 leader and 8 followers is simulated under 3 different information flow topologies. These topologies are nearest-neighbor (NN), nearest-neighbor with leader paths (NNL), and two-nearest-neighbor (2NN), as shown in Fig. 6.2. With the NNL topology, all the vehicles have access to the leader. This will allow us to demonstrate effect of the leader information on the performance of the platoon.

The distributed control law (6.10) was designed based on a nonlinear vehicle dynamics (6.1)-(6.2) for simplicity and elegance. In the simulation, we applied the control law to platoon with high-fidelity vehicle model to validate the performance of

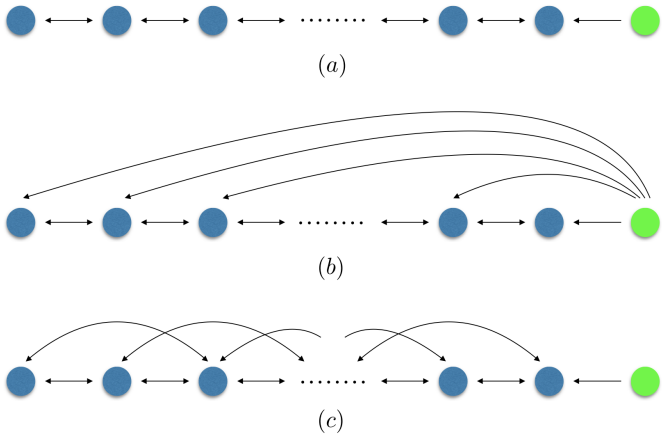

Figure 6.2: Types of bidirectional information flow topology used in this dissertation: (a) nearest-neighbor (NN); (b) nearest-neighbor with leader paths (NNL); (c) two-nearest-neighbor (2NN).

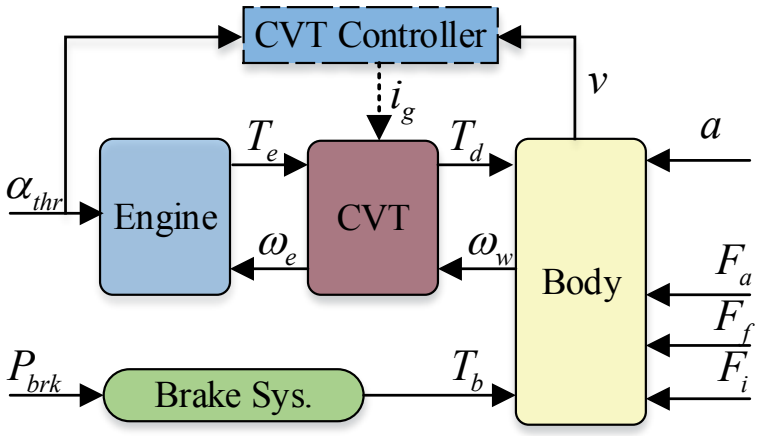

Figure 6.3: Sketch of vehicle longitudinal dynamics.

DSMC under modeling uncertainty. Each vehicle is a passenger car with a gasoline engine, a torque converter, a continuous variable transmission (CVT), two driving and two driven wheels, as well as a hydraulic braking system. Fig. 6.3 sketches the powertrain dynamics. The inputs are the throttle angle (α_{thr}) and the braking pressure (P_{brk}). In realistic driving modes, a driver can not simultaneously engage the throttle and brake pedals. Therefore, in this study we use an inverse model to allocate the driving commands (T_i) to either throttle angle or braking pressure. Interested readers can refer to [39] for further information. The outputs include

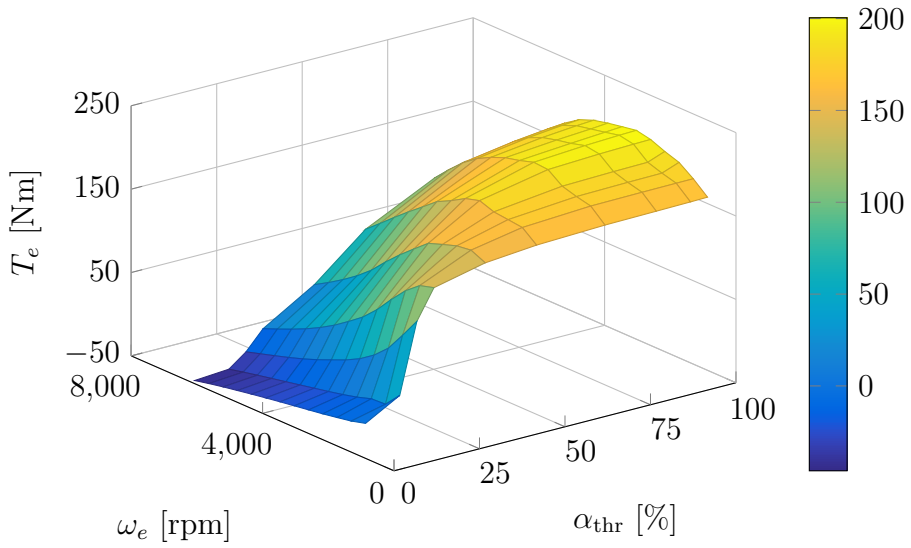

Figure 6.4: Engine torque map.

the longitudinal acceleration (a), vehicle velocity (v), as well as other measurable variables in the powertrain. When driving, the engine torque is amplified by the torque converter, CVT, and final gearing and acts on the two front driving wheels. When braking, the braking torque acts on all four wheels to dissipate the kinetic energy of the vehicle body. Fig. 6.4 shows the nonlinear engine torque map: engine torque (T_e) is a nonlinear monotonically increasing function of engine speed (ω_e) and throttle angle (α_{thr}). The vehicle parameters are offered in Table 6.1, in which the heterogeneity is represented by the difference in vehicle mass (m_i) and wheel radius (R_i). In addition, parameter uncertainties are added in mechanical efficiency (η_i), coefficient of aerodynamic drag ($C_{A,i}$), and coefficient of rolling resistance (f). In this study, the parameter heterogeneities are known while the parameter uncertainties are unknown.

The simulation includes 2 scenarios distinguished by the speed profile of leading vehicle: constant speed ramp and modified EPA74 profile. In the former, the leading vehicle ramps from 15m/s to 20m/s in 3 seconds with constant acceleration, for the purpose of examining the stability of the distributed control law. In the latter, the leading vehicle follows a modified EPA74 speed profile to allow comparison of platooning performance under different communication topologies.

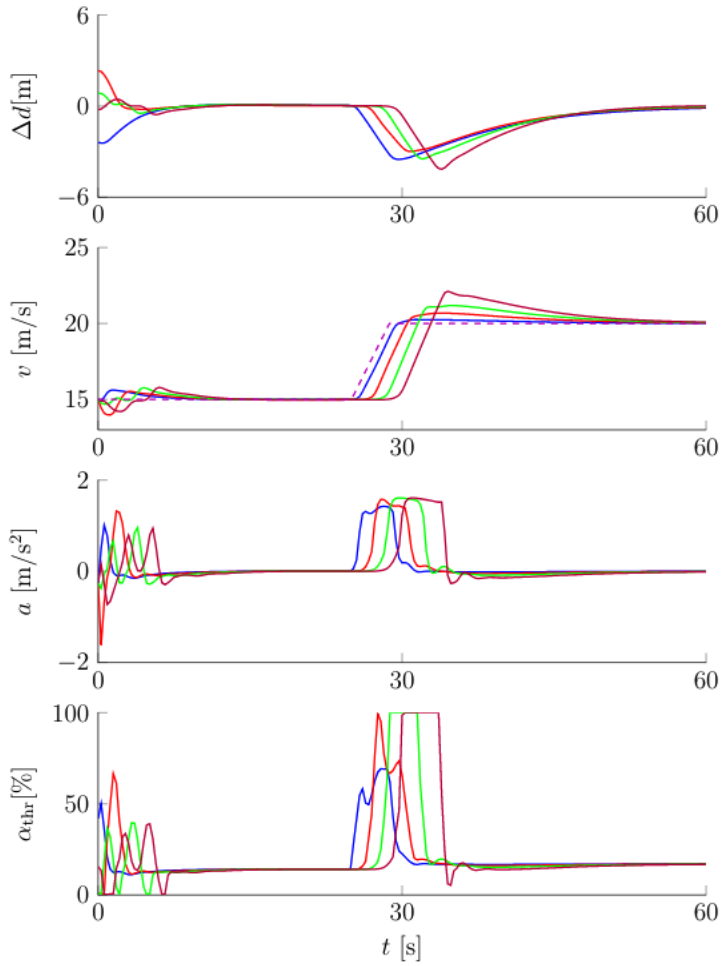

Figure 6.5: Simulation result in ramp speed profile under NN topology. 1st, 3rd, 5th, and 7th vehicle are denoted by (——), (——), (——), and (——), respectively. (- - -) denotes leader velocity.

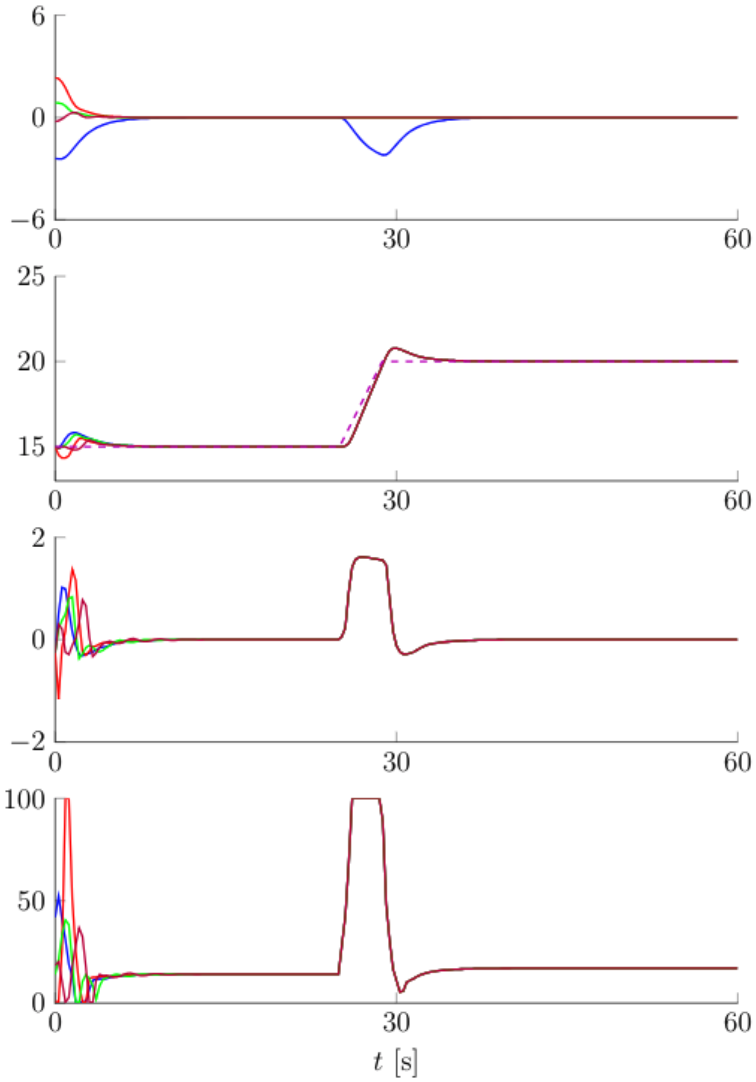

Figure 6.6: Simulation result in ramp speed profile under NNL topology. 1st, 3rd, 5th, and 7th vehicle are denoted by (——), (——), (——), and (——), respectively. (- - -) denotes leader velocity.

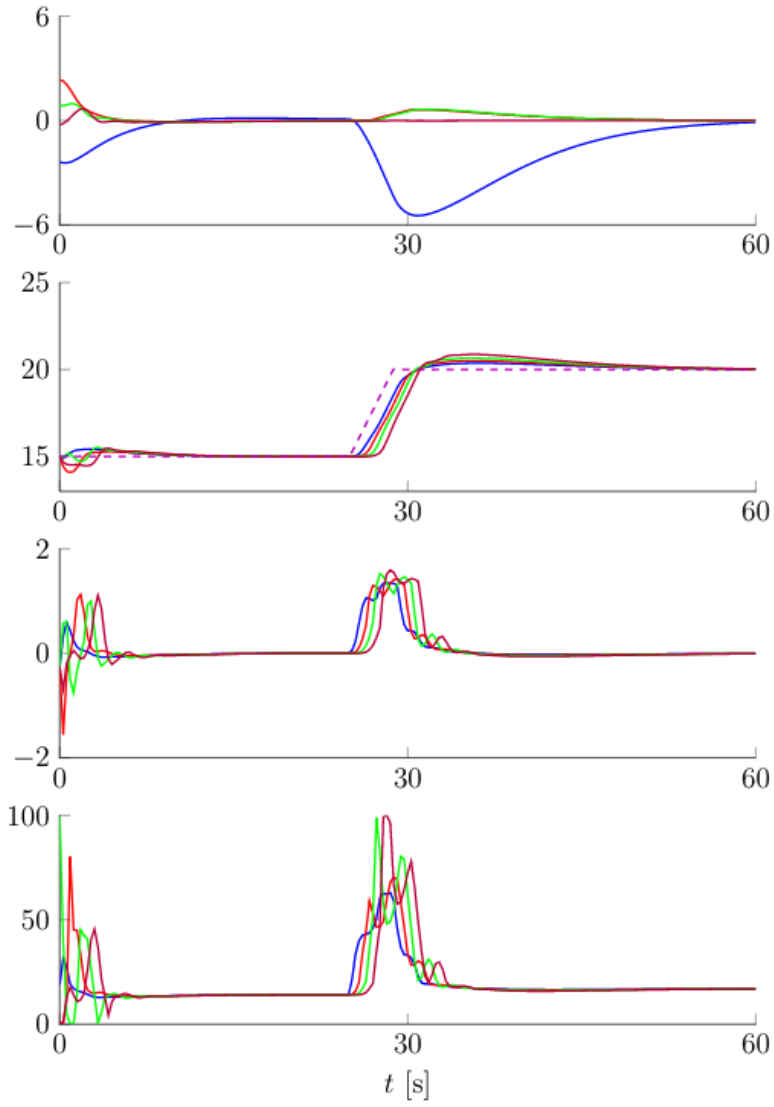

Figure 6.7: Simulation result in ramp speed profile under 2NN topology. 1st, 3rd, 5th, and 7th vehicle are denoted by (——), (——), (——), and (——), respectively. (- - -) denotes leader velocity.

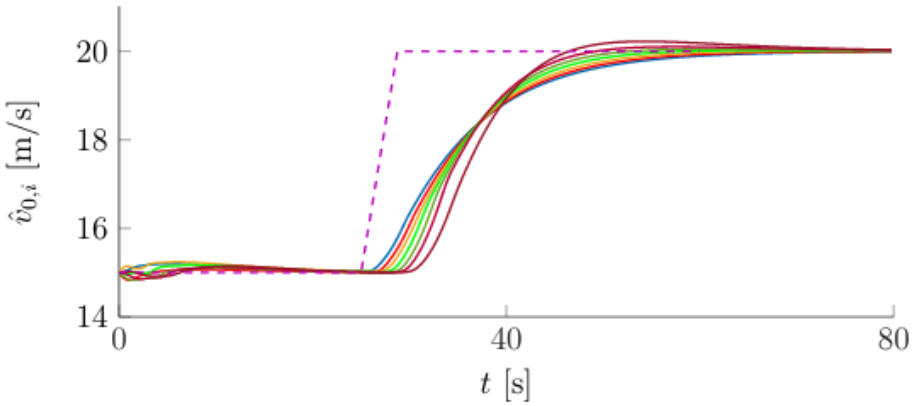

(a) NN

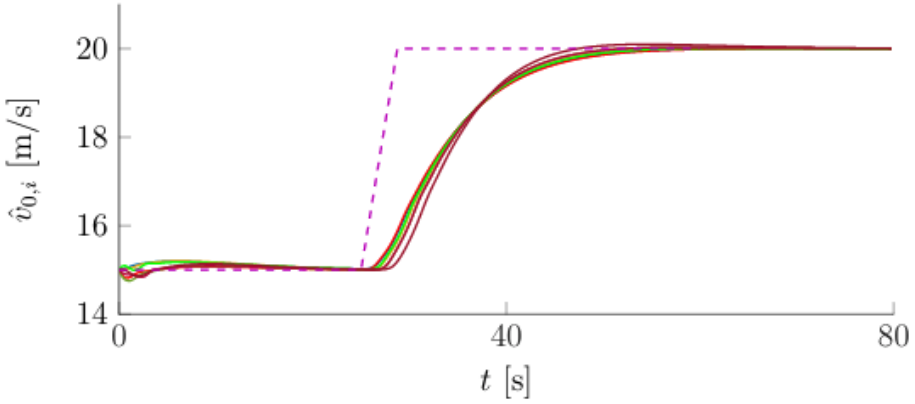

(b) 2NN

Figure 6.8: Result of topologically structured velocity observer. The map between vehicles and lines are: 2nd vehicle (—), 3rd vehicle (—), 4th vehicle (—), 5th vehicle (—), 6th vehicle (—), 7th vehicle (—), 8th vehicle (—).

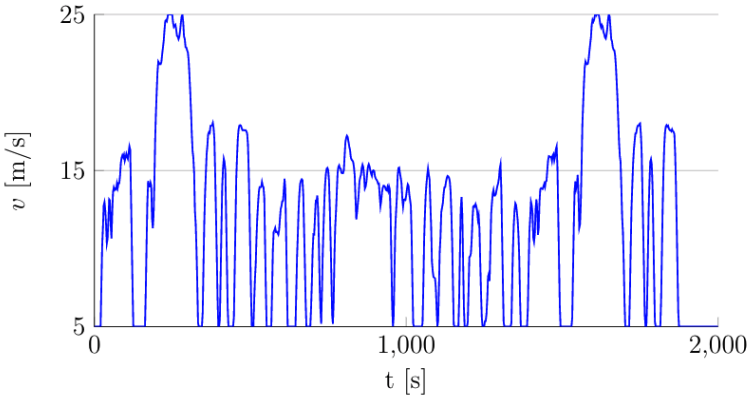

Figure 6.9: The velocity profile of leading vehicle when running EPA74 standard driving cycle.

Simulation of Leader's Ramp Speed Profile

The simulation results of the 3 topologies, i.e., NN, NNL, and 2NN, are shown in Fig. 6.5- 6.7, (a)-(c) respectively. In each figure, there are 4 subplots from top to bottom, including distance error between 2 consecutive vehicles ($\Delta d_i = e_i - e_{i-1}$), vehicle velocity ($v_i$), vehicle acceleration (a_i), and throttle angle ($\alpha_{\text{thr},i}$). One can observe that the tracking error converges to zero asymptotically for both non-zero initial condition and time-varying leader velocity. The velocity estimation of NN and 2NN topology is shown in Fig. 6.8.

Simulation of modified EPA74 speed profile

The simulation results are shown in Fig. 6.10. The used speed profile, shown in Fig 6.9, is modified from the standard EPA74 by multiplying 0.8 and then adding 5m/s point-wise. Three performance indices – tracking index (TI), acceleration standard deviation (ASD), and fuel economy (Fuel) – are used to assess the performance. The tracking index for i-th vehicle is calculated by

$$\text{TI}_i = \frac{1}{T}\int_0^T \left(|\dot{e}_i(t) \cdot SVE| + |\Delta d_i(t) \cdot SDE|\right) \mathrm{d}t,$$

where T is the simulation length, $SVE = 10$ denotes sensitivity of velocity error, and $SDE = 1$ denotes sensitivity to distance error [14]. The ASD for i-th vehicle is calculated by

$$\text{ASD}_i = \text{std}(a_i(t)),$$

where std denotes standard deviation in $t \in [0,\, T]$. The fuel economy for i-th vehicle is calculated with

$$\text{Fuel}_i = \frac{\int_0^T Q_i(t)\mathrm{d}t}{x_i(T)},$$

where Q_i denotes the engine fuel injecting rate and $x_i(t)$ is the traveling distance.

We observe from Fig. 6.10 that 2NN has superior tracking performance compared to NN, due to access to more information from neighboring nodes, in combination with the constant-distance spacing policy. The topology with full leader access (NNL), have significantly improved tracking ability compared with other topologies. These results confirm our intuitive analysis. The topological selection has less influence on the acceleration noise. In addition it is found that 2NN has worse fuel economy than NN. This phenomenon is caused by more aggressive control inputs, which come from a tighter information connection with other neighboring vehicles. More neighbor information is then beneficial to the tracking capability but unfavorable to the fuel economy. Fortunately, more leading information contributes to both tracking capability and fuel economy. Similar conclusions can be drawn from Fig. 6.12.

Remark 18. *We used a high-fidelity model in this section. The simulation result (tracking performance, velocity profile and acceleration) of the design model* (6.1)-(6.2) *is similar to the result presented in this section.*

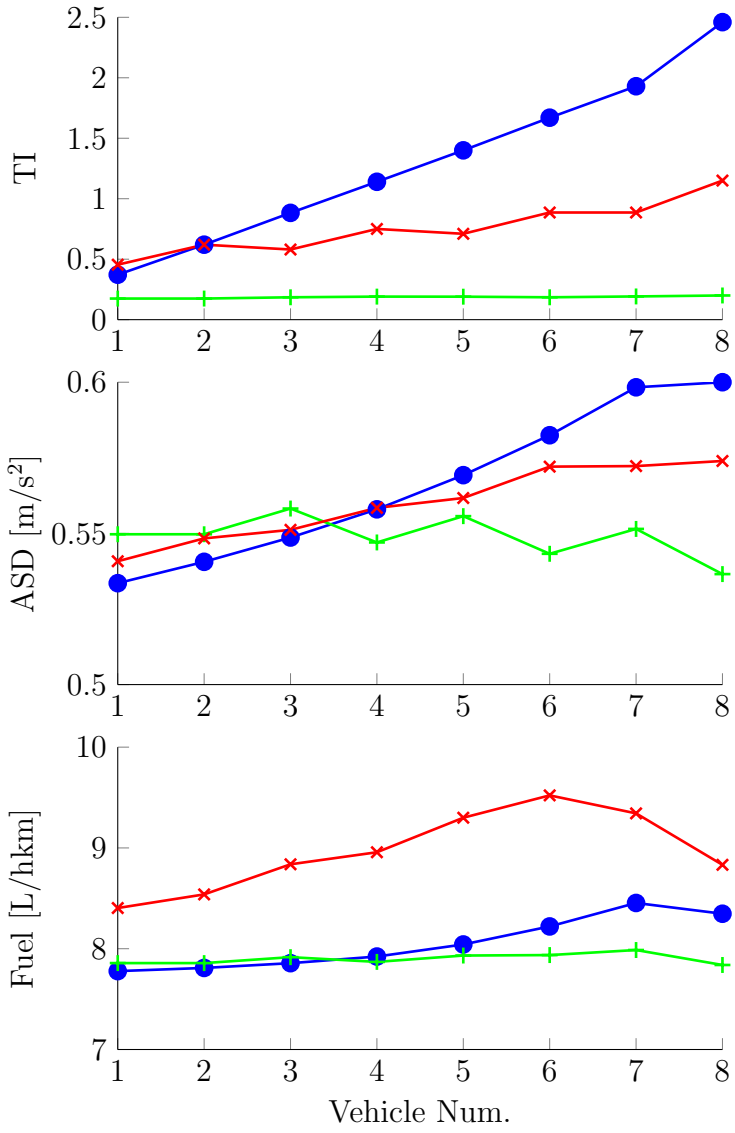

Figure 6.10: Simulation result under EPA74 scenario. From top to bottom, each subplot shows tracking index, acceleration standard deviation and fuel consumption for each vehicle. The NN, NNL, and 2NN are denoted by (—●—), (—+—), and (—×—).

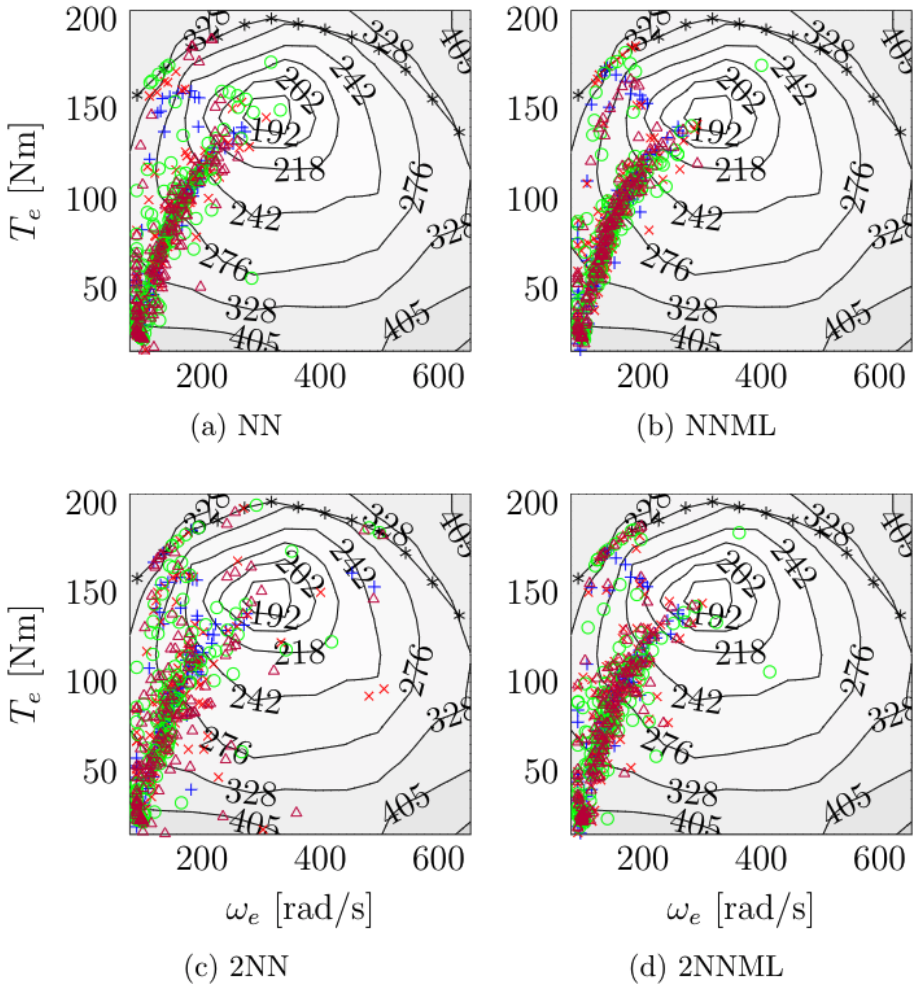

Figure 6.11: Engine operating points with a leader running EPA74 cycle. The 1st, 3rd, 5th, and 8th vehicle are denoted by (+), (×), (○), (△).

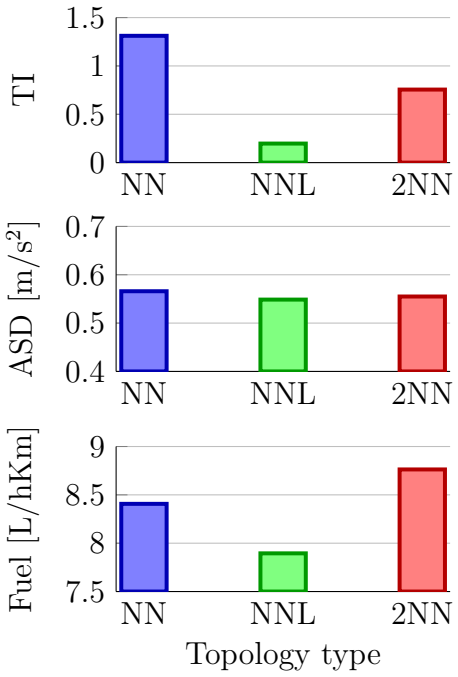

Figure 6.12: Performance analysis of 3 different topologies. Each subplot shows average performance indexes.

Chapter 7

Extensions of DSMC

7.1 Extension to MIMO systems

Consider a network of agents with multi-input-multi-output dynamics,

$$\begin{aligned}
\dot{x}_{i,1}^k =& x_{i,2}^k, \\
\dot{x}_{i,2}^k =& x_{i,3}^k, \\
&\vdots \qquad\qquad\qquad\qquad \forall k \in \{1, \cdots, M\} \\
\dot{x}_{i,n}^k =& f_i^k(\mathbf{x}_i) + \sum_{j=1}^{M} g_{i,j}^k(\mathbf{x}_i) u_i^j, \\
y_i^k =& x_{i,1}^k,
\end{aligned} \tag{7.1}$$

where u_i^k and y_i^k are the k-th input and output for the i-th node. The input, output and state vector of i-th agent are denoted as

$$\begin{aligned}
\mathbf{u}_i &= [u_i^1, u_i^2, \cdots, u_i^M]^\top \in \mathbb{R}^M, \\
\mathbf{y}_i &= [y_i^1, y_i^2, \cdots, y_i^M]^\top \in \mathbb{R}^M, \\
\mathbf{x}_i &= [\underbrace{x_{i,1}^1, x_{i,2}^1, \cdots, x_{i,n}^1}_{\mathbf{x}_i^1}, \cdots, \underbrace{x_{i,1}^M, x_{i,2}^M, \cdots, x_{i,n}^M}_{\mathbf{x}_i^M}]^\top \in \mathbb{R}^{Mn}.
\end{aligned}$$

For simpler explanation, define

$$\begin{aligned}\mathbf{f}_i(\mathbf{x}_i) =&[f_i^1(\mathbf{x}_i), f_i^2(\mathbf{x}_i), \cdots, f_i^M(\mathbf{x}_i)]^\top,\\ \mathbf{g}_i(\mathbf{x}_i) =&\begin{bmatrix} g_{i,1}^1(\mathbf{x}_i) & g_{i,2}^1(\mathbf{x}_i) & \cdots & g_{i,M}^1(\mathbf{x}_i)\\ g_{i,1}^2(\mathbf{x}_i) & g_{i,2}^2(\mathbf{x}_i) & \cdots & g_{i,M}^2(\mathbf{x}_i)\\ \vdots & \vdots & \ddots & \vdots\\ g_{i,1}^M(\mathbf{x}_i) & g_{i,2}^M(\mathbf{x}_i) & \cdots & g_{i,M}^M(\mathbf{x}_i)\end{bmatrix},\end{aligned}$$

we assume $\mathbf{g}_i(\mathbf{x}_i)$ is nonsingular for all $\mathbf{x}_i \in \mathbb{R}^{Mn}$.

Assume the output of the virtual reference model $\mathbf{y}_0 = [y_0^1, y_0^2, \cdots, y_0^M]^\top \in \mathbb{R}^M$. The consensus problem is said to be solved if

$$\mathbf{y}_i \to \mathbf{y}_0, \text{ as } t \to +\infty, \ \forall\, i \in \mathcal{V}.$$

We define the tracking error vector as

$$\mathbf{e}_i = \mathbf{y}_i - \mathbf{y}_0,$$

and the intermediate error vector as

$$\boldsymbol{\delta}_i = (I_M \otimes (\frac{\mathrm{d}}{\mathrm{d}t} + \rho)^{n-1})\mathbf{e}_i,$$

where I_M is the identity matrix of dimension M and $\rho \in \mathbb{R}_+$.

The topological sliding variable for the whole system is:

$$\mathbf{S} = (\mathcal{L} + \mathcal{P}) \otimes I_M \begin{bmatrix} \boldsymbol{\delta}_1\\ \boldsymbol{\delta}_2\\ \vdots\\ \boldsymbol{\delta}_N\end{bmatrix} = (\mathcal{L} + \mathcal{P}) \otimes I_M \boldsymbol{\Delta}, \tag{7.2}$$

where $\boldsymbol{\Delta} = [\boldsymbol{\delta}_1^\top, \boldsymbol{\delta}_2^\top, \cdots, \boldsymbol{\delta}_N^\top]^\top$. For simpler description, we define $\mathbf{s}_i \in \mathbb{R}^M$ as

$$\mathbf{s}_i = t_i^{TS}(\boldsymbol{\Delta}) = \sum_{j=1, j\neq i}^{N} a_{ij}(\boldsymbol{\delta}_i - \boldsymbol{\delta}_j) + p_i\boldsymbol{\delta}_i.$$

Therefore, we have $\mathbf{S} = [\mathbf{s}_1^\top, \mathbf{s}_2^\top, \cdots, \mathbf{s}_N^\top]^\top \in \mathbb{R}^{MN}$.

We introduce the topological reaching law as

$$\dot{\mathbf{S}} = -(\mathcal{L} + \mathcal{P}) \otimes I_M(\psi\mathbf{S} + \phi\,\mathrm{sgn}(\mathbf{S})), \tag{7.3}$$

with ψ and ϕ positive.

Static reference model

The SMC control law for static reference model based on design principal (7.2) and (7.3) is

$$\mathbf{u}_i = -\mathbf{g}_i^{-1}(\mathbf{x}_i)(\psi \mathbf{s}_i + \phi \operatorname{sgn}(\mathbf{s}_i) + \mathbf{f}_i(\mathbf{x}_i) + \boldsymbol{\gamma}(\mathbf{x}_i)), \tag{7.4}$$

where $\boldsymbol{\gamma}(\mathbf{x}_i) = [\gamma(\mathbf{x}_i^1), \gamma(\mathbf{x}_i^2), \cdots, \gamma(\mathbf{x}_i^M)]$, and $\gamma : \mathbb{R}^N \to \mathbb{R}$ is defined in (4.10).

Similar to the SISO case, we give stability justification here.

Theorem 19. *Consider a network of agents with nonlinear heterogeneous node dynamics* (7.1) *and communication topology* $\mathcal{G}$ *under Assumption 3. With the distributed control law* (7.4)*, and tuning parameters* ψ, ϕ, $\rho \in \mathbb{R}_+$*, the sliding variable* S*, defined by* (7.2)*, converges to* $\mathbf{0}$ *asymptotically.*

Proof. With the control law (7.4), the dynamics of sliding variable is

$$\dot{\mathbf{S}} = -(\mathcal{L} + \mathcal{P}) \otimes I_M(\psi \mathbf{S} + \phi \operatorname{sgn}(\mathbf{S})), \tag{7.5}$$

Define $f_{sld} : \mathbb{R}^{MN} \to \mathbb{R}^{MN}$ as

$$f_{sld}(\mathbf{S}) = -(\mathcal{L} + \mathcal{P}) \otimes I_M(\psi \mathbf{S} + \phi \operatorname{sgn}(\mathbf{S})). \tag{7.6}$$

Although f_{sld} is not Lipschitz continuous, it is measurable and essentially locally bounded. Therefore, Lemma 1 is satisfied, the Filippov solution of (7.5) exists.

From (2.5), the Filippov set-valued map associated with (7.6) is

$$\mathcal{F}[f_{sld}](S) = -(\mathcal{L} + \mathcal{P}) \otimes I_M(\psi \mathbf{S} + \phi \operatorname{sgn}(\mathcal{W})),$$

where $\mathcal{W}$ is the set defined by

$$\begin{aligned} \mathcal{W} \triangleq \operatorname{co}\{\bar{S} = [\bar{s}_1, \cdots, \bar{s}_{MN}]^\top : & \bar{s}_i = \operatorname{sgn}(s_i), \text{ if } s_i \neq 0; \\ & \bar{s}_i = \{-1, 1\}, \text{ if } s_i = 0\}, \\ \mathbf{S} = [s_1, s_2 \cdots, s_{MN}]. & \end{aligned} \tag{7.7}$$

Define $\overline{\mathcal{L} + \mathcal{P}} = (\mathcal{L} + \mathcal{P}) \otimes I_M$, and

$$\begin{aligned} \mathbf{a} =& [a_1, \cdots, a_N]^\top = (\overline{\mathcal{L} + \mathcal{P}})^{-1}\mathbf{1}, \\ \mathbf{b} =& [b_1, \cdots, b_N]^\top = (\overline{\mathcal{L} + \mathcal{P}})^{-\top}\mathbf{1}, \\ \overline{\mathcal{D}} =& \operatorname{diag}\left(\frac{b_1}{a_1}, \frac{b_2}{a_2}, \cdots, \frac{b_N}{a_N}\right), \end{aligned} \tag{7.8}$$

$$\overline{\mathcal{Q}} = \overline{\mathcal{D}}\overline{(\mathcal{L} + \mathcal{P})} + \overline{(\mathcal{L} + \mathcal{P})}^\top \overline{\mathcal{D}}, \tag{7.9}$$

then according to theorem 8, $\overline{\mathcal{D}} \succ 0$ and $\overline{\mathcal{Q}} \succ 0$.

We choose a Lyapunov candidate as

$$V_4(S) = \mathbf{S}^\top \overline{\mathcal{D}} \mathbf{S}. \tag{7.10}$$

The set-valued Lie derivative of (7.10) is

$$\begin{aligned} \mathscr{L}_{\mathcal{F}[f_{sld}]} V_3(\mathbf{S}) =& \{\nabla V_3(\mathbf{S})^\top v : v \in \mathcal{F}[f_{sld}](\mathbf{S})\} \\ =& -\psi \mathbf{S}^\top \overline{\mathcal{Q}} \mathbf{S} - 2\phi \mathbf{S}^\top \overline{\mathcal{D}(\mathcal{L}+\mathcal{P})} \mathcal{W}, \end{aligned} \tag{7.11}$$

By Theorem 8, we have $\overline{\mathcal{Q}} \succ 0$, thus the first term of (7.11) is negative for all $\mathbf{S} \in \mathbb{R}^{MN} \setminus \{\mathbf{0}\}$. By Theorem 10, all elements in the second term of (7.11) is non-positive.

Then, for all $S \in \mathbb{R}^{MN} \setminus \{\mathbf{0}\}$, we have

$$\max \mathscr{L}_{\mathcal{F}[f_{sld}]} V_3(\mathbf{S}) < 0. \tag{7.12}$$

By Lemma 3, we establish asymptotic stability of system. □

Next, we give a sufficient condition for finite-time convergence.

Corollary 6. *Consider a network of agents satisfies the hypotheses of Theorem 19. Let $\mathcal{G}_{agent}$ be undirected. Then, the sliding variable $\mathbf{S}$ converges to $\mathbf{0}$ in finite time.*

Proof. With Theorem 6, we have $\overline{\mathcal{L}+\mathcal{P}} \succ 0$. Choose the Lyapunov candidate,

$$V_4(\mathbf{S}) = \frac{1}{2} \mathbf{S}^\top \overline{(\mathcal{L}+\mathcal{P})}^{-1} \mathbf{S}.$$

Taking the set-valued Lie derivative, we have

$$\begin{aligned} \mathscr{L}_{\mathcal{F}[f_{sld}]} V_4(\mathbf{S}) =& \{-\psi \|\mathbf{S}\|_2^2 - \phi \mathbf{S}^\top \operatorname{sgn}(\mathbf{S})\} \\ =& \{-\psi \|\mathbf{S}\|_2^2 - \phi \|\mathbf{S}\|_1\} \end{aligned}$$

Since $\|\mathbf{S}\|_1 \geq \|\mathbf{S}\|_2$, we have

$$\max \mathscr{L}_{\mathcal{F}[f_{sld}]} V_4(\mathbf{S}) \leq -\psi \|\mathbf{S}\|_2^2 - \phi \|\mathbf{S}\|_2. \tag{7.13}$$

Instead of proving the finite-time convergence of S directly, we prove that $\sqrt{2V_4} = \|(\overline{\mathcal{L}+\mathcal{P}})^{-\frac{1}{2}} \mathbf{S}\|_2$ converges to 0 in finite time. For $\mathbf{S} \in \mathbb{R}^{MN} \setminus \{\mathbf{0}\}$, the set-valued Lie derivative of $\sqrt{2V_4}$ is

$$\mathscr{L}_{\mathcal{F}[f_{sld}]}\sqrt{2V_4} = \frac{1}{\|(\overline{\mathcal{L}+\mathcal{P}})^{-\frac{1}{2}}\mathbf{S}\|_2}\mathscr{L}_{\mathcal{F}[f_{sld}]}V_4. \tag{7.14}$$

By Rayleigh's quotient, we have

$$\|(\overline{\mathcal{L}+\mathcal{P}})^{-\frac{1}{2}}\mathbf{S}\|_2 \leq \frac{1}{\sqrt{\lambda_{\min}(\overline{\mathcal{L}+\mathcal{P}})}}\|\mathbf{S}\|_2. \tag{7.15}$$

From (7.13), (7.14), and (7.15), one can establish

$$\max \mathscr{L}_{\mathcal{F}[f_{sld}]}\sqrt{2V_4} \leq -\sqrt{\lambda_{\min}(\overline{\mathcal{L}+\mathcal{P}})}\phi.$$

From Lemma 2, we have

$$\frac{\mathrm{d}}{\mathrm{d}t}\|(\overline{\mathcal{L}+\mathcal{P}})^{-\frac{1}{2}}\mathbf{S}(t)\|_2 \in \mathscr{L}_{\mathcal{F}[f_{sld}]}\sqrt{2V_4} \tag{7.16}$$

for almost every $t \in [0, +\infty)$. We have

$$\begin{aligned}\|(\overline{\mathcal{L}+\mathcal{P}})^{-\frac{1}{2}}\mathbf{S}(t_f)\|_2 =& \|(\overline{\mathcal{L}+\mathcal{P}})^{-\frac{1}{2}}\mathbf{S}(0)\|_2 \\ &+ \int_0^{t_f}\frac{\mathrm{d}}{\mathrm{d}\tau}\|(\overline{\mathcal{L}+\mathcal{P}})^{-\frac{1}{2}}\mathbf{S}(\tau)\|_2\mathrm{d}\tau.\end{aligned} \tag{7.17}$$

With (7.16) and (7.17), in the region $\mathbb{R}^{MN} \setminus \{\mathbf{0}\}$, we have

$$\begin{aligned}\|(\overline{\mathcal{L}+\mathcal{P}})^{-\frac{1}{2}}\mathbf{S}(t_f)\|_2 \leq& \|(\overline{\mathcal{L}+\mathcal{P}})^{-\frac{1}{2}}\mathbf{S}(0)\|_2 \\ &-t_f\phi\sqrt{\lambda_{\min}(\overline{\mathcal{L}+\mathcal{P}})}.\end{aligned}$$

We argue that there must exist t_f such that $\mathbf{S}(t_f) = \mathbf{0}$. Otherwise, $\|(\overline{\mathcal{L}+\mathcal{P}})^{-\frac{1}{2}}\mathbf{S}(t_f)\|_2 \to -\infty$ as $t_f \to +\infty$. □

In the sliding phase we also use Lemma 7 to justify the following theorem.

Theorem 20. *Consider a network of agents satisfies the hypotheses of Theorem 19. The tracking error* $\mathbf{e}_i(t)$ *for each agent converges to* $\mathbf{0}$ *asymptotically.*

Active reference model

Assume active reference model

$$\begin{aligned}\dot{\mathbf{x}}_0 =& A_0\mathbf{x}_0,\\ \mathbf{y}_0 =& C_0\mathbf{x}_0,\end{aligned}$$

where $\mathbf{x}_0 \in \mathbb{R}^q$, $\mathbf{y}_0 \in \mathbb{R}^M$, $A_0 \in \mathbb{R}^{q\times q}$, and $C_0 \in \mathbb{R}^{M\times q}$. The objective of control design is to achieve:

$$\mathbf{y}_i(t) \to \mathbf{y}_0(t), \text{ as } t \to +\infty, \forall i \in \mathcal{V}.$$

with the same sliding variable (7.2), reaching law (7.3) and distributed observer (4.14), we get the distributed control law:

$$\mathbf{u}_i = -\mathbf{g}_i^{-1}(\mathbf{x}_i)(\psi\mathbf{s}_i + \mathbf{f}_i(\mathbf{x}_i) + \boldsymbol{\gamma}(\mathbf{x}_i) - \boldsymbol{\zeta}(\hat{\mathbf{x}}_{0,i})), \tag{7.18}$$

where $\boldsymbol{\zeta} : \mathbb{R}^q \to \mathbb{R}^M$ is defined as:

$$\boldsymbol{\zeta}(\hat{\mathbf{x}}_{0,i}) = \sum_{k=0}^{n-1} \binom{n-1}{k} \rho^k C_0 A_0^{n-k} \hat{\mathbf{x}}_{0,i}.$$

The stability result is similar to the SISO case and is presented as follows.

Theorem 21. *Consider a network of agents with nonlinear heterogeneous node dynamics* (7.1) *and communication topology* $\mathcal{G}$ *under Assumption 1. With the distributed control law* (7.18)*, and the distributed observer* (4.14) *with a sufficient large positive* k*, both the sliding variable* S *in* (7.2) *and the observing error* E *converge to* $\mathbf{0}$ *asymptotically.*

Proof. First, we prove observing error E converges to $\mathbf{0}$ asymptotically. The observing error dynamics is

$$\dot{E} = (I_N \otimes A_0 - k(\mathcal{L} + \mathcal{P}) \otimes I_q)E. \tag{7.19}$$

From [65], the eigenvalues of $I_N \otimes A_0 - k(\mathcal{L} + \mathcal{P}) \otimes I_q$ are:

$$\{\lambda_i(A_0) - k\lambda_j(\mathcal{L} + \mathcal{P}) : i \in \{1, \cdots, q\};\, j \in \{1, \cdots, N\}\}$$

where $\lambda_i(A_0)$ and $\lambda_j(\mathcal{L} + \mathcal{P})$ are the eigenvalues of A_0 and $\mathcal{L} + \mathcal{P}$, respectively. With a sufficient large k, we can ensure all the eigenvalues of $I_N \otimes A_0 - k(\mathcal{L} + \mathcal{P}) \otimes I_q$ on the left-half complex plane. Then, we conclude asymptotic stability of system (7.19).

Secondly, we prove the asymptotic convergence of sliding variable. The dynamics of sliding variable is

$$\dot{\mathbf{S}} = -\psi(\overline{\mathcal{L}+\mathcal{P}})S + \overline{\zeta}(E),$$

where $\overline{\zeta} : \mathbb{R}^{qN} \to \mathbb{R}^{MN}$ defined as

$$\begin{aligned}\overline{\zeta}(E) =& T^{TS}(\begin{bmatrix} \zeta(\epsilon_1) \\ \vdots \\ \zeta(\epsilon_N) \end{bmatrix}) \\ =& (\overline{\mathcal{L}+\mathcal{P}}) \begin{bmatrix} \zeta(\epsilon_1) \\ \vdots \\ \zeta(\epsilon_N) \end{bmatrix} = (\mathcal{L}+\mathcal{P}\otimes I_M) \begin{bmatrix} \zeta(\epsilon_1) \\ \vdots \\ \zeta(\epsilon_N) \end{bmatrix}.\end{aligned} \tag{7.20}$$

From (7.20), we see $\overline{\zeta}$ is linear. Since $\overline{\zeta}(E) \to \mathbf{0}$ and $-\psi(\overline{\mathcal{L}+\mathcal{P}})$ is Hurwitz, we conclude $\mathbf{S} \to \mathbf{0}$ as $t \to +\infty$ by Lemma 7. □

Leaderless Consensus

For leaderless consensus, the consensus problem is said to be solved if

$$\|\mathbf{y}_i - \mathbf{y}_j\| \to 0, \text{ as } t \to +\infty, \ \forall\, i, j \in \mathcal{V}.$$

We define the intermediate error vector as:

$$\boldsymbol{\delta}_i = (I_M \otimes (\frac{\mathrm{d}}{\mathrm{d}t} + \rho)^{n-1})\mathbf{y}_i, \tag{7.21}$$

where I_M is the identity matrix of dimension M and $\rho \in \mathbb{R}_+$. Since the multi-agent system is leaderless, the topological sliding variable for the whole system is:

$$\mathbf{S} = \mathcal{L} \otimes I_M \begin{bmatrix} \boldsymbol{\delta}_1 \\ \boldsymbol{\delta}_2 \\ \vdots \\ \boldsymbol{\delta}_N \end{bmatrix} = \mathcal{L} \otimes I_M \boldsymbol{\Delta}, \tag{7.22}$$

where $\boldsymbol{\Delta} = [\boldsymbol{\delta}_1^\top, \boldsymbol{\delta}_2^\top, \cdots, \boldsymbol{\delta}_N^\top]^\top$.

For simpler description, we define $\mathbf{s}_i \in \mathbb{R}^M$ as

$$\begin{aligned}\mathbf{s}_i =& t_i^{TS}(\boldsymbol{\Delta}) = \sum_{j=1, j\neq i}^{N} a_{ij}(\boldsymbol{\delta}_i - \boldsymbol{\delta}_j) + 0\boldsymbol{\delta}_i \\ =& \sum_{j=1, j\neq i}^{N} a_{ij}(\boldsymbol{\delta}_i - \boldsymbol{\delta}_j)\end{aligned}$$

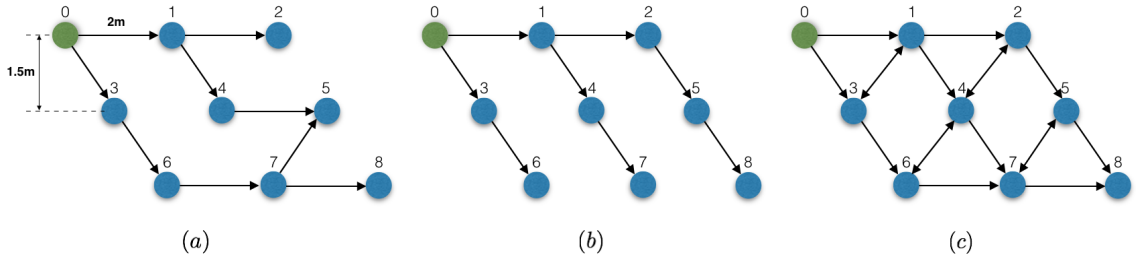

Figure 7.1: Desired formation of networked system under three different information flow topologies.

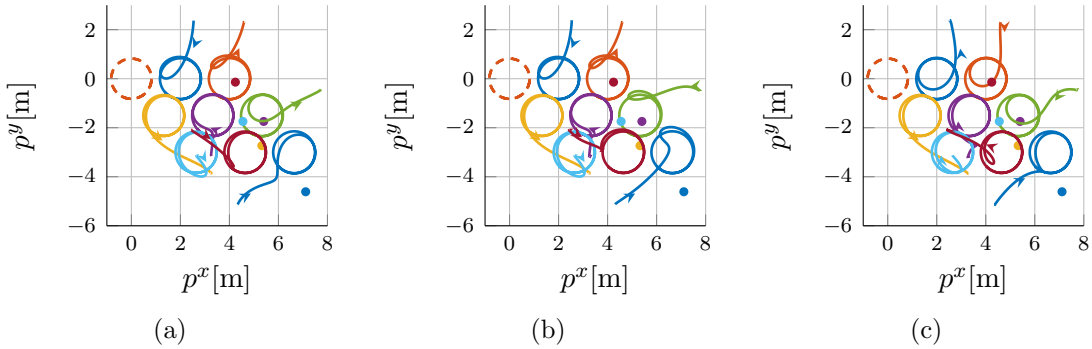

Figure 7.2: Position of the leader and agents under three different information topologies.

We then give the control law as:

$$\mathbf{u}_i = -\mathbf{g}_i^{-1}(\mathbf{x}_i)(\psi \mathbf{s}_i + \phi \operatorname{sgn}(\mathbf{s}_i) + \mathbf{f}_i(\mathbf{x}_i) + \boldsymbol{\gamma}(\mathbf{x}_i)), \tag{7.23}$$

where $\boldsymbol{\gamma}(\mathbf{x}_i) = [\gamma(\mathbf{x}_i^1), \gamma(\mathbf{x}_i^2), \cdots, \gamma(\mathbf{x}_i^M)]$, and $\gamma : \mathbb{R}^N \to \mathbb{R}$ is defined in (4.10).

The stability justification follows:

Theorem 22. *Consider a network of agents with nonlinear heterogeneous node dynamics* (7.1) *and communication topology* $\mathcal{G}$ *under Assumption 3. With the distributed control law* (7.23)*, and tuning parameters* ψ, ϕ, $\rho \in \mathbb{R}_+$, *the sliding variable* $\mathbf{S}$, *defined by* (7.22)*, converges to a consensus equilibrium* $\mathbf{S}^* = c\mathbf{1}$ *asymptotically, where* $c \in \mathbb{R}$. *This means* $\lim_{t\to\infty} \|\mathbf{s}_i(t) - \mathbf{s}_j(t)\| = 0$.

The proof is similar to theorem 15.

7.2 Applications of MIMO DSMC

In this section, we apply the DSMC to a consensus problem with MIMO dynamics.

Consider a unicycle model with extended dynamics [59] on a 2D plane,

$$\begin{aligned} \dot{p}_i^x =& \cos\theta_i v_i, \\ \dot{p}_i^y =& \sin\theta_i v_i, \\ \dot{v}_i =& u_{i,1}, \\ \dot{\theta}_i =& u_{i,2}, \end{aligned} \tag{7.24}$$

where the input is $\mathbf{u}_i = [u_{i,1},\, u_{i,2}]^\top$, position $\mathbf{p}_i = [p_i^x,\, p_i^y]^\top$ is the output.

The dynamics (7.24) can also be written as

$$\ddot{\mathbf{p}}_i = \begin{bmatrix} \cos\theta_i & -v_i\sin\theta_i \\ \sin\theta_i & v_i\cos\theta_i \end{bmatrix} \mathbf{u}_i. \tag{7.25}$$

We assume the reference signal $\mathbf{p}_0$ generated by

$$\dot{\mathbf{p}}_0(t) = \underbrace{\begin{bmatrix} 0 & 1 \\ -1 & 0 \end{bmatrix}}_{A_0} \mathbf{p}_0(t),$$

with initial condition $\mathbf{p}_0(0) = [0.82,\, 0]^\top$.

We define the tracking error and intermediate error as

$$\begin{aligned} \mathbf{e}_i =& \mathbf{p}_i - \mathbf{p}_0, \\ \boldsymbol{\delta}_i =& (I_2 \otimes (\frac{\mathrm{d}}{\mathrm{d}t} + \rho))\mathbf{e}_i. \end{aligned}$$

With the sliding variable (7.2), reaching law (7.3) and distributed observer (4.14), we get the following distributed control law:

$$\begin{aligned} \mathbf{u}_i = & \begin{bmatrix} \cos\theta_i & \sin\theta_i \\ -\frac{\sin\theta_i}{v_i} & \frac{\cos\theta_i}{v_i} \end{bmatrix} \cdot (-\psi\mathbf{s}_i - \phi\,\mathrm{sgn}(\mathbf{s}_i) \\ & - \rho \begin{bmatrix} \cos\theta_i v_i \\ \sin\theta_i v_i \end{bmatrix} + (A_0^2 + \rho A_0)\hat{\mathbf{p}}_{0,i}), \end{aligned} \tag{7.26}$$

where $\hat{\mathbf{p}}_{0,i}$ is the estimated $\mathbf{p}_0$ for the i-th node.

We conducted numerical simulation under three different information flow topologies, shown in Fig. 7.1. We choose the tuning parameter as follows: $k = 2$, $\psi = 2$, $\phi = 0$, and $\rho = 1$. Fig. 7.2 shows the position portrait of the multi-agent system.

7.3 Graph Robustness and DSMC

One of the important aspect of consensus is to study the influence of information exchange topology on the closed-loop performance with respect to consensus and robustness. In this section, we will discuss MIMO DSMC as the tool to study graph robustness.

In [42, 30], an optimal control framework specialized to large-scale distributed systems is developed. This framework introduces a sparsity penalty on the controller structure into a standard optimal control setting, indicating a design preference for decentralized and localized control schemes with limited communication between subsystems. Recent work by [76, 24] extend these ideas to the consensus and synchronization setting. Here, the pursuit of sparsity is particularly well motivated. For example, the application of classical optimal control strategies can often result in feedback laws that require dense communication networks which are not practical for real-world implementation. Penalizing the structure of the control law is critical to constructing an effective framework for control design. Naturally, balancing the performance of the closed-loop system (e.g. response times and robustness to disturbances/uncertainty) with the sparsity of the feedback law leads to an interesting tradeoff problem.

The sparsity-promoting optimal control framework for multi-agent consensus

Here, we review the *sparsity-promoting optimal control* method in the context of consensus and synchronization problems. This approach was developed in [42, 30] and specialized to consensus and synchronization in recent work by [76, 24].

Consider the following undirected consensus network,

$$\begin{aligned} \dot{\mathbf{x}} &= -\mathcal{L}_p\mathbf{x} + \mathbf{u} + \mathbf{d}, \\ \mathbf{u} &= -\mathcal{L}_c\mathbf{x} \end{aligned} \tag{7.27}$$

where $\mathbf{x} \in \mathbb{R}^N$ is the state, $\mathcal{L}_p$ is the Laplacian of the open-loop system (i.e., the plant), $\mathbf{u}$ is the control action, and $\mathbf{d}$ represent a disturbance. $\mathcal{L}_c$ is a weighted Laplacian, which implies that the control associated with the ith node takes the form $u_i = -\sum_{j=1}^{n} w_{ij}(x_i - x_j)$.

In the context of control design, $\mathcal{L}_p$ is given and $\mathcal{L}_c$ is to be designed. Let $\mathcal{I}_c$ be the collection of all nodal pairs (i, j) that we are allowed to connect using the controller. For example, this set may contain all edges not contained in the open-loop

system. The control Laplacian may be rewritten as,

$$\mathcal{L}_c = \sum_{l \in \mathcal{I}_c} w_l \xi_l \xi_l^\top = \mathbf{E}_c \mathrm{diag}(\mathbf{w}) \mathbf{E}_c^\top \tag{7.28}$$

where $\mathbf{E}_c$ is the incidence matrix associated with $\mathcal{I}_c$ and the ξ are the corresponding column vectors. Note that the weight vector $\mathbf{w}$ is the design variable.

The sparsity-promoting optimal control framework is made up of a two-stage process. First, the sparsity structure of the optimal control is identified by solving,

$$w' = \underset{w}{\mathrm{argmin}} \; J(w) + \gamma \|w\|_1 \tag{7.29}$$

where $J(w)$ is the performance objective and γ is a regularization parameter. The second stage, referred to as *polishing*, solves the unregularized problem ($\gamma = 0$) but subject to the previously identified sparsity structure,

$$\begin{aligned} w^\star = \underset{w}{\mathrm{argmin}} \; & J(w) + \gamma \|w\|_1 \\ \text{s.t.} \quad & \mathrm{supp}(w) \subseteq \mathrm{supp}(w') \end{aligned} \tag{7.30}$$

In [42, 76], the performance objective is chosen as the $\mathcal{H}_2$ norm of the closed-loop system, which quantifies the steady-state variance amplification (of the disturbance) and is parameterized by two penalty matrices: $\mathbf{Q}$, which is used to form a quadratic penalty on the state, and $\mathbf{R}$, which is used to form a quadratic penalty on the control. Typically, $\mathbf{Q} = \mathbf{I} - \frac{1}{n}\mathbf{1}\mathbf{1}^\top$ and $\mathbf{R} = \mathbf{I}$. Note, the state penalty $\mathbf{x}^\top \mathbf{Q} \mathbf{x} = \|\mathbf{x} - [\frac{1}{n}\mathbf{1}^\top x]\mathbf{1}\|_2^2$ and thus punishes deviations from the network average.

As demonstrated in [24], the sparsity-promoting framework described above can be specialized to the consensus setting by,

$$J(w) = \langle G(w)^{-1}, Q + L_c R L_c \rangle \tag{7.31}$$

where $G(w) = L_p + L_c + \frac{1}{n}\mathbf{1}\mathbf{1}^\top$ is the "strengthened" closed-loop plant and adding the constraint $G(w) \succ 0$ to produce

$$\begin{aligned} w' = & \underset{w}{\mathrm{argmin}} \; J(w) + \gamma \|w\|_1 \\ & \text{s.t.} \quad G(w) \succ 0. \end{aligned} \tag{7.32}$$

Note, the linear matrix inequality constraint $G(w) \succ 0$ implies that the closed-loop plant is positive definite on the space $\mathbf{1}^\perp$. To see this, note that the constraint implies that for any $\mathbf{z} \in \mathbf{1}^\perp$, $\mathbf{z}^\top G(w) \mathbf{z} = \mathbf{z}^\top (\mathcal{L}_p + \mathcal{L}_c) \mathbf{z} > 0$. Hence, the closed-loop

Laplacian has only a single zero eigenvalue and the resulting network is connected, thus guaranteeing consensus. Importantly, (7.32) is a convex optimization. $J(w)$ is convex with a Lipschitz continuous gradient, with derivatives computed in [24, 20].

Following standard techniques, the objective in (7.32) can minimized by the proximal gradient method, leading to the following iteration.

$$w^{k+1} = \text{soft}(w^k - \alpha_k \nabla J(w^k), \gamma\alpha_k). \tag{7.33}$$

where $\text{soft}(\cdot,\cdot)$ refers to the soft-thresholding function (proximal operator of $\|\cdot\|_1$). A key challenge, however, is the choice of stepsize α_k since the Lipschitz constant of ∇J exists but is unknown. To address this, [24] suggests the stepsize to be determined at each iteration by backtracking to ensure the appropriate descent condition as well as feasibility:

- $J(w^{k+1}) \leq J(w^k) + \nabla J(w^k)^\top (w^{k+1} - w^k) + \dfrac{1}{2\alpha_k}\|w^{k+1} - w^k\|_2^2$ (7.34)
- $G(w^{k+1}) \succ 0$

Interestingly, we found that we could not replicate the results of [24] by simply applying the proximal gradient method for a wide selection of γ. In several trials, we ended up with weight vectors with many small but non-negligible entries, which corresponded to dense communication networks. In order to verify our implementation, we compared our results to that of the *graphsp* MATLAB implementation developed by [24]. We found that the inclusion of a greedy modification significantly improved the result. This modification essentially applied the proximal gradient method iteratively for increasing γ, where at each iteration the support of the decision variable w was restricted to the support found in the previous iteration. The results in the following section were produced using this algorithm.

DSMC control example

Consider agent dynamics (7.25), we define an intermediate variable for each agent:

$$\boldsymbol{\delta}_i = (\mathbf{I}_2 \otimes (\frac{\mathrm{d}}{\mathrm{d}t} + \rho))\mathbf{p}_i, \tag{7.35}$$

where I_2 denotes the second order identity matrix, and $\rho \in \mathbb{R}_+$ is a tuning parameter.

We define the topological sliding mode variable for the whole system

$$\mathbf{S} := (\mathcal{L}_p + \mathcal{L}_c) \otimes \mathbf{I}_2 \begin{bmatrix} \boldsymbol{\delta}_1 \\ \boldsymbol{\delta}_2 \\ \vdots \\ \boldsymbol{\delta}_N \end{bmatrix} = (\mathcal{L} \otimes \mathbf{I}_2)\boldsymbol{\Delta}, \tag{7.36}$$

where $\mathcal{L} := \mathcal{L}_c + \mathcal{L}_p$, and $\boldsymbol{\Delta} = [\boldsymbol{\delta}_1^\top, \boldsymbol{\delta}_2^\top, \cdots, \boldsymbol{\delta}_N^\top]^\top$.

For simpler description, we denote the adjacency matrix corresponding to $\mathcal{L} = \mathcal{L}_c + \mathcal{L}_p$ as $\mathcal{A}$. Then we define $\mathbf{s}_i \in \mathbb{R}^2$ as

$$\mathbf{s}_i := \sum_{j=1, j\neq i}^{N} a_{ij}(\boldsymbol{\delta}_i - \boldsymbol{\delta}_j), \tag{7.37}$$

where a_{ij} is the (i,j)-th term of $\mathcal{A}$. Therefore, we have $\mathbf{S} = [\mathbf{s}_1^\top, \mathbf{s}_2^\top, \cdots, \mathbf{s}_N^\top]^\top \in \mathbb{R}^{2N}$.

With the sliding variable (7.36), we present the following distributed control law:

$$\begin{aligned} \mathbf{u}_i = &\begin{bmatrix} \cos\theta_i & \sin\theta_i \\ -\frac{\sin\theta_i}{v_i} & \frac{\cos\theta_i}{v_i} \end{bmatrix} \cdot (-\psi \mathbf{s}_i - \phi\, \mathrm{sgn}(\mathbf{s}_i) \\ &- \rho \begin{bmatrix} \cos\theta_i v_i \\ \sin\theta_i v_i \end{bmatrix}), \end{aligned} \tag{7.38}$$

with ψ and ϕ positive.

The stability is justified with Theorem 22.

We conducted numerical simulation under two different randomly generated plant topologies. In Fig.7.3-7.8, we showed the simulation of how the sparsity-promoted control completes the disconnected graph with different sparsity weights. In the first row of both figures, we plot the information topologies; the second row showcases the phase portrait; and the third row displays the time-domain signal plots.

In Figure 7.3 and Fig. 7.6, we witnessed the fragmentation phenomena of the closed-loop system with a disconnected information topology. In systems with connected topologies, we see the consensus is achieved; also we find that under different linkages, the convergence behaviors/patterns and rates are significantly different.

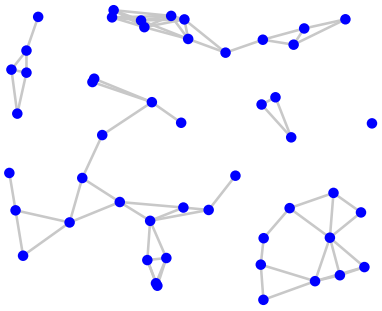

(a) plant topology (A)

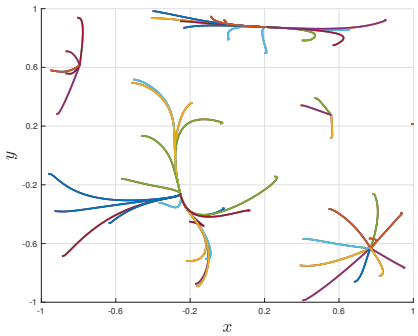

(b) Consensus of plant (A)

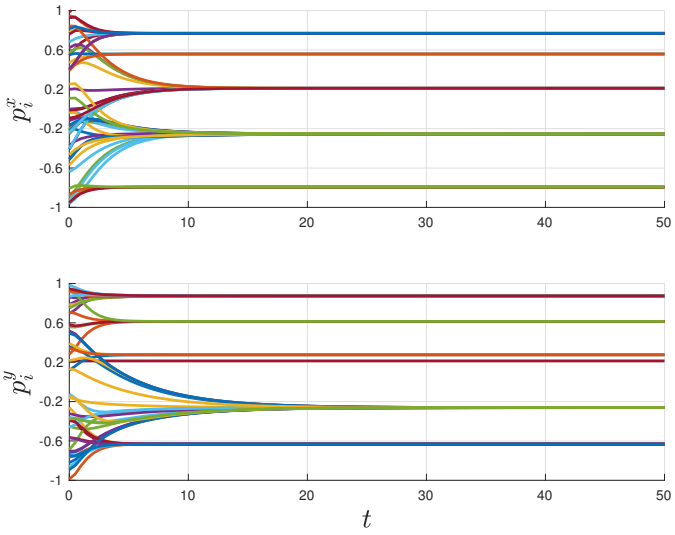

(c) time signal

Figure 7.3: Topology (A). The first row is the information flow topology (A), the second row is the phase portrait, the third row is the response in time domain.

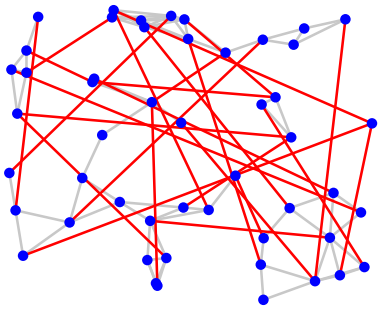

(a) plant topology (A) with dense link

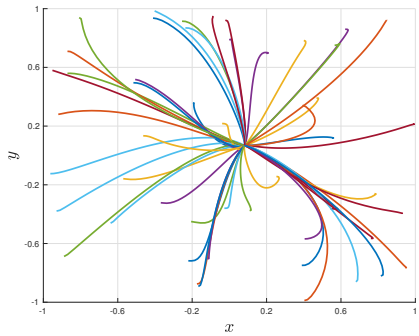

(b) Consensus of plant (A) with dense link

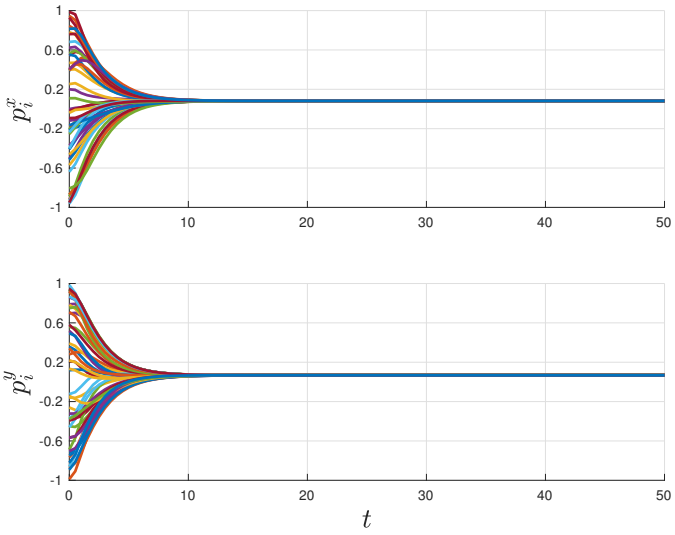

(c) time signal

Figure 7.4: Topology (A) with dense link. The first row is the information flow topology (A) with dense link, the second row is the phase portrait, the third row is the response in time domain.

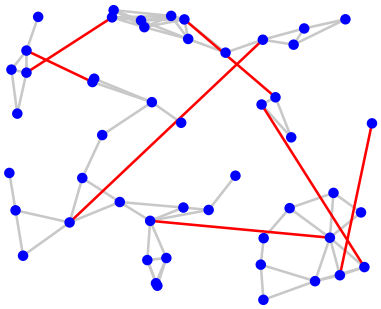

(a) plant topology (A) with sparse link

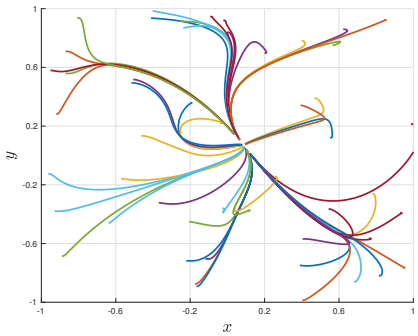

(b) Consensus of plant (A) with sparse link

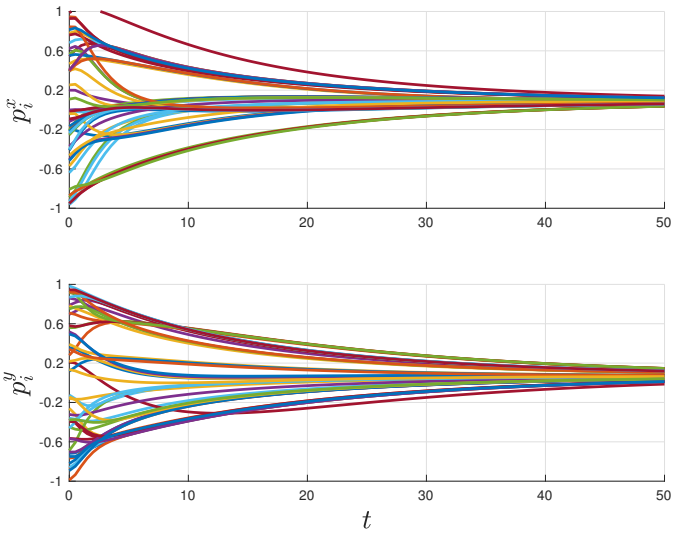

(c) time signal

Figure 7.5: Topology (A) with sparse link. The first row is the information flow topology (A) with sparse link, the second row is the phase portrait, the third row is the response in time domain.

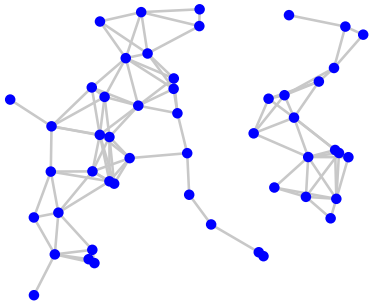

(a) plant topology (B)

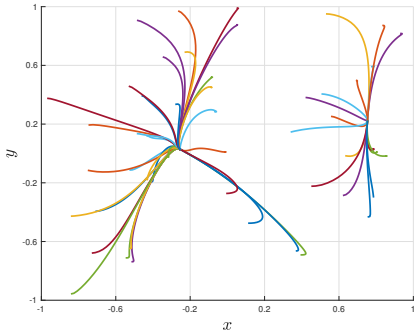

(b) Consensus of plant (B)

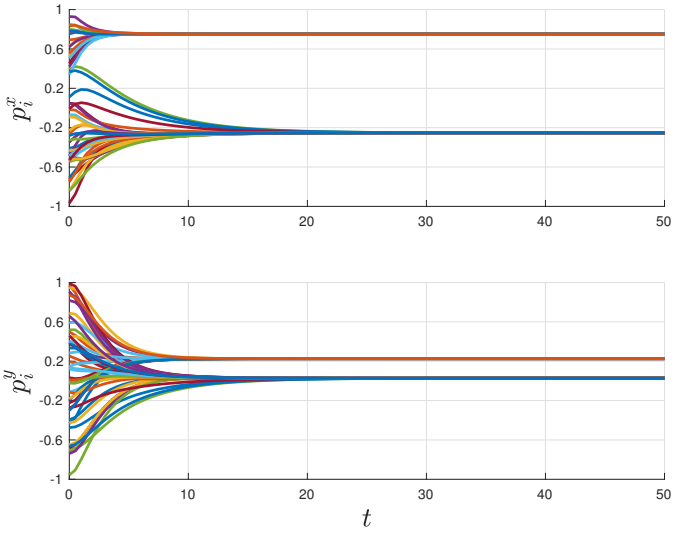

(c) time signal

Figure 7.6: Topology (8). The first row is the information flow topology (A), the second row is the phase portrait, the third row is the response in time domain.

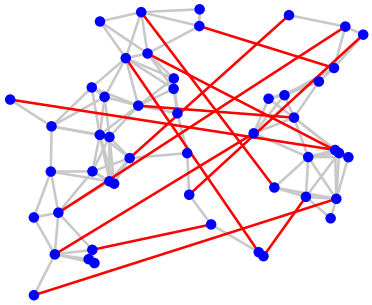

(a) plant topology (B) with dense link

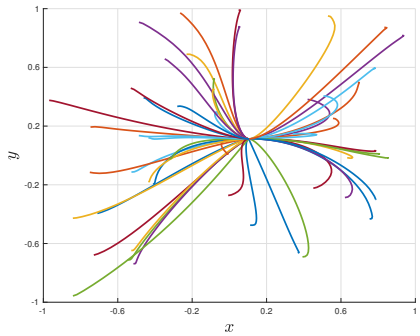

(b) Consensus of plant (B) with dense link

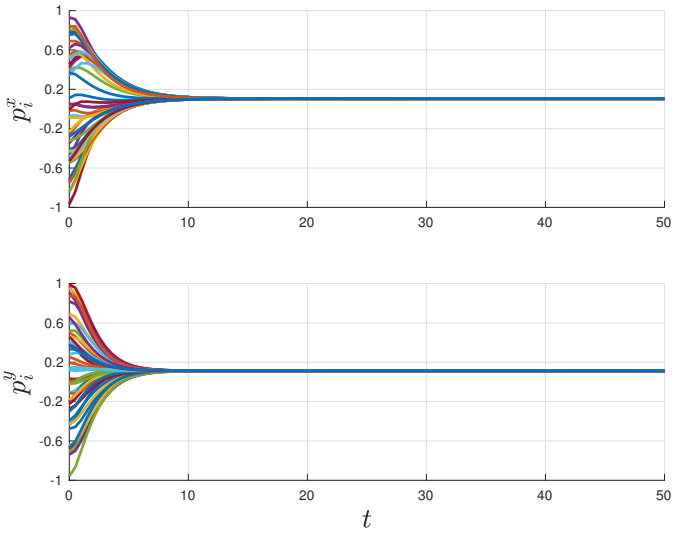

(c) time signal

Figure 7.7: Topology (B) with dense link. The first row is the information flow topology (B) with dense link, the second row is the phase portrait, the third row is the response in time domain.

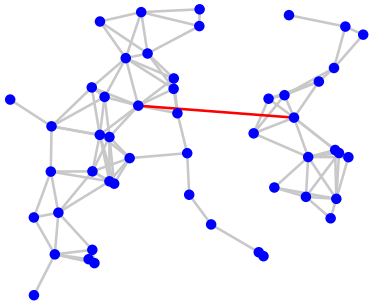

(a) plant topology (B) with sparse link

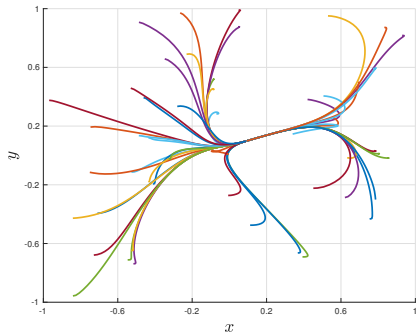

(b) Consensus of plant (B) with sparse link

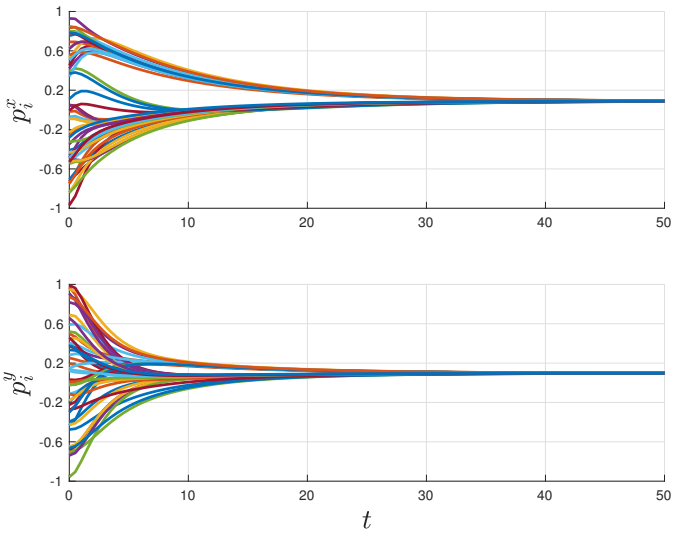

(c) time signal

Figure 7.8: Topology (B) with sparse link. The first row is the information flow topology (B) with sparse link, the second row is the phase portrait, the third row is the response in time domain.

Chapter 8

Conclusion

In this dissertation, we presented a distributed sliding mode control design framework for nonlinear heterogeneous multi-agent systems. We proposed a new "topologically structured function" that is used to construct the topological sliding surface and reaching law. This design results naturally in a distributed control architecture. The distributed control law is obtained by properly matching the topological sliding surface and topological reaching law. The consensus problem is significantly simplified by casting N interconnected higher-order dynamics into N-th order sliding variable. The stability and convergence property are proved in the sense of Filippov to cope with the discontinuity originated from switching terms.

The advantage of this framework is it explicitly supports both consensus problems with/without leader. It also incorporates all possible information topologies ranging from undirected topology to directed topologies with a spanning tree, and gives stability justifications for each one of them. Also, it fits all nonlinear feedback-linearizable systems.

8.1 Summary

In Chapter 2, we reviewed the contents in discontinuous dynamical systems since in sliding mode control, discontinuities are intentionally designed to achieve regulation and stabilization.

In Chapter 3 we have introduced basic concepts of graph theory, adjacency matrix, Laplacian matrix, and incident matrix. Then we introduced how the connectivity of the graph affects the algebraic results of these matrices.

In Chapter 4, we presented the problem formulation. We started construction from the definition of the topological structured function, then used this function

to construct both topological sliding surface and topological reaching law. We also introduced variation of the design under three different cases: 1. without a leader, 2. with a static leader, 3. with an active leader.

In Chapter 5, we have studied the stability results of the DSMC. We discussed that under different topologies, the stability results can vary. We give sufficient conditions on Lyapunov stability, finite-convergence, and input-to-state stability. We made the discussion on robustness by characterizing the input-output relations.

In Chapter 6, we applied the DSMC framework to a platooning system. We introduced a simplified velocity observer for easier implementation. In addition, we have a discussion on the propagation of disturbance and topology.

In Chapter 7, we extend the DSMC framework to MIMO systems. We showed corresponding stability results. We also illustrated an application of using DSMC to study the sparsity-promoting optimal control framework.

8.2 Future directions

Despite the recent progress in the study of consensus problems, numerous open questions of scientific and practical interest remain unanswered. We describe a few promising projects, emphasizing motivations, prospects and potential rewards for each of them.

How to characterize disturbance propagation for a multi-agent system with general topologies?

In vehicle platooning, there is a commonly used definition called "string stability". As discussed earlier, the definition of "strong string stability" as given in (6.32) or as given in [51] relies on a specific information flow topology. The structure of the system (6.32) implies that the error propagates from the front cars to the rear cars. Without (6.32), the definition reduces to normal Lyapunov stability of the whole platoon. The definition in [51] is based on the predecessor following topology, and does not apply to other other information flow topology, since the existence of $G_{i-1,i}$ is not guaranteed.

The question for us is to develop so-called "string stability" for general consensus problem. This notion will be useful for future autonomous driving systems with V2V and V2X for the purpose of collision avoidance.

How to keep a balance between graph sparsity and system robustness?

A critical issue arising from multi-agent systems is the influence of the information exchange topology on the closed-loop performance with respect to consensus and robustness. Designing information topologies that are both efficient and satisfy these important criteria can become a challenge, particularly when only limited communication between individual agents or groups of agents is possible. Many of the recent researches [24, 20, 42, 76], gives us a direction. However, there is a still a gap between the theory and application here. Maybe some of the theorems in compressed sensing, and sparsity promoting optimization can give us an answer in the future.

How to tame under-actuated dynamics?

In traditional nonlinear control, we deal with mostly fully actuated systems. Currently, the DSMC control can deal with all feedback-linearizable systems. However, many of the prospective applications of consensus have under-actuated systems, for example: airplanes, automobiles, and robots. There are many explorations in this area to be done. The geometric control [7] provides us some ideas on how to deal with the under-actuated systems.

Bibliography

[1] Luigi Ambrosio. "A lower closure theorem for autonomous orientor fields". In: *Proceedings of the Royal Society of Edinburgh Section A: Mathematics* 110.3-4 (1988), pp. 249–254.

[2] Murat Arcak. "Passivity as a design tool for group coordination". In: *IEEE Transactions on Automatic Control* 52.8 (2007), pp. 1380–1390.

[3] Andrea Bacciotti. "Some remarks on generalized solutions of discontinuous differential equations". In: *INTERNATIONAL JOURNAL OF PURE AND APPLIED MATHEMATICS.* 10 (2004), pp. 257–266.

[4] Prabir Barooah and Joao P Hespanha. "Error amplification and disturbance propagation in vehicle strings with decentralized linear control". In: *Proceedings of the 44th IEEE conference on Decision and Control*. IEEE. 2005, pp. 4964–4969.

[5] Bart Besselink and Karl H Johansson. "String stability and a delay-based spacing policy for vehicle platoons subject to disturbances". In: *IEEE Transactions on Automatic Control* 62.9 (2017), pp. 4376–4391.

[6] Vivek Borkar and Pravin Varaiya. "Asymptotic agreement in distributed estimation". In: *IEEE Transactions on Automatic Control* 27.3 (1982), pp. 650–655.

[7] Francesco Bullo and Andrew D Lewis. *Geometric control of mechanical systems: modeling, analysis, and design for simple mechanical control systems*. Vol. 49. Springer Science & Business Media, 2004.

[8] Frank H Clarke. *Optimization and nonsmooth analysis*. SIAM, 1990.

[9] Jorge Cortés. "Discontinuous dynamical systems". In: *IEEE Control Systems Magazine* 28.3 (2008), pp. 36–73.

[10] Jorge Cortés. "Finite-time convergent gradient flows with applications to network consensus". In: *Automatica* 42.11 (2006), pp. 1993–2000. ISSN: 0005-1098. DOI: http://dx.doi.org/10.1016/j.automatica.2006.06.015. URL: http://www.sciencedirect.com/science/article/pii/S000510980600269X.

[11] Jorge Cortés and Francesco Bullo. "Coordination and geometric optimization via distributed dynamical systems". In: *SIAM Journal on Control and Optimization* 44.5 (2005), pp. 1543–1574.

[12] Morris H DeGroot. "Reaching a consensus". In: *Journal of the American Statistical Association* 69.345 (1974), pp. 118–121.

[13] Stefano Di Cairano et al. "Vehicle yaw stability control by coordinated active front steering and differential braking in the tire sideslip angles domain". In: *IEEE Transactions on Control Systems Technology* 21.4 (2013), pp. 1236–1248.

[14] Shengbo Eben Li, Keqiang Li, and Jianqiang Wang. "Economy-oriented vehicle adaptive cruise control with coordinating multiple objectives function". In: *Vehicle System Dynamics* 51.1 (2013), pp. 1–17.

[15] Shengbo Eben Li et al. "Minimum fuel control strategy in automated car-following scenarios". In: *Vehicular Technology, IEEE Transactions on* 61.3 (2012), pp. 998–1007.

[16] J Alexander Fax and Richard M Murray. "Information flow and cooperative control of vehicle formations". In: *IEEE transactions on automatic control* 49.9 (2004), pp. 1465–1476.

[17] Antonella Ferrara and Claudio Vecchio. "Second order sliding mode control of vehicles with distributed collision avoidance capabilities". In: *Mechatronics* 19.4 (2009), pp. 471–477.

[18] Aleksei Fedorovich Filippov. *Differential equations with discontinuous right-hand sides: control systems*. Vol. 18. Springer Science & Business Media, 2013.

[19] Feng Gao et al. "Robust control of heterogeneous vehicular platoon with uncertain dynamics and communication delay". In: *IET Intelligent Transport Systems* 10.7 (2016), pp. 503–513.

[20] Arpita Ghosh, Stephen Boyd, and Amin Saberi. "Minimizing Effective Resistance of a Graph". In: *SIAM Review* 50 (2008), pp. 37–66.

[21] Chris Godsil and Gordon F Royle. *Algebraic graph theory*. Vol. 207. Springer Science & Business Media, 2013.

[22] Ge Guo and Wei Yue. "Hierarchical platoon control with heterogeneous information feedback". In: *IET control theory & applications* 5.15 (2011), pp. 1766–1781.

[23] Xianggui Guo et al. "Distributed adaptive integrated-sliding-mode controller synthesis for string stability of vehicle platoons". In: *IEEE Transactions on Intelligent Transportation Systems* 17.9 (2016), pp. 2419–2429.

[24] Sepideh Hassan-Moghaddam and Mihailo R Jovanović. "Topology Design for Stochastically Forced Consensus Networks". In: *IEEE Transactions on Control of Network Systems* 5 (2018), pp. 1075–1086.

[25] JK Hedrick et al. "Longitudinal vehicle controller design for IVHS systems". In: *American Control Conference, 1991*. IEEE. 1991, pp. 3107–3112.

[26] Henry Hermes. "Discontinuous vector fields and feedback control." In: *Differential Equations and Dynamical Systems* (1967).

[27] Yiguang Hong, Guanrong Chen, and Linda Bushnell. "Distributed observers design for leader-following control of multi-agent networks". In: *Automatica* 44.3 (2008), pp. 846–850.

[28] Yiguang Hong, Jiangping Hu, and Linxin Gao. "Tracking control for multi-agent consensus with an active leader and variable topology". In: *Automatica* 42.7 (2006), pp. 1177–1182.

[29] R. Horowitz and P. Varaiya. "Control design of an automated highway system". In: *Proceedings of the IEEE* 88.7 (July 2000), pp. 913–925. ISSN: 0018-9219. DOI: 10.1109/5.871301.

[30] Mihailo R Jovanović and Neil K Dhingra. "Controller architectures: Tradeoffs between performance and structure". In: *European Journal of Control* 30 (2016), pp. 76–91.

[31] Gelig Arkadii Kh et al. *Stability of stationary sets in control systems with discontinuous nonlinearities*. Vol. 14. World Scientific, 2004.

[32] Hassan K Khalil. *Noninear Systems*. Prentice-Hall, New Jersey, 1996.

[33] Nikolai Nikolaevich Krasovskii, Andrei Izmailovich Subbotin, and Samuel Kotz. *Game-theoretical control problems*. Springer-Verlag, 1987.

[34] NN Krasovskii and JL Brenner. "Stability of Motion, Applications of Lyapunov's Second Method to Differential Systems and Equations with Delay". In: *View at MathSciNet* (1963).

[35] Ji-Wook Kwon and Dongkyoung Chwa. "Adaptive bidirectional platoon control using a coupled sliding mode control method". In: *IEEE Transactions on Intelligent Transportation Systems* 15.5 (2014), pp. 2040–2048.

[36] GD Lee and SW Kim. "A longitudinal control system for a platoon of vehicles using a fuzzy-sliding mode algorithm". In: *Mechatronics* 12.1 (2002), pp. 97–118.

[37] Shengbo Eben Li et al. "An overview of vehicular platoon control under the four-component framework". In: *Intelligent Vehicles Symposium (IV), 2015 IEEE*. IEEE. 2015, pp. 286–291.

[38] Shengbo Eben Li et al. "Dynamical modeling and distributed control of connected and automated vehicles: Challenges and opportunities". In: *IEEE Intelligent Transportation Systems Magazine* 9.3 (2017), pp. 46–58.

[39] Shengbo Eben Li et al. "Multiple-model switching control of vehicle longitudinal dynamics for platoon-level automation". In: *IEEE Transactions on Vehicular Technology* 65.6 (2016), pp. 4480–4492.

[40] Zhongkui Li et al. "Consensus of multiagent systems and synchronization of complex networks: a unified viewpoint". In: *Circuits and Systems I: Regular Papers, IEEE Transactions on* 57.1 (2010), pp. 213–224.

[41] Zhongkui Li et al. "Designing fully distributed consensus protocols for linear multi-agent systems with directed graphs". In: *IEEE Transactions on Automatic Control* 60.4 (2015), pp. 1152–1157.

[42] Fu Lin, Makan Fardad, and Mihailo R Jovanović. "Design of Optimal Sparse Feedback Gains via the Alternating Direction Method of Multipliers". In: *IEEE Transactions on Automatic Control* 58 (2013), pp. 2426–2431.

[43] Jie Lin, A Stephen Morse, and Brian DO Anderson. "The multi-agent rendezvous problem". In: *42nd IEEE International Conference on Decision and Control (IEEE Cat. No. 03CH37475)*. Vol. 2. IEEE. 2003, pp. 1508–1513.

[44] Peng Lin, Yingmin Jia, and Lin Li. "Distributed robust H_∞ consensus control in directed networks of agents with time-delay". In: *Systems & Control Letters* 57.8 (2008), pp. 643–653.

[45] Xiangheng Liu et al. "Effects of communication delay on string stability in vehicle platoons". In: *ITSC 2001. 2001 IEEE Intelligent Transportation Systems. Proceedings (Cat. No.01TH8585)*. 2001, pp. 625–630. DOI: 10.1109/ITSC.2001.948732.

[46] Nancy A Lynch. *Distributed algorithms*. Elsevier, 1996.

[47] Kwang-Kyo Oh, Myoung-Chul Park, and Hyo-Sung Ahn. "A survey of multi-agent formation control". In: *Automatica* 53 (2015), pp. 424–440.

[48] R. Olfati-Saber and R.M. Murray. "Consensus problems in networks of agents with switching topology and time-delays". In: *Automatic Control, IEEE Transactions on* 49.9 (Sept. 2004), pp. 1520–1533. ISSN: 0018-9286. DOI: 10.1109/TAC.2004.834113.

[49] Fernando Paganini, John Doyle, and Steven Low. "Scalable laws for stable network congestion control". In: *Decision and Control, 2001. Proceedings of the 40th IEEE Conference on*. Vol. 1. IEEE. 2001, pp. 185–190.

[50] L Peppard. "String stability of relative-motion PID vehicle control systems". In: *IEEE Transactions on Automatic Control* 19.5 (1974), pp. 579–581.

[51] Jeroen Ploeg, Nathan Van De Wouw, and Henk Nijmeijer. "Lp string stability of cascaded systems: Application to vehicle platooning". In: *IEEE Transactions on Control Systems Technology* 22.2 (2014), pp. 786–793.

[52] Jiahu Qin et al. "Recent advances in consensus of multi-agent systems: A brief survey". In: *IEEE Transactions on Industrial Electronics* 64.6 (2017), pp. 4972–4983.

[53] Zhihua Qu. *Cooperative control of dynamical systems: applications to autonomous vehicles*. Springer Science & Business Media, 2009.

[54] Wei Ren and Ella Atkins. "Distributed multi-vehicle coordinated control via local information exchange". In: *International Journal of Robust and Nonlinear Control: IFAC-Affiliated Journal* 17.10-11 (2007), pp. 1002–1033.

[55] Wei Ren, Randal W Beard, and Timothy W McLain. "Coordination variables and consensus building in multiple vehicle systems". In: *Cooperative control*. Springer, 2005, pp. 171–188.

[56] Wei Ren, Kevin L Moore, and YangQuan Chen. "High-order and model reference consensus algorithms in cooperative control of multi-vehicle systems". In: *Journal of Dynamic Systems, Measurement, and Control* 129.5 (2007), pp. 678–688.

[57] Craig W Reynolds. "Flocks, herds and schools: A distributed behavioral model". In: *ACM SIGGRAPH computer graphics*. Vol. 21. 4. ACM. 1987, pp. 25–34.

[58] Jonathan A Rogge and Dirk Aeyels. "Vehicle platoons through ring coupling". In: *IEEE Transactions on Automatic Control* 53.6 (2008), pp. 1370–1377.

[59] Shankar Sastry. *Nonlinear systems: analysis, stability, and control*. Vol. 10. Springer Science & Business Media, 2013.

[60] E. Shaw and J.K. Hedrick. "String Stability Analysis for Heterogeneous Vehicle Strings". In: *American Control Conference* (July 2007), pp. 3118–3125. ISSN: 0743-1619. DOI: 10.1109/ACC.2007.4282789.

[61] S.E. Shladover et al. "Automated vehicle control developments in the PATH program". In: *Vehicular Technology, IEEE Transactions on* 40.1 (Feb. 1991), pp. 114–130. ISSN: 0018-9545. DOI: 10.1109/25.69979.

[62] Jean-Jacques E Slotine, Weiping Li, et al. *Applied nonlinear control*. Vol. 199. 1. Prentice hall Englewood Cliffs, NJ, 1991.

[63] Srdjan S Stankovic, Milorad J Stanojevic, and Dragoslav D Siljak. "Decentralized overlapping control of a platoon of vehicles". In: *IEEE Transactions on Control Systems Technology* 8.5 (2000), pp. 816–832.

[64] Sonja Stüdli, María M Seron, and Richard H Middleton. "From vehicular platoons to general networked systems: String stability and related concepts". In: *Annual Reviews in Control* 44 (2017), pp. 157–172.

[65] Youfeng Su and Jie Huang. "Cooperative output regulation of linear multi-agent systems". In: *IEEE Transactions on Automatic Control* 57.4 (2012), pp. 1062–1066.

[66] D Swaroop and J Karl Hedrick. "String stability of interconnected systems". In: *IEEE transactions on automatic control* 41.3 (1996), pp. 349–357.

[67] D Swaroop and JK Hedrick. "Direct adaptive longitudinal control of vehicle platoons". In: *Conference of Decision and Control, 1994*. IEEE. 1994, pp. 5116–5121.

[68] DVAHG Swaroop et al. "A comparision of spacing and headway control laws for automatically controlled vehicles". In: *Vehicle System Dynamics* 23.1 (1994), pp. 597–625.

[69] John Nikolas Tsitsiklis. *Problems in decentralized decision making and computation.* Tech. rep. Massachusetts Inst of Tech Cambridge Lab for Information and Decision Systems, 1984.

[70] John Tsitsiklis, Dimitri Bertsekas, and Michael Athans. "Distributed asynchronous deterministic and stochastic gradient optimization algorithms". In: *IEEE transactions on automatic control* 31.9 (1986), pp. 803–812.

[71] Vadim I Utkin. *Sliding modes in control and optimization*. Springer Science & Business Media, 2013.

[72] Jian-Qiang Wang et al. "Longitudinal collision mitigation via coordinated braking of multiple vehicles using model predictive control". In: *Integrated Computer-Aided Engineering* 22.2 (2015), pp. 171–185.

[73] Susan C Weller and N Clay Mann. "Assessing rater performance without a" gold standard" using consensus theory". In: *Medical Decision Making* 17.1 (1997), pp. 71–79.

[74] Guanghui Wen et al. "Distributed consensus of multi-agent systems with general linear node dynamics and intermittent communications". In: *International Journal of Robust and Nonlinear Control* 24.16 (2014), pp. 2438–2457.

[75] T.L. Willke, P. Tientrakool, and N.F. Maxemchuk. "A survey of inter-vehicle communication protocols and their applications". In: *Communications Surveys Tutorials, IEEE* 11.2 (Second 2009), pp. 3–20. ISSN: 1553-877X. DOI: 10.1109/SURV.2009.090202.

[76] Xiaofan Wu and Mihailo R Jovanović. "Sparsity-promoting optimal control of systems with symmetries, consensus, and synchronization networks". In: *Systems & Control Letters* 103 (2017), pp. 1–8.

[77] Yujia Wu et al. "Distributed sliding mode control for multi-vehicle systems with positive definite topologies". In: *2016 IEEE 55th Conference on Decision and Control (CDC)*. IEEE. 2016, pp. 5213–5219.

[78] Y. Wu et al. "Distributed Sliding Mode Control for Nonlinear Heterogeneous Platoon Systems With Positive Definite Topologies". In: *IEEE Transactions on Control Systems Technology* (2019), pp. 1–12. ISSN: 1063-6536. DOI: 10.1109/TCST.2019.2908146.

[79] Lingyun Xiao and Feng Gao. "Practical String Stability of Platoon of Adaptive Cruise Control Vehicles". In: *Intelligent Transportation Systems, IEEE Transactions on* 12.4 (Dec. 2011), pp. 1184–1194. ISSN: 1524-9050. DOI: 10.1109/TITS.2011.2143407.

[80] Sai Krishna Yadlapalli, Swaroop Darbha, and KR Rajagopal. "Information Flow and Its Relation to Stability of the Motion of Vehicles in a Rigid Formation". In: *IEEE Transactions on Automatic Control* 51.8 (2006), pp. 1315–1319.

[81] Fuzhen Zhang. *The Schur complement and its applications*. Vol. 4. Springer Science & Business Media, 2006.

[82] Hongwei Zhang et al. "On constructing Lyapunov functions for multi-agent systems". In: *Automatica* 58 (2015), pp. 39–42.

[83] Yang Zheng et al. "Distributed model predictive control for heterogeneous vehicle platoons under unidirectional topologies". In: *IEEE Transactions on Control Systems Technology* 25.3 (2017), pp. 899–910.

[84] Yang Zheng et al. "Stability and Scalability of Homogeneous Vehicular Platoon: Study on the Influence of Information Flow Topologies". In: *Intelligent Transportation Systems, IEEE Transactions on* 17.1 (2016), pp. 14–26.

[85] Yang Zheng et al. "Stability Margin Improvement of Vehicular Platoon Considering Undirected Topology and Asymmetric Control". In: *Control Systems Technology, IEEE Transactions on* pp.99 (2016).